Durham University

Durham Research Online

Deposited in DRO:

27 November 2020

Version of attached file:

Published Version

Peer-review status of attached file:

Peer-reviewed

Citation for published item:

Flewelling, H. A. and Magnier, E. A. and Chambers, K. C. and Heasley, J. N. and Holmberg, C. and Huber, M. E. and Sweeney, W. and Waters, C. Z. and Calamida, A. and Casertano, S. and Chen, X. and Farrow, D. and Hasinger, G. and Henderson, R. and Long, K. S. and Metcalfe, N. and Narayan, G. and Nieto-Santisteban, M. A. and Norberg, P. and Rest, A. and Saglia, R. P. and Szalay, A. and Thakar, A. R. and Tonry, J. L. and Valenti, J. and Werner, S. and White, R. and Denneau, L. and Draper, P. W. and Hodapp, K. W. and Jedicke, R. and Kaiser, N. and Kudritzki, R. P. and Price, P. A. and Wainscoat, R. J. and Chastel, S. and McLean, B. and Postman, M. and Shiao, B. (2020) 'The Pan-STARRS1 database and data products.', Astrophysical journal supplement series., 251 (1). p. 7.

Further information on publisher's website:

https://doi.org/10.3847/1538-4365/abb82d

Publisher's copyright statement:

© 2020. The American Astronomical Society. All rights reserved.

Use policy

The full-text may be used and/or reproduced, and given to third parties in any format or medium, without prior permission or charge, for personal research or study, educational, or not-for-profit purposes provided that:

- a full bibliographic reference is made to the original source
- a link is made to the metadata record in DRO
- the full-text is not changed in any way

The full-text must not be sold in any format or medium without the formal permission of the copyright holders.

Please consult the full DRO policy for further details.

Durham University Library, Stockton Road, Durham DH1 3LY, United Kingdom
Tel : +44 (0)191 334 3042 | Fax : +44 (0)191 334 2971
https://dro.dur.ac.uk

The Astrophysical Journal Supplement Series, 251:7 (62pp), 2020 November https://doi.org/10.3847/1538-4365/abb82d
© 2020. The American Astronomical Society. All rights reserved.

The Pan-STARRS1 Database and Data Products

H. A. Flewelling[1,2], E. A. Magnier[1], K. C. Chambers[1], J. N. Heasley[3], C. Holmberg[1], M. E. Huber[1], W. Sweeney[1], C. Z. Waters[1], A. Calamida[4], S. Casertano[4], X. Chen[5], D. Farrow[6], G. Hasinger[1], R. Henderson[7], K. S. Long[4], N. Metcalfe[8], G. Narayan[4], M. A. Nieto-Santisteban[4], P. Norberg[9,10], A. Rest[4], R. P. Saglia[6], A. Szalay[11], A. R. Thakar[11], J. L. Tonry[1], J. Valenti[4], S. Werner[11], R. White[4], L. Denneau[1], P. W. Draper[8], K. W. Hodapp[1], R. Jedicke[1], N. Kaiser[1], R. P. Kudritzki[1], P. A. Price[12], R. J. Wainscoat[1], S. Chastel[1], B. McLean[4], M. Postman[4], and B. Shiao[4]
[1] Institute for Astronomy, University of Hawai'i, 2680 Woodlawn Drive, Honolulu, HI 96822, USA
[2] Canada-France-Hawai'i Telescope, 65-1238 Mamalahoa Hwy, Kamuela, HI 96743, USA
[3] Back Yard Observatory, P.O. BOX 68856, Tucson, AZ 85737, USA
[4] Space Telescope Science Institute, 3700 San Martin Drive, Baltimore, MD 21218, USA
[5] Google Inc., 1600 Amphitheatre Parkway, Mountain View, CA 94043, USA
[6] Max-Planck Institut für extraterrestrische Physik, Giessenbachstraß e 1, D-85748 Garching, Germany
[7] Spire Global, Sky Park 5, 45 Finnieston Street, Glasgow, G3 8JU, UK
[8] Department of Physics, Durham University, South Road, Durham DH1 3LE, UK
[9] Institute for Computational Cosmology, Department of Physics, Durham University, South Road, Durham DH1 3LE, UK
[10] Centre for Extragalactic Astronomy, Department of Physics, Durham University, South Road, Durham DH1 3LE, UK
[11] Department of Physics and Astronomy, The Johns Hopkins University, 3400 North Charles Street, Baltimore, MD 21218, USA
[12] Department of Astrophysical Sciences, Princeton University, Princeton, NJ 08544, USA
Received 2020 February 7; revised 2020 August 27; accepted 2020 September 12; published 2020 October 30

Abstract

This paper describes the organization of the database and the catalog data products from the Pan-STARRS1 3π Steradian Survey. The catalog data products are available in the form of an SQL-based relational database from MAST, the Mikulski Archive for Space Telescopes at STScI. The database is described in detail, including the construction of the database, the provenance of the data, the schema, and how the database tables are related. Examples of queries for a range of science goals are included.

Unified Astronomy Thesaurus concepts: Astronomy databases (83); Sky surveys (1464); Photometry (1234); Astrometry (80)

1. Introduction

For nearly 4 yr, from 2010 May through 2014 March, the 1.8 m Pan-STARRS1 telescope (PS1) was used to perform a set of astronomical surveys with wide-ranging scientific goals. The largest portion of the observing time (56%) was used for the so-called 3π Survey, covering the three-quarters of the sky north of $-30°$ decl., easily observable by PS1 from its site on the summit of Haleakala on the Hawaiian island of Maui. The wide-field optical design of the telescope (Hodapp et al. 2004) allowed PS1 to observe most of the 3π Survey area in each of five filters (g_{P1}, r_{P1}, i_{P1}, z_{P1}, y_{P1}) between 10 and 15 times. Another 25% of the observing time was dedicated to the Medium-Deep (MD) Survey, in which 10 fields were repeatedly observed over the course of the 4 yr mission. The Pan-STARRS1 Gigapixel Camera (GPC1), consisting of an 8×8 grid of 4846×4868 pixel CCDs covering roughly 7 deg^2, has a pixel scale of $0\farcs257$. The telescope optics and the natural seeing of the site result in good image quality which is fully sampled by the GPC1 pixels: 75% of the 3π Survey images have FWHM values less than ($1\farcs51$, $1\farcs39$, $1\farcs34$, $1\farcs27$, $1\farcs21$) for (g_{P1}, r_{P1}, i_{P1}, z_{P1}, y_{P1}), with a floor of $\sim 0\farcs7$.

This is the sixth in a series of seven papers that describe the Pan-STARRS1 Surveys, the data processing algorithms, calibration, and the resulting data products. Chambers et al. (2016, Paper I) describe the Pan-STARRS1 Surveys, an overview of the Pan-STARRS1 System, the resulting image and catalog data products, a discussion of the overall data quality and basic characteristics, and a summary of important results. Magnier et al. (2020a, Paper II) describe how the various data processing stages of the Pan-STARRS Image Processing Pipeline (IPP) are organized and implemented. Waters et al. (2020, Paper III) describe the details of the pixel processing algorithms, including detrending, warping, and adding (to create stacked images) and subtracting (to create difference images), and the resulting image products and their properties. Magnier et al. (2020b, Paper IV) describe the details of the source detection and photometry, including point-spread-function (PSF) and extended source fitting models, and the techniques for forced photometry measurements. Magnier et al. (2020c, Paper V) describe the final calibration process and the resulting photometric and astrometric quality. This paper (Paper VI) describes the Pan-STARRS1 database, the data products, and details of their organization in the Pan-STARRS1 database. M. Huber et al. (2020, in preparation, Paper VII) will describe the MD Survey in detail, including the unique issues and data products specific to that survey.

In this article, we use the following typefaces to distinguish different concepts:

1. SMALL CAPS for the analysis stages.
2. *Italics* for database tables and columns.
3. `Fixed-width` font for program names, variables, and miscellaneous constants.

2. Background

The Pan-STARRS Project teamed with Alex Szalay's database development group at The Johns Hopkins University (JHU) to undertake the task of providing a publicly accessible database for Pan-STARRS1 (Heasley 2008). The JHU team was the major developer of the Sloan Digital Sky Survey

(SDSS) public database (Thakar et al. 2003), and it was an early goal of the Pan-STARRS team to reuse as much of the existing software as possible. However, for a number of reasons, including the much larger size of the Pan-STARRS1 data set, the wide variety of image and measurement types, and the importance of temporal information, major changes to the code base were required. Like the SDSS database, the database implementation for Pan-STARRS1 is based on the Microsoft SQL Server product line, with supporting code forked from the SDSS Catalog Archive Server Jobs System (CasJobs). Staying with SQL Server allows the use of a wealth of software developed for SDSS, including the Hierarchical Triangular Mesh tools (Szalay et al. 2007). The system developed for Pan-STARRS1 is called the *Published Science Products Subsystem*, or PSPS (Heasley et al. 2006).

As a widely used database engine, the Microsoft SQL Server provides a robust tool to define, build, and query the full database. The engine implements the SQL relational database language: data within different tables of the database are related to data in other tables by common fields, or indexes. In the PSPS implementation, the relationships are largely hierarchical: many measurements are linked to the images from which they came; associated measurements from the same astrophysical object are linked together to those objects. The tables use unique indexes to form these relationships, as detailed throughput this article.

The most significant challenge for the PSPS relative to the SDSS database implementation was the need to address the very large volume of Pan-STARRS1 data. The single monolithic database design of SDSS could not scale to the level needed for PS1 data. While SQL Server does not have (at present) a cluster implementation, a bespoke version can be crafted using a combination of distributed partition views and data slices (Heasley 2008). Partitioning data into smaller databases spread over multiple server machines allows the information to be presented to the users as a single, unified table.

3. Processing Versions and Data Releases

The Pan-STARRS data released to the community has been processed several times. All data is processed immediately by the data analysis system in order to discover moving and transient objects. This nightly science processing is streamlined and designed to allow fast access to the results by the Pan-STARRS1 *Moving Object Processing System* (MOPS; Denneau et al. 2013) and the PS1 science consortium, typically within a few hours after observation, for the discovery of moving objects, supernovae, and other time-sensitive transients. We refer to the nightly science processing as Processing Version 0 (PV0). On longer timescales, large portions of the data have been reprocessed, either for internal use or for external release. The 3π Survey data spans >4 yr of observations (2010–2014, with some observations in 2009 and 2015), a time during which the IPP was actively being developed and improved. To make a consistent set of data, both for internal use as well as for the public release, all of the raw images were reprocessed from scratch using a specific revision number of the IPP code. During the survey, the 3π Survey data were reprocessed twice for internal access by the consortium members, making use of improvements to the calibrations and the processing algorithms. These internal releases are considered PV1 and PV2. The data released to the public in DR1 and DR2 represent a third full-scale reprocessing of the data, PV3.

This paper covers multiple data releases. The first Pan-STARRS1 data release (DR1, database opened to public in 2016 December) covers the 3π STACK images and the static sky catalog. The DR1 image products are deep stacked images along with ancillary data including signal, masks, variance, and number maps. The DR1 catalog data products available from the PSPS include the PS1 static sky 3π catalog. Source properties are organized into several tables, as described in Table 1; only tables referring to the static results, without time domain information, are included in DR1.

Data Release 2 (DR2, database opened to public in 2019 January), adds more of the PS1 image products from the 3π Survey, including the single-epoch WARP images and their ancillary data, such as signal, masks, and variance maps. DR2 provides the *Detection* tables and *Forced**[13] tables, containing the single-epoch source detections and the forced photometry. DR2 also contains numerous improvements to the data products in DR1, which it supersedes. Future data releases are anticipated to provide the 3π DIFF image products and catalogs and analogous data products for the MD surveys.

4. Overview of the Data Products

Public access to the Pan-STARRS data is through the web server located at https://panstarrs.stsci.edu and is hosted by the Barbara A. Mikulski Archive for Space Telescopes (MAST) at STScI. MAST provides the access point for downloading different pixel data products and their associated metadata and source catalogs. This includes FITS images, FITS and JPEG image cutouts, scriptable image access, color JPEG images, and an interactive image browser with catalog overlays through the MAST portal and the MAST PS1 image cutout server. In addition, MAST provides a simple web-based interface to access the Pan-STARRS catalog database. Full database access to the Pan-STARRS tables is available through the CasJobs interface (see description at https://mastweb.stsci.edu/mcasjobs). CasJobs emulates local free-form SQL access in a web environment and provides both synchronous and asynchronous query execution. The interface can execute complex, large queries of the PS1 (DR1/DR2) catalogs, with results saved to a private space allocated to each registered user. The Pan-STARRS catalog database accessible through CasJobs contains calibrated catalogs of photometric and astrometric parameters for single-epoch exposures, stacks, difference images, and forced photometry. The database schema for the Pan-STARRS catalog database is briefly described in Section 7 and is fully expanded in Appendix D. Examples of queries are described in Appendix A.

The Pan-STARRS1 catalog database schema is organized into four sections:

1. Fundamental Data Products. These are attributes that are calculated from either detrended but untransformed pixels or warped pixels. It should be noted that, once in the database, the instrumental fluxes and magnitudes have been subject to recalibration, as have the sky coordinates. Because of these recalibrations on the catalogs, the catalog values are to be preferred to making a new

[13] In this article, we refer to groups of tables with the same base name using the file "glob" convention where, e.g., *Forced** refers to a collection of tables starting with *Forced*.

Table 1
Summary of the Different Database Tables, Their Types, and Other Comments

PSPS Table Name	Table Type	Release
Filter	System Metadata	DR1
FitModel	System Metadata	DR1
Survey	System Metadata	DR1
PhotoCal	System Metadata	DR1
StackType	System Metadata	DR1
DiffType	System Metadata	DR1
TessellationType	System Metadata	DR1
ImageFlags	System Metadata	DR1
DetectionFlags	System Metadata	DR1
DetectionFlags2	System Metadata	DR1
DetectionFlags3	System Metadata	DR1
ObjectInfoFlags	System Metadata	DR1
ObjectFilterFlags	System Metadata	DR1
ObjectQualityFlags	System Metadata	DR1
ForcedGalaxyShapeFlags	System Metadata	DR1
ObjectThin	Object/Mean	DR1
MeanObject	Object/Mean	DR1
GaiaFrameCoordinate	Object/Mean	DR1 only
FrameMeta	Obs. Metadata	DR2
ImageMeta	Obs. Metadata	DR1
Detection	Detection table	DR2
ImageDetEffMeta	Obs. Metadata	DR2
StackMeta	Obs. Metadata	DR1
StackObjectThin	Detection table	DR1
StackObjectAttributes	Detection table	DR1
StackApFlx	Detection table	DR1
StackModelFitExp	Detection table	DR1
StackModelFitDeV	Detection table	DR1
StackModelFitSer	Detection table	DR1
StackApFlxExGalUnc	Detection table	DR1
StackApFlxExGalCon6	Detection table	DR1
StackApFlxExGalCon8	Detection table	DR1
StackPetrosian	Detection table	DR1
StackToImage	Obs. Metadata	DR1
StackToFrame	Obs. Metadata	DR1
StackDetEffMeta	Obs. Metadata	DR1
ForcedMeanObject	Object/Mean	DR1
ForcedMeanLensing	Object/Mean	DR1
ForcedGalaxyShape	Object/Mean	DR2
ForcedWarpMeta	Obs. Metadata	DR2
ForcedWarpMeasurement	Detection table	DR2
ForcedWarpMasked	Detection table	DR2
ForcedWarpExtended	Detection table	DR2
ForcedWarpLensing	Detection table	DR2
ForcedWarpToImage	Obs. Metadata	DR2
DiffDetObject	Object/Mean	DR3
DiffMeta	Obs. Metadata	DR3
DiffDetection	Detection table	DR3
DiffToImage	Obs. Metadata	DR3
DiffDetEffMeta	Obs. Metadata	DR3

Note. The column labeled "Release" specifies the first Data Release a specific product became available. Note that all of the DR1 tables were regenerated for DR2, in order to address minor bugs and inconsistencies discovered in DR1.

measurement directly from the available released pixel data, and care should be taken when using the recalibrated astrometry with the original images (see Table 2).

Table 2
Fundamental IPP Data Product Database Tables

Table Class	PSPS Table Name	Source	Release
Object	ObjectThin	dvo	DR1
	MeanObject	dvo	DR1
	GaiaFrameCoordinate	dvo	DR1
Detection	Detection	dvo and cam smf	DR2
Stack	StackObjectThin	dvo and skycal cmf	DR1
	StackObjectAttributes	dvo and skycal cmf	DR1
	StackApFlx	dvo and skycal cmf	DR1
	StackApFlxExGalUnc	dvo and skycal cmf	DR1
	StackApFlxExGalCon6	dvo and skycal cmf	DR1
	StackApFlxExGalCon8	dvo and skycal cmf	DR1
	StackPetrosian	dvo and skycal cmf	DR1
	StackModelFitExp	dvo and skycal cmf	DR1
	StackModelFitDeV	dvo and skycal cmf	DR1
	StackModelFitSer	dvo and skycal cmf	DR1
Forced	ForcedMeanObject	dvo	DR1
	ForcedWarpMeasurement	dvo and forced warp cmf	DR2
	ForcedMeanLensing	dvo	DR2
	ForcedWarpLensing	dvo and forced warp cmf	DR2
	ForcedGalaxyShape	dvo	DR2
	ForcedWarpMasked	dvo and forced warp cmf	DR2
Difference	DiffDetection	dvo and diff skycal cmf	DR3
	DiffDetObject	dvo	DR3

2. Derived Data Products. These are higher-order science products that have been calculated from the fundamental data products, such as proper motions and photometric redshifts. These data products are not yet available and will come in later data releases.
3. Observational Metadata. These metadata provide detailed information about the individual exposures (e.g., information like exposure time, filter used, etc.) or about which exposures went into an image combination (stacks and diffs), as well as information such as detection efficiencies.
4. System Metadata. These tables have fixed information about the system and the database itself, primarily descriptions of various flags and their bits, but also for other metadata such as filter information.

Various database "Views" are also constructed as an aid to the user for standard types of queries. Views act like tables and primarily consist of joins of different commonly used tables, in order to simplify queries. Views are also used to join slices of tables (sliced by area of sky) into a full sky view. For example, "*Detection*" is a view of 32 *Detection* tables, but the individual tables are hidden from the user. For more information on views, including the currently defines ones, see Table 8.

This paper covers the data products and schema for the 3π data releases, though most details also apply to the MD fields. Additional documentation is available together with the data products through MAST.

5. Flow of Data from Pipeline to the Pan-STARRS Catalog Database

This section presents a condensed version of the flow of data starting with raw image processing by the Pan-STARRS IPP

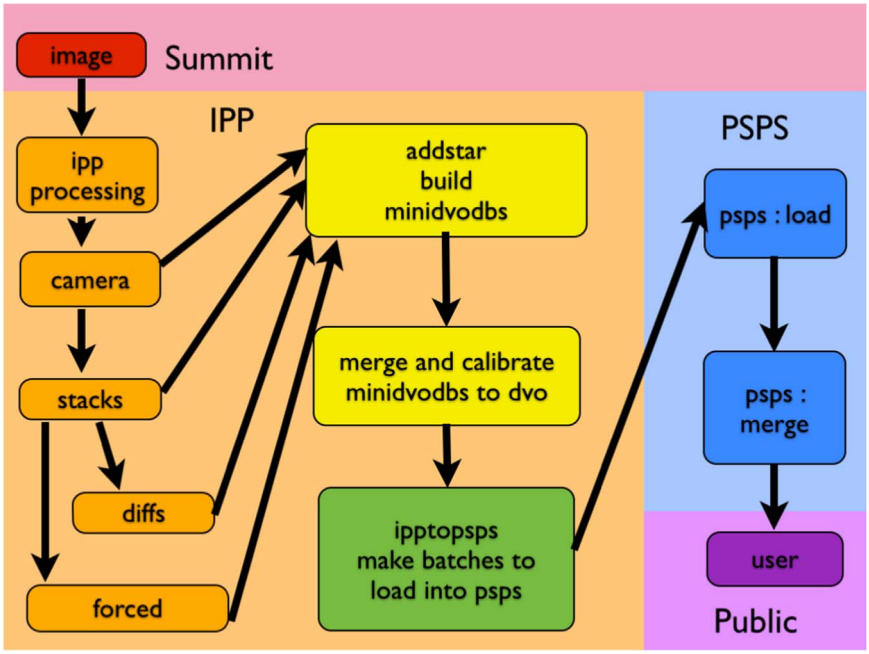

Figure 1. An overview of the steps necessary to create publicly accessible Pan-STARRS1 data. The first step is to take exposures from the summit, process them via the image processing pipeline (IPP), ingest the data into the PSPS, and then provide public access to the user. The IPP has many processing steps; not all are shown here. The *camera*, *stacks*, *difference images*, and *forced photometry* stages produce binary catalog FITS files, which are the foundation of building the DVO database, which is then calibrated. The final step of IPP processing is to use *IppToPsps* to generate small batches of data in the appropriate database schema to be ingested into PSPS. This paper primarily focuses on the PSPS and the database schema. The other steps are explained in enough detail to describe known and potential sources of inconsistencies within the database.

and ending with the steps used to generate the PSPS database. The description includes an overview of the various terms used to describe different data products. For the full description of these steps, see Paper II. A flowchart of the whole process is shown in Figure 1.

Exposures are first processed by the IPP, producing measurements of the sources in the individual images, stacks, and difference images. These measurements are then ingested into an instance of the "Desktop Virtual Observatory" database system (DVO, described briefly in Section 5.2 and more extensively in Paper V). The DVO database is then calibrated (Paper V). Next, the IPPTOPSPS combines the measurements with the calibrations and transforms them into the appropriate format for the PSPS. Data in this form are loaded into the PSPS database at the University of Hawaii's Institute for Astronomy (IfA). The PSPS database is then copied to STScI and made available to the users.

5.1. Processing Stages

Processing with the IPP takes place in several stages. Because the organization of the PSPS database is tied to these processing stages, we describe them in some detail here. For further information, see Paper II for the overall analysis sequence, Paper III for the details in the detrending and other pixel manipulation, Paper IV for the source detection and characterization, and Paper V for the photometric and astrometric calibration.

5.1.1. Download and Registry of Images

Before processing of images can take place, they must first be transferred to the IPP cluster from the summit and registered in a metadata database to ensure that all of the >1.3 million images taken by Pan-STARRS have been properly handled. This is represented as the "image" → "ipp processing" step in Figure 1. The IPP uses an internal database to track all parts of the image processing. This database keeps basic metrics relevant to each stage, including details on what type of image was taken, when an image was processed, how long processing took, flags and other metrics on the quality, etc. This internal processing database is referenced to in this paper as the "GPC1" database.

5.1.2. Chip and Camera Stages

The CHIP stage takes the raw images—generally 60 FITS files, one FITS file per orthogonal transfer array (OTA)—and detrends them, one chip per computing job. Dark, flat, bias, background, and other corrections, as described in Paper III, are applied to each chip image, followed by source detection and photometry using the `psphot` program (Paper IV). Next, the CAMERA stage combines the outputs of the CHIP stage, performs basic astrometry on the detected sources, and generates a binary FITS table, called an smf file, holding the catalog information for the entire exposure. These files are later ingested into a DVO-style database for internal use. These two stages are represented as the "ipp processing" → "camera" steps in Figure 1. Camera-stage products are available to the user in the PSPS "Detection" tables, starting with DR2.

5.1.3. Warp Stage

The next step, the WARP stage, is represented as "camera" → "stacks" in Figure 1. The WARP stage geometrically transforms the output images from the CHIP stage to a common pixel grid

defined on a tangential R.A./decl. plane, with 0.″25 pixels. The output images, called "skycells," cover the entire sky; thus, an image from a PS1 exposure can be split and projected onto a common layout for its portion of the sky. For 3π, the skycell tessellation[14] is called `Rings.V3` and is described in detail in Paper II. This tessellation subdivides the sky into projection cell rings with centers at constant decl. Each projection cell is ∼4.°0 × ∼4.°0, subdivided into 10 × 10 skycells, each with 60″ of overlap on a side, yielding square image with size ranging from 6240 to 6500 pixels on a side. All image data products beyond WARP (STACKS/FORCED WARPS/DIFFS/ etc.) are laid out in skycells as well.

The warp image products are available to users via MAST for the 3π Survey as part of DR2.

5.1.4. Stack, Staticsky, Skycal Stages

There are three stack-related stages: STACK, STATICSKY, and SKYCAL. The STACK stage generates the stacked images, STATICSKY generates the source catalogs files, while SKYCAL calibrates the source catalogs. All of the stack-related stages are represented as "stacks" in Figure 1.

STACKS are generated by adding together WARP skycells, with bad-pixel rejection and internal calibration as described in Paper III. Depending on the survey, stacks may be generated from different sets of raw exposures. For the deepest possible stacks, essentially all available exposures are combined, with only weak cuts on the data quality. Stacks may also be generated with a constraint on the image quality of the input exposures in order to yield a deep reference image with good image quality. In order to limit contamination from ongoing transient events, stacks may also be generated with constraints on the time range of the input exposures: out-of-season stacks would include only exposures not taken within a given year or period to act as a reference for transient events within that period. The different stack types are listed in the *StackType* table in the PSPS database. For the DR1 and DR2 3π databases, only the `DEEP_STACK` STACK type is used, i.e., all available WARPS of sufficiently good quality for a given skycell and filter within the 3π Survey data set are used to generate the STACKS, yielding one STACK per skycell per filter. Mask images, variance images, and related pixel images are also generated for each stack.

Once each STACK image is created, source detection and characterization, including galaxy morphological analysis, are performed by the STATICSKY stage. The source analysis is run on all five filters at once. PSF photometry is forced for sources that are detected in at least two filter images on the other filter images for which the source was not detected above the 5σ threshold. This forced photometry is also performed for sources detected in only the $y_{\rm P1}$ band.

Aperture photometry, for a series of circular apertures specified by SDSS (Stoughton et al. 2002), is performed on the raw stacks and also on stack images that have been convolved to a common 6 pixel FWHM, and again to a common 8 pixel FWHM. These latter seeing-matched images are only kept in memory for the analysis and are not written to disk. Up to nine of the SDSS apertures are used for this measurement: R3 ($r = 1.''03$), R4 ($r = 1.''76$), R5 ($r = 3.''00$), R6 ($r = 4.''63$), R7 ($r = 7.''43$), R8 ($r = 11.''42$), R9 ($r = 18.''20$), R10 ($r = 28.''20$), and R11 ($r = 44.''21$). Note that the measurement is performed in apertures with the same angular diameter as used for SDSS, which necessarily results in different radii in pixels from those used by SDSS apertures (see Table 7 in Stoughton et al. 2002). For more details on the photometric analysis of the stack images, see Paper IV.

Catalog files, one per filter, are generated with sources spatially matched between filters using a 5 pixel ($1.''25$) correlation radius. Sources matched as across filters are linked in the output catalog by the detection ID. The SKYCAL stage calibrates the STATICSKY catalogs relative to the reference catalog. The calibrated catalog files are later ingested into the DVO database and then into the PSPS database. Due to the overlap between skycells, sources that land in the overlaps can be reported two, three, or four times in the DVO and PSPS database. See the discussion in Section 7.4.2 regarding the "primary" and "best" stack measurements.

Stack data products are available for the 3π Survey as part of DR1 and DR2. Stack image products are available to users via MAST, and Stack-related tables are available in the PSPS database.

5.1.5. Forced Warp Photometry Stage

Sources that are detected in the stack images are used to measure forced photometry on each of the input warps in the FORCED WARP PHOTOMETRY stage. Two types of forced photometry analysis are performed on the WARP exposures: PSF photometry and galaxy model analysis.

In the forced warp photometry stage, the positions of sources located in the deep STACKS are used to fix the position in the warp images. The software then measures the PSF model flux at those positions on each of the individual warps. This measurement also yields the Kron and aperture fluxes for the warp image at that location. The catalogs generated by this process are ingested into the DVO database and average values are then calculated. Note that the fluxes on the warps for faint objects may be insignificant or even negative; the average values are calculated using all flux values (both positive and negative) properly weighted by the detection flux errors. Only measurements for which the warp pixels were excessively masked are rejected in this average flux calculation. The individual measurements and the averages are translated by the IPPTOPSPS stage into the *ForcedWarp** tables for the PSPS. For the 3π Survey, these tables are available starting with DR2.

For extended sources, galaxy models are fitted on the STACK images. These models are then used as a seed to determine galaxy models for each warp image. The position, aspect ratio, and (where appropriate) Sérsic radius are kept fixed to the values determined for the stack image. A grid of major and minor axis values is tested around the values from the stack fit for each warp image, with the galaxy model convolved with the PSF appropriate to the specific warp image. The software reports the model normalization and χ^2 value at each grid point; these are combined together across all warp exposures and the interpolated minimum χ^2 value is used to determine a best-fit galaxy model. Due to size constraints, only the average galaxy model results are propagated to the PSPS database. These are later ingested into the PSPS database as the *ForcedGalaxy** tables.

The extended source (galaxy) models described above are not applied to all sources. Galaxy models are only applied if the measured Kron magnitudes are brighter than the following limits for at least one filter: ($g_{\rm P1}$, $r_{\rm P1}$, $i_{\rm P1}$, $z_{\rm P1}$, $y_{\rm P1}$) = (21.5, 21.5,

[14] Note that our use of the term "tessellation" is inaccurate because the skycell sizes are variable and neighbors overlap each other.

21.5, 20.5, 19.5). In addition, galaxy models and Petrosian fluxes are only measured for skycells with centers outside of a Galactic plane exclusion zone defined for the 3π Survey as

$$|b| > b_0 + r_b e^{\frac{-l^2}{2\sigma_b^2}},$$

where $b_0 = 20°$, $r_b = 15°$, and $\sigma_b = 50°$ and l, the Galactic longitude, is constructed to have a domain of $-180°$ to $+180°$. Thus, both apparently stellar and nonstellar sources outside of the dense portions of the Galactic plane and bulge have galaxy models and Petrosian fluxes measured (see full discussion in Paper IV).

5.1.6. Diff Stage

Difference images are generated by the IPP in order to detect transient and moving objects. Several types of difference images may be generated by the IPP depending on the type of images that are involved in the subtraction. The WARP_WARP diffs are generated by subtracting warps from a pair of exposures, usually taken within a short period of time; these are primarily used by the nightly science processing and the MOPS analysis for inner solar system sources and for transient detections from the 3π Survey data. STACK_STACK diffs are generated by subtracting a deep reference stack from a stack of multiple exposures taken over a shorter period. The STACK_STACK diffs are used for supernova discovery in the MD survey fields with eight exposures taken in sequence and stacked to make a more sensitive single-epoch observation. The WARP_STACK diffs were generated for the 3π Survey by combining warps from single exposures with a deep reference stack. These diffs are also used for MOPS and transient discoveries, and will be provided for the full 3π Survey as a temporal reference. There is one DIFF image for each single exposure within the 3π Survey. Finally, STACK_WARP diffs could be made in principle but are not in practice used by the IPP.

For the difference image analysis, the input images (STACK or WARP) are convolved to have similar PSFs (Waters et al. 2020) and one subtracted from the other. Sources are detected on the difference image, basic photometry is performed on the sources, and DIFF catalog files are created. The DIFF catalog files are then ingested into the DIFF DVO and later ingested into the PSPS. The results from this stage of processing include diff catalog files, which will be available in a future release (nominally DR3). At this time, it is undecided if, as part of DR3, the complete collection of PV3 difference images will be stored at MAST or if they will be generated on demand. Within the IPP, difference images are generally stored on disk only for a short period of time (days to weeks) in order to save on storage space. When needed, historical difference images are regularly regenerated based on stored results (difference kernels and PSF models). MAST may rely on this process for DR3.

5.2. DVO Database Steps

The DVO (Magnier & Cuillandre 2004; Magnier et al. 2020c) is a database that tracks the measurements of astronomical sources detected in the various types of images and associates them into unique astronomical objects based on positional coincidence. This database system also tracks the metadata for each image that provided the measurements. The DVO database is loaded with a subset of photometric, astrometric, and other information from the catalog FITS files (smf/cmf) from various IPP stages. The DVO database is then used to determine the astrometric and photometric calibrations for all survey images. These calibrations are in turn used to calculate the average properties of the astronomical objects (see Paper V).

Catalog files from several stages of IPP processing are ingested into the DVO database via the IPP program addstar. The relevant stages are CAMERA (all measurements from the individual exposures), SKYCAL (measurements from the stacks), and FORCED WARP (forced photometry and the forced galaxy model fits from the warps). Difference image catalogs are ingested into the separate diff DVO database.

Measurements from 2MASS, WISE, and Gaia are also merged into the DVO database; flags within the DVO database, and inherited by the PSPS database, note the presence of data from these surveys. Gaia DR1 (Gaia Collaboration et al. 2016) was released before the Pan-STARRS DR1 was complete, but after all of the object tables were already ingested into the PSPS database. We used the Gaia DR1 data to recalibrate the DVO object positions, which improved the astrometry significantly. Rather than regenerate the database and start over (with corrected R.A. and decl. positions), we arranged for the IPPTOPSPS system to export just the newly calibrated positions along with minimal metadata to link the new coordinates with the existing objects. See Section 5.3 for the special table that carries the Gaia DR1 calibration into the 3π Survey DR1 release. For the 3π Survey DR2, the calibration is tied directly to the Gaia DR1 astrometric system (Paper V).

The DVO databasing system uses a collection of binary FITS tables as the backend. These files define a spatial partition of the database, divided on lines of constant R.A. and decl. For a given file type, the database contains several thousand such files. Several categories of DVO files are used by IPPTOPSPS to populate the PSPS database. Here we give a short summary of the subset of DVO files that are most relevant for IPPTOPSPS (see Paper II for more details).

.cpt: Object information—each .cpt table has one entry for each object in that region of the sky. It summarizes the average properties of that object as long as those properties can be derived independently of the filter used. Information such as mean R.A. and decl. is listed in these files.

.cpm: Measurements—each .cpm table contains all of the measurement information for each object in the .cpt file. Contains measurement information for detections from the stack/skycal cmf, camera smfs, and forced warp smfs.

.cps: Mean properties—the .cps table has filter-dependent average property information for each object listed in the .cpt file. Information such as mean magnitudes is located in these files.

.cpx: Lensing measurements—the .cpx files contains lensing parameters measured from all the forced warp cmfs.

.cpy: Lensing Objects—the .cpy table has one entry per filter for each object in that region of the sky, same object ids as for objects in the .cpt file. It summarizes the average properties of the lensing measurements.

.cpq: Forced Galaxy—the .cpq table has one entry per filter for each object in that region of the sky, same object IDs as for objects in the .cpt files. It summarizes the extended source galaxy shape measurements.

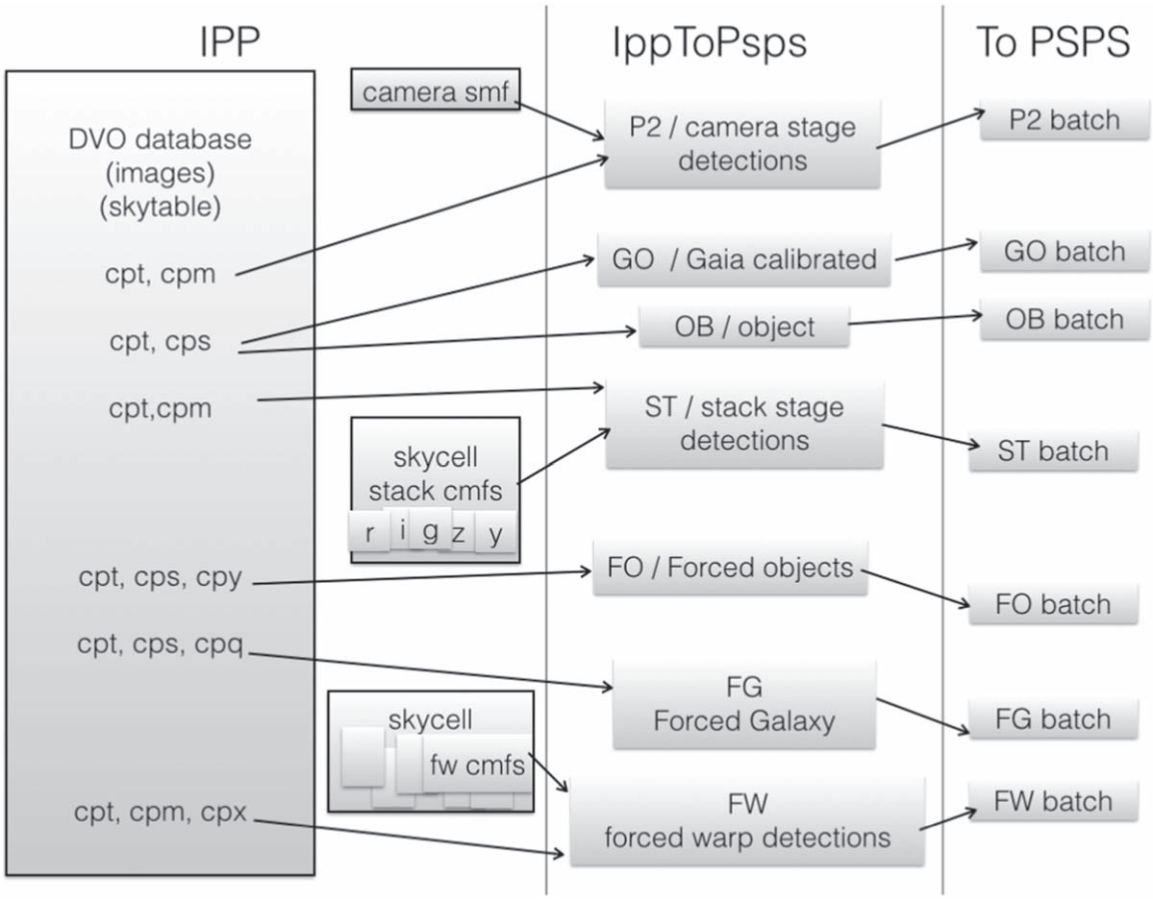

Figure 2. This figure shows a flowchart of how data flows from the IPP side into batches for PSPS, using *IppToPsps*. On the IPP side, the DVO database shows cpt/cpm/cps/cpx/cpy/cpq files, organized and grouped by which *IppToPsps* batch type uses them. The IPP side also has the smf/cmf files from the camera stage, forced warp stage, and stack (skycal) stages; these smf/cmf files are also needed for *IppToPsps*. *IppToPsps* has several different batch types, extracting data from different sources and generating batches for ingest into PSPS. Batches related to diffs are not shown here; it is a similar process (cpt, cpm) files from the diff DVO and cmf files from the diff skycells go through *IppToPsps* to create DF batches (analagous to P2 or ST but using diff cmfs). DO batches are created using cpt, cps files from the diff DVO (similar to how OB or GO batches are created).

5.3. *IppToPsps* Steps

The DVO database contains the calculated astrometric and photometric calibrations and average properties of the astronomical objects but only a subset of the information recorded by the IPP in the output catalog files. It is therefore necessary, when building the PSPS database, to combine the calibrations from the DVO database with the full set of data from the individual smf and cmf catalog files. It is also necessary to extract the average quantities from the DVO database to be uploaded to the PSPS database. The IPPTOPSPS system is responsible for both of these actions.

The IPPTOPSPS system extracts the average properties from the DVO database in units of the DVO sky partition files and generates file sets called "batches" containing the information formatted according to the PSPS schema. IPPTOPSPS generates average property batches separately for measurements from individual exposures, difference exposures, and exposures measured at the FORCED WARP stage. In addition, for the 3π Survey DR1, mean property batches are generated for the astrometry tied to the Gaia DR1 catalog (Gaia Collaboration et al. 2016).

The IPPTOPSPS system also extracts calibration information and calibrated measurements for the CAMERA, STACK, FORCED WARP, and DIFFERENCE stages and combines those values with the raw measurements stored in the smf/cmf files. Batch files are generated for the CAMERA-stage data for each exposure. For data from the other three stages, batches are generated for individual skycells. In the case of the STACK data, the batch contains data for the stack images from all five filters. For the FORCED WARP stage, the batch contains data from all warp epochs for a given skycell.

The batches generated by the IPPTOPSPS are made available to the PSPS ingest system using an internal web-based interface called a "datastore." The IPPTOPSPS software is written in Python/Jython, using the STILTS library (Taylor 2006) to interact with the FITS tables. IPPTOPSPS also uses as MySQL database to track the processing and for temporary scratch databases. This process also queries the IPP processing database, retrieves files from the IPP cluster, and reads data from the DVO database.

Below we provide additional details on the different batch types generated by the IPPTOPSPS system. An overview of the different batch types and associated DVO files and smf/cmf files is shown in the flowchart in Figure 2.

Init batch (IN): Defines elements of the PSPS database structure and is the first to be ingested into PSPS. It includes the system metadata tables described in Section 7.2, with flag bits listed in Appendix C.

Object batches (OB): Populate the *ObjectThin* and *MeanObject* tables, described in more detail in Section 7.3. Each

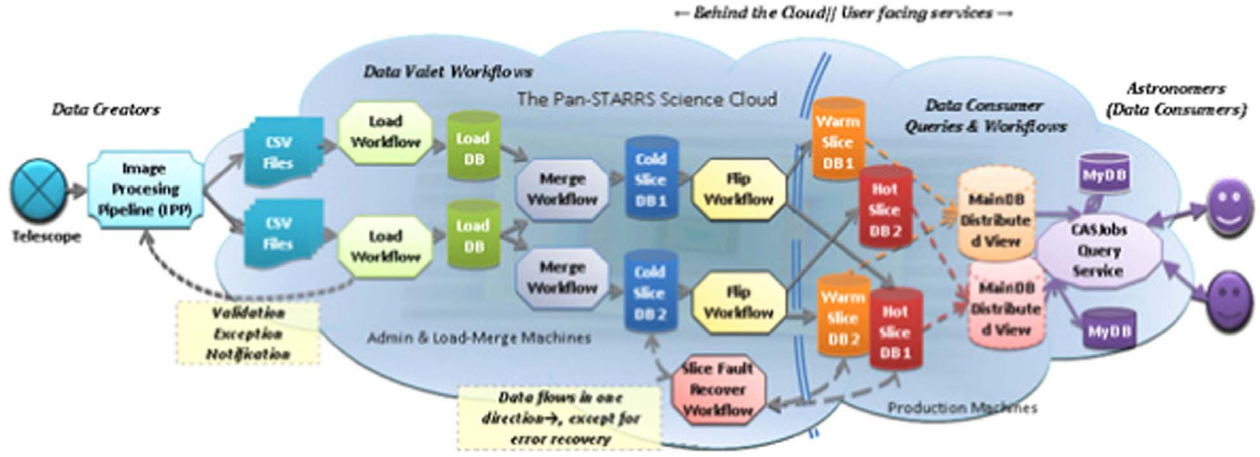

Figure 3. This figure shows a flowchart of how data flow from the IPP (via IppToPsps) into the load merge machines, which are then copied to the slice machines to allow for users to query the data (via a modified CasJobs).

batch represents individual DVO files, which are subdivided into small rectangular patches of sky. Columns are filled from the DVO database (*cpt* and *cps* files).

Detection batches (P2): Populate the *Detection* tables, described in more detail in Section 7.4.1. Each batch corresponds to a single exposure from Pan-STARRS1. Columns within are filled from the DVO database (cpt and cpm files) as well as the CAMERA stage catalog file (smf).

Stack batches (ST): Populate the *stack* tables, described in more detail in Section 7.4.2. Each batch corresponds to a skycell from the SKYCAL stage. Columns are filled from the DVO database (cpt and cpm files) as well as from the corresponding SKYCAL catalog files (cmf) for all five filters (or what is available).

Forced mean object batches (FO): Populate the *ForcedMeanObject* and *ForcedMeanLensing* tables, described in more detail in Section 7.3. Each batch contains data from individual DVO files (cpt, cps, cpy).

Forced galaxy batches (FG): Populate the *ForcedGalaxyShape* table, described in more detail in Section 7.3. Each batch contains data from individual DVO files (cpt, cps, cpq).

Forced warp batches (FW): Populate the *ForcedWarp** tables, described in more detail in Section 7.4.3. Each batch corresponds to a different skycell, and contains all of the FORCED WARP catalog measurements for that skycell. Each batch contains data from individual DVO files (cpt, cps, cpx) as well as from the corresponding FORCED WARP catalog files (cmf).

Diff object batches (DO): Populate the *DiffDetObject* table, described in more detail in Section 7.3. Columns are filled from the DVO DIFF database (cpt and cps files).

Diff detection batches (DF): Populate the *DiffDetection* table, described in more detail in Section 7.4.4. Each batch corresponds to a difference image catalog file created in the DIFF stage and contains all of the skycells for a given exposure. Columns are filled from the DVO database (cpt and cpm files), and from the corresponding DIFF catalog file (cmf).

Gaia object batches (GO): Populate the *GaiaFrameCoordinate* table, linking the Gaia DR1 calibrated positions to the *ObjectThin* entries by *objID*. It is based on exactly the same DVO files as OB batches, has updated R.A. and decl. calibrated to Gaia, and ignores the rest of the DVO columns. These batches, and this table, are only present for DR1. For DR2, additional calibration improvements were made within the DVO database (see Paper V). The average property batches were regenerated, making the GO batch irrelevant for that release.

Within IPPTOPSPS, it is possible to verify that the expected batches were generated, and to requeue and regenerate batches that failed. Batches fail for a variety of reasons, but none of the failures are terminal. Batches can fail if any of the associated mysql databases time out or are unavailable, or if there are disk or network I/O glitches or other disk/network problems. The DVO database sets the expected number of batches to generate, and failures are investigated and retried until they are resolved. Within IPPTOPSPS, it is also possible to poll the PSPS to verify if batches have been ingested, thus closing the loop.

6. PSPS

The PSPS consists of several parts: the data transformation layer (DXLayer), the Object Database Manager (ODM), the Workflow Manager Database (WMD), and the data retrieval layer (DRL). The user accesses the data through the DRL, using either scripts, the STScI CasJobs interface, or if the user is a Pan-STARRS1 Consortium member, the Published Science Interface (PSI). The DXLayer polls the IPPTOPSPS datastores for new batches and prepares them for loading. The ODM is the software used to load, merge, copy, and publish the PSPS databases. The WMD is the database containing all the logs about the PSPS databases. The DRL is the intermediate layer between the client and the PSPS database. The PSI is the web-based interface for PS1 consortium members, for interacting with the DRL. Each of these components is described in more detail below, and a diagram of the process is shown in Figure 3.

6.1. Partitioning the PSPS

The PSPS uses Distributed Partitioned Views, a mechanism that allows tables to be partitioned into files that reside in different linked servers. For the PSPS, the largest tables are partitioned into "slices," which divide the sky into decl. bands. The database tables exposed to the end users (e.g., *Detection*, *ForcedWarpMeasurement*, etc.) are composed of views

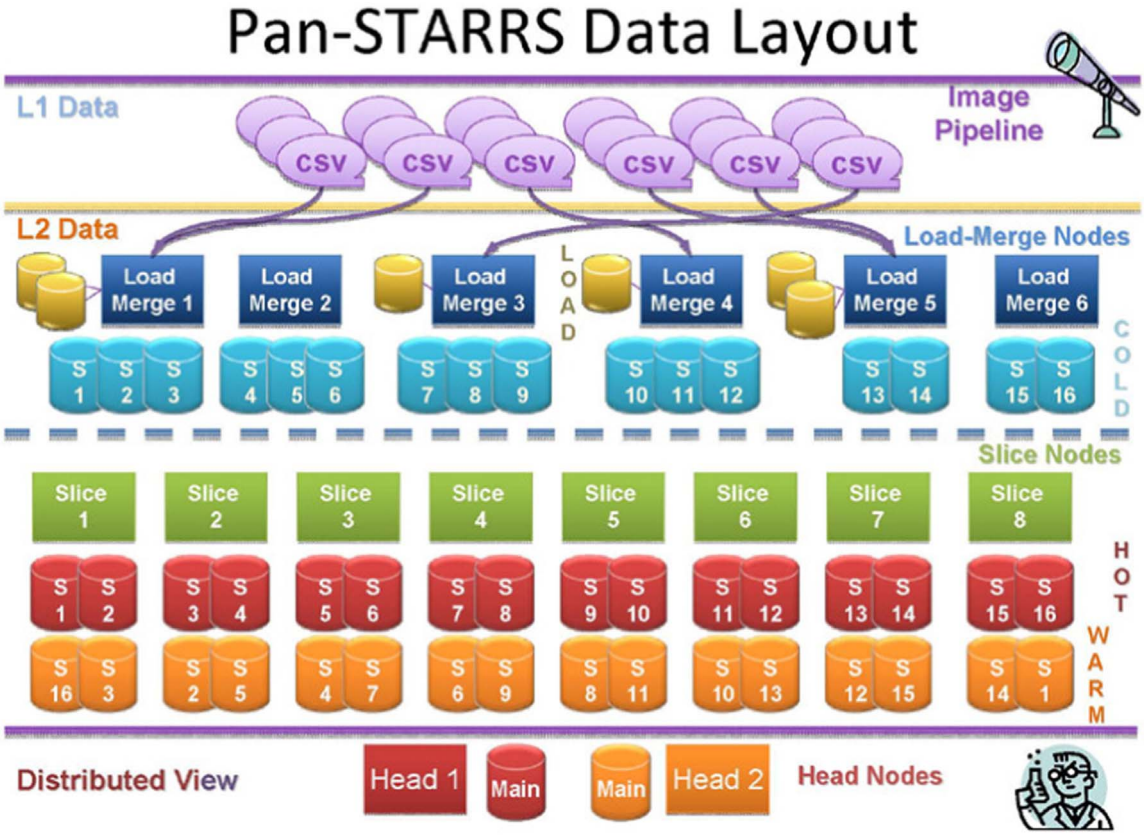

Figure 4. This shows how the data (L1 data/csv files/Image Pipeline) is loaded into L2 data (the load merge machines—responsible for loading the data and merging it into the "cold" part of the database. In this figure, there are eight slice machines that hold hot and warm copies of the database. At the bottom is the head nodes and the main database. The hot database serves the fast response queue, and the warm database serves the slow queue. The fast queue is specifically for queries that take less than one minute to complete. The cold database is never accessible by users.

combining the distributed slices. This aspect of the database design is intended to be transparent to the user, but power users may find it useful to know how the slices are subdivided. The dividing decl. cuts are defined to ensure each slice contains a similar amount of data, with the constraint that no slice spans less than a full camera footprint (3.″3) due to the loading implementation. Partition slices are customized for each database version (e.g., 3π DR1, DR2 versus MD). Figure 4 shows how the data is partitioned across a subset of the machines. For the 3π Survey, the PSPS database is partitioned into 32 slices. Table 3 lists the names of the slices and the decl. ranges for each slice for the 3π Survey.

6.2. Loading Data into PSPS

The process of loading data into the PSPS is split into several stages in order to manage the large data volume, to ensure data integrity, and to allow portions of the database to be exposed to internal users for testing while loading proceeds. A top-level outline of the process is as follows. First, the PSPS DXLayer retrieves the batch files, generated by the IPPTOPSPS system, from the IPP datastore interface. These batch files are loaded into an initial set of database machines (the Load/Merge Nodes; see Figure 4). As batches are loaded, they populate a temporary set of tables, which grows as more batches are added. When enough batches have been loaded, these temporary tables are merged into the corresponding tables in the first instance of the PSPS database. This initial instance, called the Cold database, naturally changes on a regular basis as more data are added. When the PSPS team is ready to expose the database to end users, the Cold database is copied to one of the two database instances exposed to end users. In this period, the database, which is the target of the copy, cannot be queried, but users may continue to query the other database while the copy proceeds. When the copy is complete, the newly copied version is "flipped" with the active query database, and a second copy is performed. Now the end users are able to query the updated database while the second copy is made. After the copies are completed, one of the two user-end databases is used for short-lived queries (the Hot database), while the other is used for long-running queries (the Warm database). Below, we discuss in more detail the PSPS components involved in various loading stages as well as those used for the user query operations.

6.3. The Data Transformation Layer (DXLayer)

The DXLayer is the first stage in the PSPS to receive data from IPPTOPSPS. This stage polls the IPP datastore interface for new batches to load and prepares them for the next step (ODM). Figure 5 shows the flowchart of the DXLayer process, and Figure 6 shows a more detailed flowchart of how batches are loaded and verified within the DXLayer and ODM. Figure 7 illustrates the merge of the batches and the flip between Warm and Cold databases. PSPS loads batches created by the IPPTOPSPS (Section 5.3). Batches contain a manifest file that describes the batch information such as type of batch, min/max *objID*, MD5 checksum, and the tables to load. Batch data

Table 3
PSPS Decl. Slice Boundaries

Slice Name	Min Decl.	Max Decl.
Slice 1	−54.82	−28.68
Slice 2	−28.68	−26.41
Slice 3	−26.41	−24.12
Slice 4	−24.12	−21.88
Slice 5	−21.88	−19.55
Slice 6	−19.55	−17.20
Slice 7	−17.20	−14.78
Slice 8	−14.78	−12.24
Slice 9	−12.24	−9.64
Slice 10	−9.64	−7.00
Slice 11	−7.00	−4.29
Slice 12	−4.29	−1.40
Slice 13	−1.40	+1.38
Slice 14	+1.38	+4.13
Slice 15	+4.13	+6.91
Slice 16	+6.91	+9.78
Slice 17	+9.78	+12.70
Slice 18	+12.70	+15.72
Slice 19	+15.72	+18.79
Slice 20	+18.79	+21.93
Slice 21	+21.93	+25.24
Slice 22	+25.24	+28.59
Slice 23	+28.59	+31.95
Slice 24	+31.95	+35.44
Slice 25	+35.44	+38.98
Slice 26	+38.98	+42.73
Slice 27	+42.73	+46.73
Slice 28	+46.73	+50.90
Slice 29	+50.90	+55.41
Slice 30	+55.41	+60.62
Slice 31	+60.62	+67.83
Slice 32	+67.83	+89.99

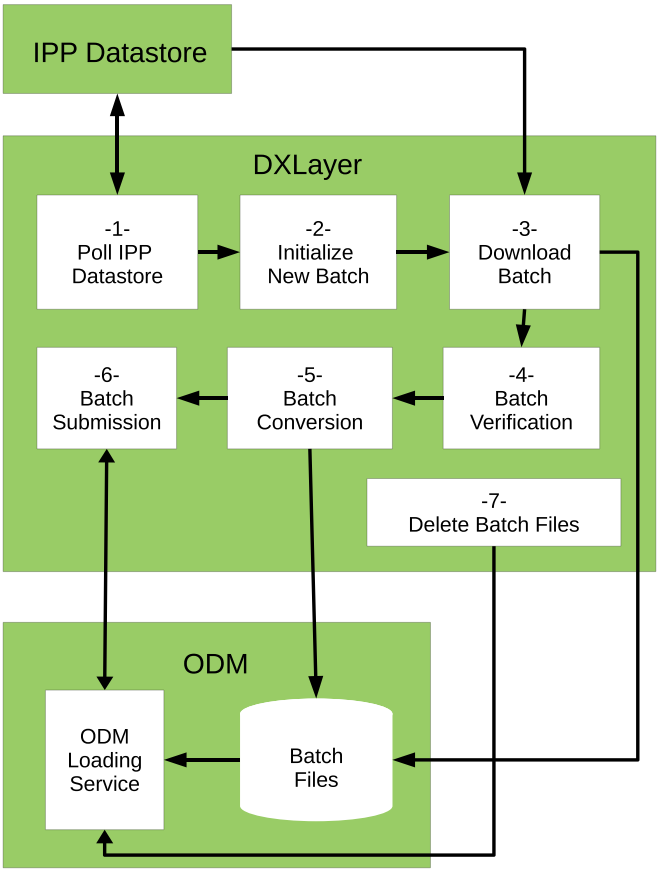

Figure 5. A flowchart of the DXLayer process, showing how batches are loaded into the DXLayer, verified, and submitted to the ODM. The shaded rectangles refer to different systems, and the white boxes and white cylinder refer to difference steps for the systems.

are stored in FITS files, which are transformed into comma-separated value (CSV) files in the DXLayer. As noted above, the batch area cannot exceed two PSPS slices or it will fail to load. The PSPS slices are constructed so that this does not happen.

6.4. The Object Data Manager (ODM)

The ODM is the software system that oversees the steps of the loading process described above. The nodes within the ODM have naming conventions for their roles: load/merge (lm), slice (s), head (h), and admin (a). The ODM processes represent each of the steps described above: load, merge, copy, flip. All logs, processes, and requests are inserted into an administration database called the Workflow Manager Database (WMD). Databases are named by the roles defined above: Load, Cold, Warm, Hot. These databases use the MS-SQL Server engine and are divided into four volumes with 96 file partitions each. While the large data tables are distributed across multiple "slice" machines, the smaller tables (the metadata tables, *ObjectThin*, *GaiaFrameCoordinate*, and *StackObjectThin*) are stored on a single "head" machine for faster queries.

6.5. The Data Retrieval Layer (DRL)

The DRL is the layer between the user and the PSPS database. The DRL is responsible for management of queries that the user submits via the DRL API. The DRL is based on CasJobs (Szalay et al. 2007) and has many similar features. It primarily keeps track of all user queries and provides progress updates of those queries in a secure way. It also kills queries that use too many resources or take too long. The DRL API is accessed via the Simple Object Access Protocol (SOAP; w3.org/TR/soap), allowing users multiple ways to access the database. Before the public releases, Pan-STARRS science consortium members used the Published Science Interface (PSI, a web-based user interface) initially based at the IfA and later at STScI. For the general public, the MAST server provides access via the CasJobs interface (https://mastweb.stsci.edu/ps1casjobs/), as well as a simple object search form which implements a basic cone search (https://catalogs.mast.stsci.edu/panstarrs). It is also possible for the consortium users to query the database via SOAP calls from command line scripts.

6.6. Published Science Interface (PSI)

The PSI is the web user interface provided to the Pan-STARRS Science Consortium members. This interface provides many useful features including a query request page, information on query progress, MyDB management tools, graphing tools, access to the pixel data products, and interactive help. The query request page allows the user to easily submit queries to a variety of databases (3pi/MD/MyDB), to upload query files or to check the syntax, to name MyDB results tables, and to select the queue to submit to. The MyDB management tools allow the user to

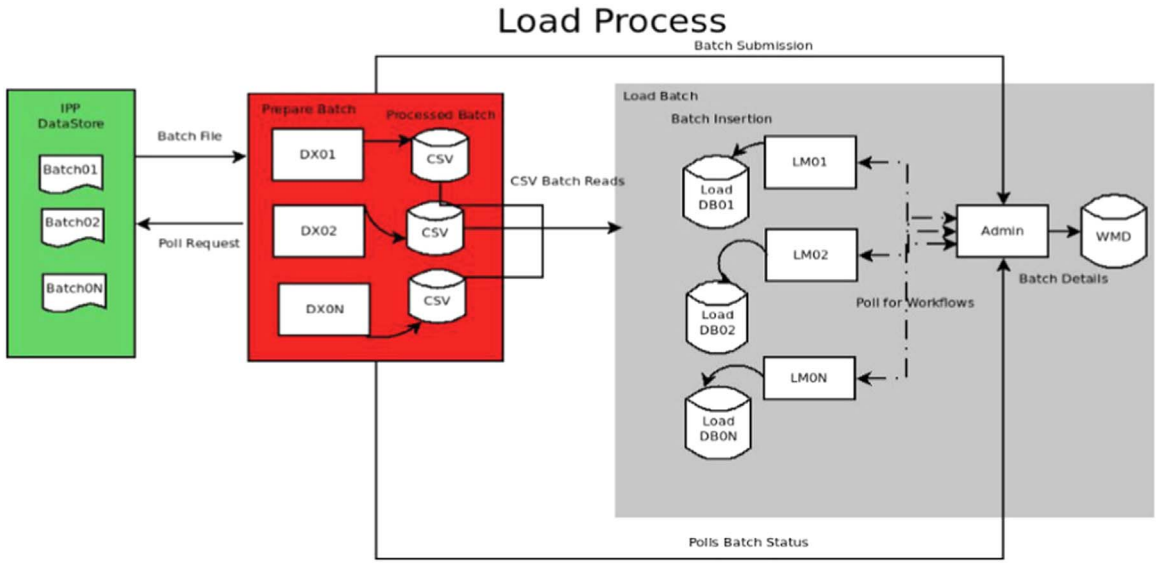

Figure 6. A flowchart of loading data from *IppToPsps*/IPP as batches into the DXLayer and ODM.

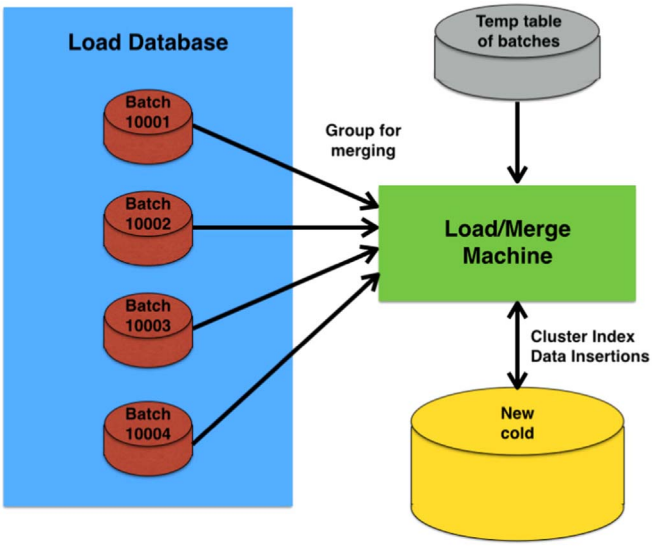

Figure 7. Flowchart showing how data from IPP/*IppToPsps* batches are loaded into the system and then merged into a new cold database.

easily select which MyDB tables to purge as well as well as methods to extract to CSV, FITS, or XML files to download. Some of the interactive features include an interactive schema browser, a query builder to easily create a query with multiple joins and conditions, and a flag generator to create bitmasks for the different types of flag tables.

7. Overview of the PSPS Database Schema

Table 1 lists the 51 different database tables that make up the PSPS schema. Here we give a brief overview of the tables and indexes to help aid the user in selecting the most appropriate table for queries.

The database has a unique *objID* for each object detected within Pan-STARRS1 data. An object that has measurable flux at a given R.A. and decl. is defined to be a source. In general, multiple detections of an object will all share the same *objID*, as well as multiple detections within 1″ of that object (which might not be physically associated with that object, e.g., blended sources). A detailed description of the source deblending algorithm and its properties is beyond the scope of this work (see Paper IV). This *objID* is the core index used to join the object and detection tables in order to select detections associated with a given object. For example, *ObjectThin* has the astrometric information for the objects; one would join against the *Detection* table, using *objID*, in order to get the individual photometric attributes for all the detections of that object within the single exposures (at a given R.A. and decl.).

The index *objID* (and *diffObjID* for difference tables) is derived from R.A. and decl. While it is possible to calculate the R.A. and decl. from the *objID*, this is not recommended. The *objID* value is determined when an object is initially instantiated in the DVO database and is based on the initial astrometric solutions from individual exposures and STACKS as they are ingested into the DVO database. These values are not calibrated against 2MASS or Gaia, nor are they authoritative. Because DR1 and DR2 use the same initial DVO database ingestion, the *objID* values are the same for the same object between the two releases. Included below is the C code for the translation between R.A. and decl. See also Figure 8.

```
uint64_t CreatePSPSObjectID(double ra,
double dec) {
    double zh = 0.0083333;
    double zid = (dec + 90.)/zh;
    // zid : 0-180*60*2 = 21600 (<15 bits)
    int izone = (int) floor(zid);
    double zresid = zid - (float) izone;
    // zresid : 0.0-1.0
    uint64_t part1, part2, part3;
    part1 = (uint64_t)
(izone*10000000000000LL);
    part2 = ((uint64_t)
(ra*1000000.))*10000;
    // part2 : 0-360*1e6 = 3.6e8 (<29 bits)
    part3 = (int) (zresid*10000.0);
    // part3 : 0-10000
    // (1 bit == 30/10000") (<14 bits)
    return part1 + part2 + part3;
  }
```

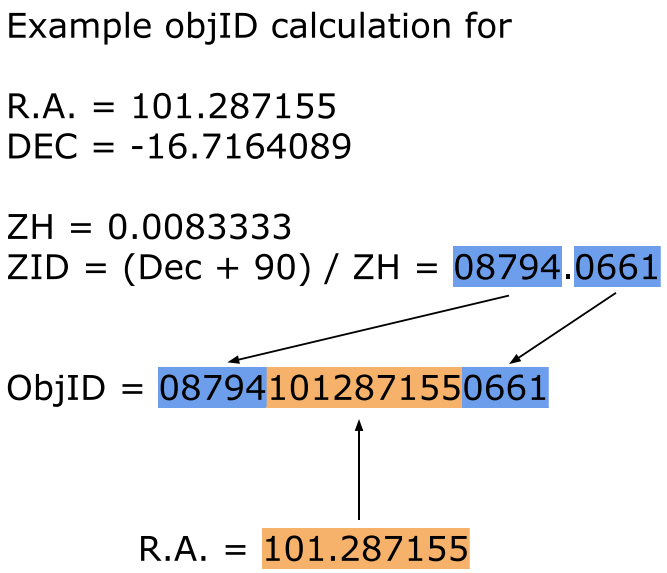

Figure 8. Graphical description of how `objID` is calculated from RA and decl. It is not recommended to derive the RA and decl. from `objID` as this will result in an inaccurate RA and decl. `ObjID` is assigned when the stack/skycal cmfs are ingested into the database and are not yet calibrated against 2MASS and Gaia. OBJID is primarily used for indexing the database.

7.1. The Main Categories of Tables

There are four main types of tables within the PSPS database: *Fundamental Data Product* tables can be categorized into either *Object* tables (Section 7.3) or *Detection* tables (Section 7.4). *Object* tables contain summary information for each source in the sky, including the mean photometric and astrometric information. *Detection* tables contain photometric and astrometric measurements from individual exposures (*Detection*), stacked images (*Stack** tables), warp images (*forcedWarp** tables), or difference images. The description of the *Detection* tables below is organized by these processing stages (see also Section 5.1). *Observational Metadata* tables (Section 7.4) contain information about the individual exposures and other image types and provide links to map from images to measurements. *Derived Data Products* (e.g., photo-z measurements) will be incorporated into the PSPS database in the future and are not described in this paper. *System Metadata* tables (Section 7.2) contain hardwired information about the PSPS, including tables describing flags, filters, tessellations and other fixed system-level quantities.

7.2. System Metadata Tables

The system metadata tables primarily contain static information of flags, filters, surveys and other information that is specific to Pan-STARRS1. Several tables describe the different flag bits used to indicate data quality or to identify details of how a measurement was made. These tables are described in Section 7.2.1. The other system metadata tables are described below:

Filter: Provides database indexes for the optical filters used in the survey (Tonry et al. 2012). Filters (g_{P1}, r_{P1}, i_{P1}, z_{P1}, y_{P1}) are assigned integer values from 1 to 5 (*filterID*).

FitModel: Provides database indexes for models used in fitting detections in images, both PSF-like and extended galaxy models including exponential, de Vaucouleurs (1948), and Sérsic (1963) profiles. Describes the values for column *psfModelID* (located in various tables).

Survey: Provides database indexes for the various PS1 Science Consortium Surveys. The 3π *SurveyID* is 0.

PhotoCal: Contains photometric calibration information for each filter and detector image combinations. Defines the values of *photoCalID* within *ImageMeta*, *StackMeta*, *ForcedWarpMeta*, and *DiffMeta*.

StackType: Provides database indexes for the types of stacked images constructed. For 3π, all STACKS are `DEEP_STACK`.

DiffType: Provides database indexes for the types of difference images constructed. For 3π, all DIFFS are `WARP_STACK`, meaning they are constructed by subtracting warps from single exposures from the deep stacks for the corresponding part of sky.

TessellationType: Provides database indexes for the types of image tessellations for the sky. For 3π, this is `RINGS.V3`. Each MD field has its own *TessellationType* (`MD01.V3`, `MD02.V3`, etc.). The RINGS.V3 Tessellations are described in more detail in Magnier et al. (2020a), and the MD tessellations in M. Huber et al. (2020, in preparation).

Table 4
Flag Types within Pan-STARRS1

Flag Type	Size	See in this Paper
ObjectInfoFlags	INT	Table D1
ObjectQualityFlags	SMALLINT	Table D2
ObjectFilterFlags	INT	Table D3
ImageFlags	INT	Table D4
ForcedGalaxyShapeFlags	SMALLINT	Table D5
Detection	BIGINT	Table D6
Detection2	INT	Table D7
Detection3	INT	Table D8

7.2.1. Flag Tables

There are 45 flag columns within the Pan-STARRS1 database schema (e.g., Detection.infoFlag) and eight different types of flags listed below (see Table 4). These flag columns use integer values to represent, e.g., different outcomes of the detection analysis. The eight different types of flags specify the meaning of the bit values for the flag columns. This section gives a brief overview of the eight different types of flags. Table 5 lists the flag columns in each of the PSPS tables and identifies the flag type for that column. Tables D1–D8 list the bit values for each of the flag types. These tables are intended to be used as a reference to select the appropriate flag information tables.

ObjectInfoFlags: These flags specify characteristics of the *object* determined during the photometric and astrometric analysis, or by external analysis or publications. For example, several bits specify if the object has been identified as a QSO, variable, transient, or a known solar system object, if it has large proper motions, if it is extended, and the source of the average position information.

ObjectQualityFlags: Contains information flag values that denote if an object is real or a possible false positive. This is a subset of flags from *ObjectInfoFlags*, specifically the ones if the object is extended, has good measurements in individual exposures, and has good measurements in the stacks. This

Table 5
Flag Columns within Pan-STARRS1

Table Name	Flag Column	Size	Flag Type
ObjectThin	objectInfoFlag	INT	ObjectInfoFlags
ObjectThin	qualityFlag	SMALLINT	ObjectQualityFlags
GaiaFrameCoordinate	gaiaFlag	INT	ObjectInfoFlags
MeanObject	(grizy)Flags	INT	ObjectFilterFlags
ForcedMeanObject	(grizy)Flags	INT	ObjectInfoFlags
DiffDetObject	objectInfoFlag	INT	ObjectInfoFlags
DiffDetObject	qualityFlag	SMALLINT	ObjectQualityFlags
ImageMeta	qaFlags	INT	ImageFlags
ForcedGalaxyShape	(grizy)GalFlags	SMALLINT	ForcedGalaxyShapeFlags
Detection	infoFlag	BIGINT	DetectionFlags
Detection	infoFlag2	INT	DetectionFlags2
Detection	infoFlag3	INT	DetectionFlags3
StackObjectThin	(grizy)infoFlag	BIGINT	DetectionFlags
StackObjectThin	(grizy)infoFlag2	INT	DetectionFlags2
StackObjectThin	(grizy)infoFlag3	INT	DetectionFlags3
DiffDetection	DinfoFlag	BIGINT	DetectionFlags
DiffDetection	DinfoFlag2	INT	DetectionFlags2
DiffDetection	DinfoFlag3	INT	DetectionFlags3
ForcedWarpMeasurement	FinfoFlag	BIGINT	DetectionFlags
ForcedWarpMeasurement	FinfoFlag2	INT	DetectionFlags2
ForcedWarpMeasurement	FinfoFlag3	INT	DetectionFlags3

describes the flags used in *ObjectThin*.qualityFlag and *DiffDetObject*.qualityFlag.

ObjectFilterFlags: These flags specify the quality of the photometric calibration for the object and are specified for each of the five filters. More detail about the meaning of these flag bits can be found in Paper V.

ImageFlags: Primarily denotes the quality of the photometric and astrometric calibration of the chip image (e.g., whether the image is bad or if there are too few measurements).

ForcedGalaxyShapeFlags: Contains information flag values that define ForcedGalaxyShape chi-squared surface fit failures.

DetectionFlags: These flag bits are generated in the pixel-level source analysis software and include information about the quality of the detection. Bits include, e.g., if the detection is blended, used for the PSF model, saturated, and many other types of defects, as well as information on types of magnitudes calculated, if it is extended, and fit information. See also Paper IV.

DetectionFlags2: Like the previous set of flags, these flags contain information about the pixel-level analysis of the detection. These bits include information specific to difference imaging, as well as quality issues such as if source is near diffraction spikes, star core, affected by the "burntool" analysis of persistence features (see Paper III), along with other analysis issues. See also Paper IV.

DetectionFlags3: These flag bits are generated by the photometric and astrometric calibration analysis. They include bits to specify, e.g., if the detection was used in the analysis of the mean astrometric or photometric properties of the object.

7.3. Object-type Tables

The object-type tables originate from the DVO database, specifically, the DVO tables that have information about objects, their mean astrometric and photometric properties, and information such as the number of detections per objects and other statistics and information. The object-type tables form the equivalent of a telephone book for all of the objects, with *objID* being the equivalent of the phone number or social security number. A key defining feature is that *objID* is unique in these object-type tables; there are no instances of two objects with the same *objID* in the same object-type table. If an object is not in these tables, it has not been detected in any of the stages of processing. Tables D9–D11 list the contents of the object-type tables. What follows is a description of each of the object-type tables, for DR1 and beyond.

ObjectThin: Contains the positional information for objects in a number of coordinate systems. The objects associate single-epoch detections and the stacked detections within a one arcsecond radius. The mean position from all the available single-epoch data is used as the basis for coordinates when available, or the mean position over each filter of an object in the STACK when it is not. The R.A. and decl. for both the STACK and single-epoch mean are provided. The number of detections in each filter from single-epoch data is listed, along with which filters the object has a STACK detection (see Szalay et al. 2007). Use *objID* to join to most tables, *uniquePspsOBid* to join to *MeanObject*. For DR1 only, the Gaia-calibrated positions were calculated after *ObjectThin* was populated; they are provided in *GaiaFrameCoordinate*. For DR2 and beyond, there is no *GaiaFrameCoordinate* table, as *ObjectThin* has be recalibrated and has the Gaia-calibrated positions.

MeanObject: Contains the mean photometric information for objects based on the single-epoch data, calculated as described in Paper V. To be included in this table, an object must be bright enough to have been detected at least once in an individual exposure. PSF, Kron (1980), and total aperture-based magnitudes and statistics are listed for all filters in a single row. The apertures are defined to match (in arcseconds) those used by SDSS (see Table 7 in Stoughton et al. 2002). Use *objID* to join to most tables, *uniquePspsOBid* to join to *MeanObject*. Average values are determined using outlier rejection based on the iteratively reweighted least-squares technique in which measurements are averaged with weights determined by their individual errors combined with a

weighting factor depending on their deviation from the previously calculated average value (see Paper IV for a full description).

GaiaFrameCoordinate: This table, only available in DR1, contains PSPS objects recalibrated against Gaia DR1 astrometry. The coordinates in this table are the best ones to use for DR1. For the DR2 version of the database, the astrometry was recalibrated against Gaia DR1; the coordinates reported in the *ObjectThin* table should be used as the best R.A. and decl. Use *objID* to join to most tables.

7.4. Individual Exposure Detection-type Tables

The majority of the data in the database are in the form of detection-type tables. These are tables that are based on individual stages of processing from the IPP. Specifically, these are tables from the catalog outputs of the CAMERA, STACK, FORCED PHOTOMETRY, and DIFF stages of the IPP. Each of these categories of tables is described below.

Note that for these tables, if it has an *objID* column, *objID* will not necessarily be unique as each measurement of the same object on different images will have the same *objID*. If doing joins between tables from the same stage, use the appropriate *uniquePspsXXid*. For example, to join between *StackObjectThin* and *StackApFlx*, use *uniquePspsSTid*.

7.4.1. Tables Based on the "Camera" Stage of IPP

Images processed through the CAMERA stage of the IPP have been detrended and have had astrometry and photometry calculated. Basic information from the images are then merged into the DVO database. The core tables based on the CAMERA stage are *FrameMeta*, *ImageMeta*, *Detection*, and *ImageDetEffMeta*. The contents of these database tables are listed in Tables D12–D15. Each image ingested into the PSPS database has a unique *imageID*; this can be used to find out, via the *FrameMeta*, *ImageMeta*, and *ImageDetEffMeta* tables, information about each image such as the filter, R.A. and decl., exposure time, etc. All of the detections measured in the image are ingested into the Detection table, which also has the *imageID*, allowing for single detections to be traced back to the OTA on which it was imaged.

FrameMeta: Contains metadata related to an individual exposure. A *Frame* refers to the collection of all images obtained by the 60 OTA devices in the camera in a single exposure. The camera configuration, telescope pointing, observation time, and astrometric solution from the detector focal plane (L, M) to the sky (R.A., decl.) is provided.

ImageMeta: Contains metadata related to an individual OTA (chip) image that comprises a portion of the full exposure. The characterization of the image quality, the detrends applied, and the astrometric solution from the raw pixels (X, Y) to the detector focal plane (L, M) is provided.

Detection: Contains single-epoch photometry of individual detections from a single exposure. The identifiers connecting the detection back to the original image and to the object association are provided. PSF, aperture, and Kron (1980) photometry are included, along with sky and detector coordinate positions. Use *objID* to join to other tables with photometry/astrometry parameters. Note that *objID* is not unique.

ImageDetEffMeta: Contains the detection efficiency information for a given individual OTA image. Provides the number of recovered sources out of 500 injected fake source and statistics about the magnitudes of the recovered sources for a range of magnitude offsets.

7.4.2. Tables Based on the "Stack" Stage of IPP

There are 15 tables based on the STACK stage of processing. The contents of these database tables are listed in Tables D16–D29. Several groups of these tables share a common schema, but are based on different convolutions of the stack images or use different extended source models. The basic table is *StackObjectThin*, which contains the positional and photometric information for point-source photometry of stack detections. The other stack tables provide additional measurements for the objects listed in *StackObjectThin*. There are several stack metadata tables, they are *StackMeta*, *StackToImage*, *StackToFrame*, and *StackDetEffMeta*. They provide general information about the stack and can be used to find out the exposures used in the stack.

Joins between any of the stack tables, except for the stack meta tables, should use *uniquePspsSTID*.

Due to overlaps in the stack tessellations, an object may appear in multiple stack images. As neighboring stack images contain nearly the same input exposures, these measurements are not statistically independent. Only one set of such measurements should be used for valid population statistics. To aid in such analysis, we define a "primary" detection for all stack measurements (from a single filter) of the same astronomical object. The "primary" detection is that detection for which the stack pixels are closest to the center of the skycell. Because the definition is purely geometric, in theory no portion of the sky can contribute more than a single stack detection. In practice, the photometric analysis of sources will occasionally split a source into multiple detections within the image. For the primary skycells, these detections will each be identified as "primary," though they come from the same astrophysical object. However, this is due to the analysis process, not the overlap of the stack boundaries.

Although the primary and secondary detections in general are derived from the same input pixels, differences can occur. It is possible that the primary detection of an object (for a particular filter) is actually more heavily masked than any secondary detections of the same object. Users who prefer a high-quality measurement of a particular object may choose to use these secondary measurements rather than the primary. We attempt to identify the "best" stack measurement for each filter by examining the signal-to-noise ratio of the measurements and the `PSF_QF_PERFECT` values, a measurement of the masked fraction for the object (see Paper IV for details of the parameter).

If the primary detection has `PSF_QF_PERFECT` > 0.95, then it is marked as the best. If multiple such measurements exist for the object, the highest signal-to-noise measurements are used. If not, but a secondary detection has `PSF_QF_PERFECT` > 0.95, then the secondary detection with the highest signal-to-noise ratio is chosen as best. If neither primary nor secondaries have `PSF_QF_PERFECT` > 0.95, the primary measurement with the highest `PSF_QF_PERFECT` is selected as the best. Finally, if no primary detection exists, the secondary with the highest `PSF_QF_PERFECT` is selected as the best.

Stack measurements that are the primary measurement have the `STACK_PRIMARY` bit set in the *StackObjectThin.*

XinfoFlag3 field for the appropriate filter while stack measurements that are identified as the "best" measurement for an object within a given filter have the STACK_PHOT_SRC bit set in the same field (see Tables D8 and D17).

If all of the "best" measurements for a stack object (across all five filters) are also primary measurements, then the BEST_STACK bit is set in the *ObjectThin.objInfoFlag* entry for the corresponding object (see Tables D1 and D9).

Several bits in the *StackObjectThin.XinfoFlag4* field for each filter may be set based on the "primary" and "best" detections (see Tables D8 and D17). If a "primary" measurement exists for a given filter, then the SECF_STACK_PRIMARY bit is set for that filter. If multiple primary stack measurements exist for a given filter, then the SECF_STACK_PRIMARY_MULTIPLE bit is also set for that filter (not set in DR1). If the "best" measurement for a filter is a significant detection (not forced from another band), then the SECF_STACK_BESTDET bit is set. If any of the "primary" measurements for a filter is a significant detection (not forced from another band), then the SECF_STACK_PRIMDET bit is set. If any stack measurements exist for a given filter, then the per-filter bit flag SECF_HAS_PS1_STACK is set.

Users should note that the fields *StackObjectThin.primaryDetection* and *StackObjectThin.bestDetection* are incorrectly set for DR1 and DR2. A coding error resulted in these bits being set based on the wrong input fields. A future update to the tables may be performed to repair these two fields.

StackObjectThin: Contains the positional and magnitude information for PSF, Kron (1980), and total aperture-based measurements of stack detections. The information for all filters are joined into a single row, with metadata indicating if this stack object represents the primary detection. In addition, a detection is flagged as "best" if it is a primary detection with a *psfQf* value greater than 0.98; if that condition is not met, then the primary or secondary detection with the highest *psfQf* value is flagged as best (see Paper V).

StackObjectAttributes: Contains the PSF, Kron (1980), and total aperture-based fluxes for all filters in a single row, along with point-source object shape parameters. Because the photometry for an object that is not detected in some filters is forced in those filters, some fluxes may have negative values. The magnitudes in *StackObjectThin* are derived from this table, where the flux is positive.

StackApFlx: Contains the fluxes within the SDSS R5 ($r = 3\farcs00$), R6 ($r = 4\farcs63$), and R7 ($r = 7\farcs43$) apertures (Stoughton et al. 2002) as measured on the raw (unconvolved) stack images. Fluxes within these same apertures are also provided for images convolved to 6 sky pixels ($1\farcs5$) and 8 sky pixels ($2\farcs0$). See Section 5.1.4 for further information. All filters are matched into a single row. These values are measured for all objects in all stacks.

StackModelFitExp: Contains the exponential galaxy model fit parameters (see Section 5.1.5 for constraints). All filters are matched into a single row.

StackModelFitDeV: Contains the de Vaucouleurs (1948) fit parameters (see Section 5.1.5 for constraints). All filters are matched into a single row.

StackModelFitSer: Contains the Sérsic (1963) fit parameters (see Section 5.1.5 for constraints). All filters are matched into a single row.

StackApFlxExGalUnc: Contains the fluxes within the nine SDSS apertures (see Section 5.1.4) as measured on the unconvolved stacks. All filters are matched into a single row.

StackApFlxExGalCon6: Contains the fluxes within the nine SDSS aperture (see Section 5.1.4) images convolved to a target of 6 sky pixels ($1\farcs5$). All filters are matched into a single row.

StackApFlxExGalCon8: Contains the fluxes within the nine SDSS aperture (see Section 5.1.4) images convolved to a target of 8 sky pixels ($2\farcs0$). All filters are matched into a single row.

StackPetrosian: Contains the Petrosian (1976) magnitudes and radii (see Section 5.1.5 for constraints). All filters are matched into a single row.

StackMeta: Contains the metadata describing the stacked image produced from the combination of a set of single-epoch exposures. The nature of the stack is given by the *StackTypeID*. The astrometric and photometric calibration of the stacked image are listed.

StackToImage: Contains the mapping of which input images were used to construct a particular stack.

StackToFrame: Contains the mapping of input frames used to construct a particular stack along with processing statistics.

StackDetEffMeta: Contains the detection efficiency information for a given stacked image. Provides the number of recovered sources out of 500 injected sources for each magnitude bin and statistics about the magnitudes of the recovered sources for a range of magnitude offsets.

7.4.3. Tables from the "Forced Photometry" Stage of IPP

The following tables contain information related to the FORCED WARP analysis stage. Joins between *ForcedWarpMeasurement*, *ForcedWarpMasked*, *ForcedWarpExtended*, and *ForcedWarpLensing* should use uniquePspsFWid. The contents of these database tables are listed in Tables D30–D38.

ForcedMeanObject: Contains the mean of single-epoch photometric information for sources detected in the stacked data, calculated as described in Paper IV. The mean is calculated for detections associated with objects within a $1''$ correlation radius. PSF, Kron (1980), and SDSS (Stoughton et al. 2002) aperture R5 ($r = 3\farcs00$), R6 ($r = 4\farcs63$), and R7 ($r = 7\farcs43$) total aperture-based magnitudes and statistics are listed for all filters. See also Paper IV. Use *objID* to join to most tables, and use *uniquePspsFOid* to join to *ForcedMeanLensing*. *objID* is not unique, but *uniquePspsFOid* is.

ForcedMeanLensing: Contains the mean Kaiser et al. (1995) lensing parameters measured from the forced photometry of objects detected in stacked images on the individual single-epoch data. Use *objID* to join to most tables; use *uniquePspsFOid* to join to *ForcedMeanObject*. *objID* is not unique, but *uniquePspsFOid* is.

ForcedGalaxyShape: Contains the extended source galaxy shape parameters. The positions, magnitudes, fluxes, and Sérsic indices are inherited from their parent measurement in the *StackModelFit* tables and are reproduced here for convenience. The major and minor axes and orientation are recalculated on a warp-by-warp basis from the best fit given these inherited properties (Sérsic 1963). Use *objID* to join to most tables. *objID* is not unique, but *uniquePspsFGid* is.

ForcedWarpMeta: Contains the metadata related to a sky-aligned distortion-corrected WARP image, upon which forced photometry is performed. The astrometric and photometric calibration of the WARP image are listed.

Table 6
Coordinate Fields in PSPS

PSPS Table	Column Names		Comments
FrameMeta	raBore	decBore	R.A./decl. of telescope boresite
ObjectThin	raMean	decMean	mean R.A. and decl. from single exposure, calibrated against 2MASS
ObjectThin	raStack	decStack	mean R.A. and decl. calculated from STACK skycells
Detection	R.A.	decl.	R.A. and decl. for single exposure detections
StackObjectThin	(grizy)ra	(grizy)dec	R.A. and decl. calculated from individual STACK skycells
DiffDetection	R.A.	decl.	R.A. and decl. for single DIFF exposure detections
DiffDetObject	R.A.	decl.	similar to raMean/decMean, calculated for DIFF objects
GaiaFrameCoordinate	R.A.	decl.	best R.A. and decl., recalibrated to Gaia (DR1 only).

ForcedWarpMeasurement: Contains single-epoch forced photometry of individual measurements for each warp image. The identifiers connecting the measurement back to the original exposure and to the object association are provided. PSF, Kron (1980), and total aperture-based fluxes are provided, along with positions in both sky and detector coordinates.

ForcedWarpMasked: Contains an entry for objects detected in the stacked images which were in the footprint of a single-epoch exposure, but for which there are no unmasked warp pixels at that epoch.

ForcedWarpExtended: Contains the single-epoch forced photometry fluxes within the SDSS R5 ($r = 3\farcs00$), R6 ($r = 4\farcs63$), and R7 ($r = 7\farcs43$) apertures (Stoughton et al. 2002) for objects detected in the stacked images.

ForcedWarpLensing: Contains the Kaiser et al. (1995) lensing parameters measured from the forced photometry of objects detected in stacked images on the individual single-epoch data.

ForcedWarpToImage: Contains the mapping of which input image comprises a particular WARP image used for forced photometry.

7.4.4. Tables Based on the "Diff" Stage of IPP

The tables described below relate to the difference image processing. The contents of these database tables are listed in Tables D39–D43. Each DIFF image has a unique *diffImageId*, and all four DIFF tables use this to join to each other.

DiffDetObject: Contains the positional information for difference detection objects in a number of coordinate systems. The objects associate difference detections within a $1''$ radius. The number of detections in each filter is listed, along with maximum coverage fractions (see Szalay et al. 2007). Use *diffObjID* to join to most diff tables. *diffObjID* and *uniquePspsDOid* are unique for *DiffDetObject*. Note that *diffObjID* and *objID* will be similar, but not identical, and it will not be easy to join to non-diff tables. We recommend comparing the R.A. and decl. for objects between Diff* and non-diff tables.

DiffMeta: Contains metadata related to a difference image constructed by subtracting a stacked image from a single-epoch image, or in the case of the MD Survey, from a nightly STACK (stack made from all exposures in a single filter in a single night). The astrometric calibration of the reference STACK is listed.

DiffDetection: Contains the photometry of individual detections from a difference image. The identifiers connecting the detection back to the difference image and to the object association are provided. PSF, aperture, and Kron (1980) photometry are included, along with sky and detector coordinate positions.

DiffToImage: Contains the mapping of which input images were used to construct a particular difference image.

DiffDetEffMeta: Contains the detection efficiency information for a given individual difference image. Provides the number of recovered sources out of 500 injected sources and statistics about the magnitudes of the recovered sources for a range of magnitude offsets.

7.5. Which R.A. and Decl. to Use?

Multiple tables contain columns that provide a measurement or representation of the R.A. and decl. This section gives information on each so that the user can choose the appropriate R.A. and decl. version to use. A summary of these tables is provided in Table 6. Generally, if the user is not interested in proper motion or moving objects, it is best to use coordinates from *GaiaFrameCoordinate* if using DR1, as this is the weighted mean R.A. and decl. (similar to *ObjectThin*), but tied to the Gaia system. This information is in a separate table and not part of *ObjectThin* because the mean properties were calculated and ingested into PSPS prior to Gaia's DR1. *ObjectThin*'s *raMean* and *decMean* are calibrated against 2MASS and thus degraded compared to Gaia. The 2MASS reference system is consistent with the ICRS to within 15 mas, but the scatter for even bright sources is ≈100 mas (Skrutskie et al. 2006).

For DR2, there is no *GaiaFrameCoordinate* table, as DR2's *ObjectThin* table is already calibrated to Gaia. The best R.A. and decl. to use for most cases are ObjectThin's *raMean* and *decMean*. If the proper motion is high, or the object is moving, and the user is interested in the single-epoch photometry, they should use *ra* and *dec* in the *Detection* table.

7.6. Indexes and Joins

There are multiple columns within the schema that are indexed and designed to be used to join tables together. Generally, if a column name ends in "*ID*," it is designed to be joined to other tables, either to system metadata tables (examples include *filterID*, *surveyID*, *ccdID*) or to fundamental data tables (for example, *objID*, *diffObjID*, *uniquePspsSTid*). There are a few exceptions: *randomID* and *random(stage)ID* should not be used for joins, the contents of each are random numbers to aid the user in selecting repeatable random subsets of data. Also, some of the *uniquePspsXXIds* are only present in one table; they are used to provide unique IDs for each stage of processing but some stages (*DiffDetObject*, for example) only have one corresponding table and therefore nothing to join to.

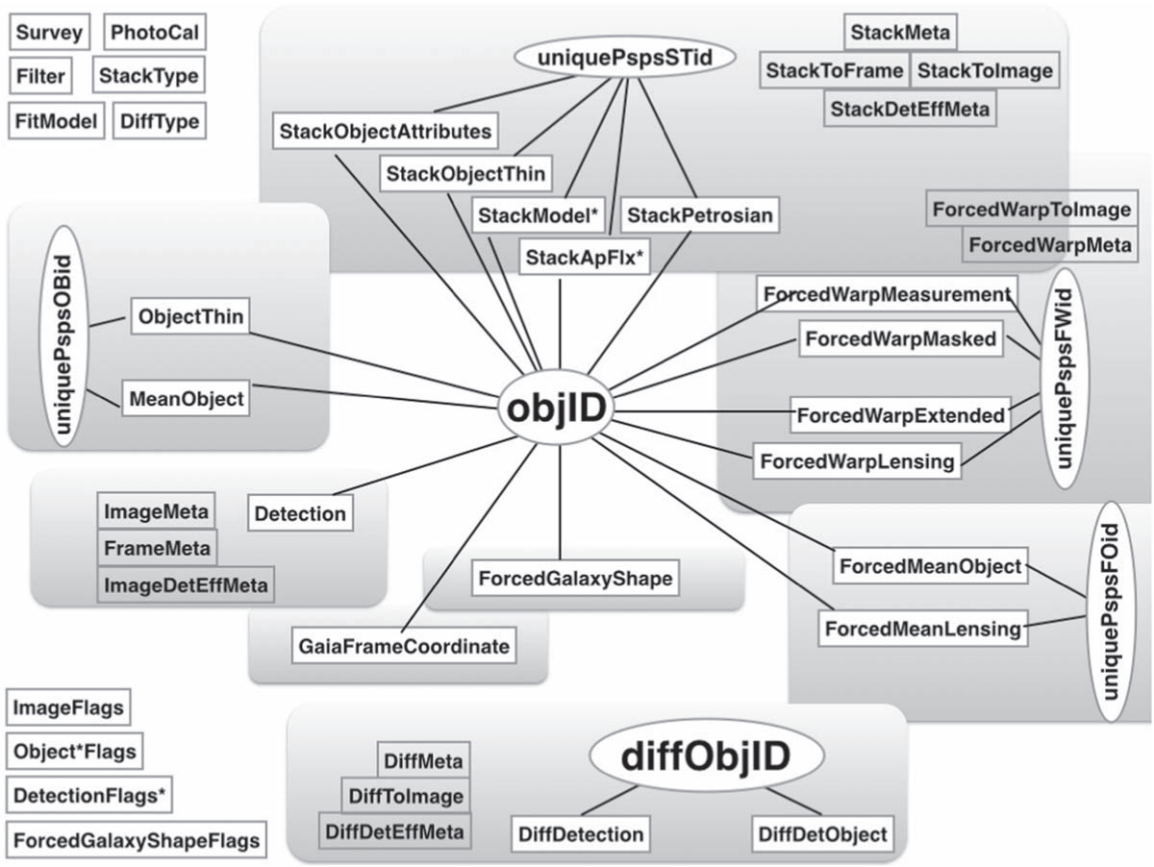

Figure 9. A summary of how the different tables are related. The rectangular boxes with words inside represent the different table names. The ovals with words inside represent the column names to use to join the tables. Black lines connect table names to columns (i.e., *Detection* has a line to `ObjID`, which has a line to *StackObjectThin*)—this shows that *Detection* can be joined to *StackObjectThin* using `ObjID`aq. The gray rounded boxes represent different stages of data processing, which corresponds to different stages of loading into the database. Tables within the gray boxes are related; connections to the (gray) metadata tables are shown in Figure 9. The tables that are not in gray rounded boxes represent system metadata, metadata that describes the Pan-STARRS1 system as well as flag information.

Figures 9 and 10 show graphical representations of how to join various tables. On these figures, the table names are boxed, while the columns to be used to join are in ovals. For the diagram with *objID* in the middle, it shows that any of the boxes connected to *objID* can be joined to each other using *objID*.

All tables with photometric or astrometric information involving different sources or objects have an index, called *objID*. *ObjID* is only unique for the object type of tables, and is loosely based on R.A. and decl.; see Section 7 for more information. It is possible to use the *objID* to get a rough estimate of the R.A. and decl., but this should not be used for the definitive R.A. and decl. Use *ObjectThin* to get the R.A. and decl. calibrated to 2MASS, and use *GaiaFrameCoordinate* (for DR1) or *ObjectThin*(for DR2)to get the R.A. and decl. calibrated to Gaia astrometry. When available and possible, if joining two tables and they both have the same column name like *uniquePspsXXId*, join those two tables using the *uniquePspsXXId*. See Table 7 to see the *uniquePsps* column name. *UniquePspsXXId* is designed to be unique; specifically for the cases when there are multiple detections that are sufficiently close by, they will have the same *objID* but different *uniquePspsXXId*s.

It is possible to join every detection, no matter what stage of processing it is from, back to the original exposure(s) and to the OTAs. Figure 10 shows how to do this. For each stage of processing, there is an associated (stage)imageID that is mapped back to the *imageID* via tables of the name `(stage)ToImage`. For example, if one wanted to find out which exposures contributed to a detection in *StackObjectThin*, they would join to *StackToImage* using the *stackImageID*. This allows the user to find data within the database as well as to find out the corresponding images to download from MAST.

7.7. NULLS as −999

The PSPS uses `−999` to denote `NULL` values, as PSPS is based off of CasJobs, which also does not use NULL. The justification for this is explained by Szalay et al. (2002; page 7): "We also insist that all fields are non-null. These integrity constraints are invaluable tools in detecting errors during loading and they aid tools that automatically navigate the database" (see also Gray et al. 2002). Because our own database design has in its roots many of the same parts as the SDSS database, we also adopt this convention of non-null fields.

7.8. Tables and Views

The PSPS has defined several views to aid the user in making database queries. A view is a virtual table that is based on the results from an SQL statement and looks like a table to the user. These views are constructed to aid the user, to alleviate the need for common joins, and to produce query

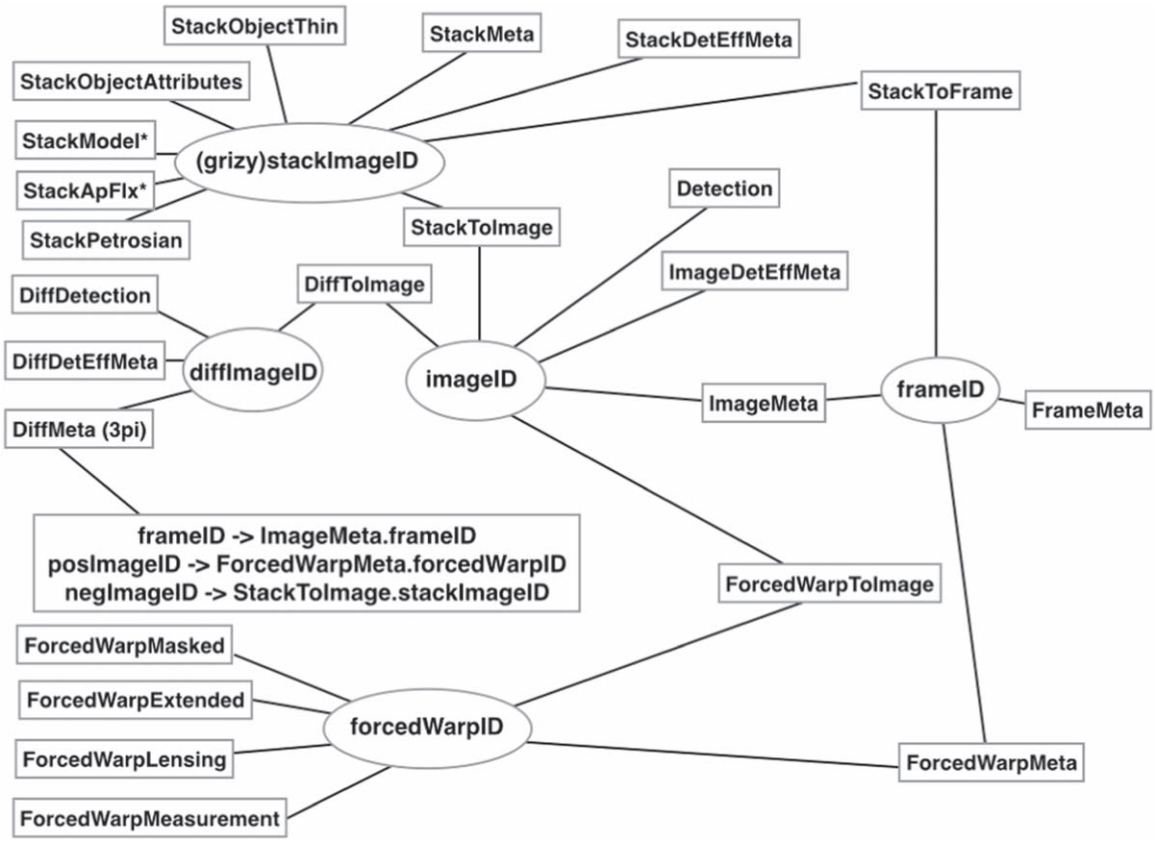

Figure 10. This diagram shows how to find the `imageID` and `frameID` from each of the different detection tables and metadata tables. The rectangular boxes with words inside represent the different table names. The ovals with words inside represent the column names to use to join the tables. Black lines connect table names to columns (i.e., *Detection* has a line to `imageID` which has a line to *ImageMeta*)—this shows that *Detection* and *ImageMeta* share the same index `imageID`.

Table 7
Unique Indices for Various PSPS Tables

PSPS Table	uniquePspsID Name	Release
ObjectThin	uniquePspsOBid	DR1
MeanObject	uniquePspsOBid	DR1
Detection	uniquePspsP2id	DR2
DiffDetection	uniquePspsDFid	DR2
DiffDetObject	uniquePspsDOid	DR2
ForcedGalaxyShape	uniquePspsFGid	DR2
ForcedMeanObject	uniquePspsFOid	DR1
ForcedMeanLensing	uniquePspsFOid	DR1
ForcedWarpMeasurement	uniquePspsFWid	DR2
ForcedWarpExtended	uniquePspsFWid	DR2
ForcedWarpLensing	uniquePspsFWid	DR2
ForcedWarpMasked	uniquePspsFWid	DR2
GaiaFrameCoordinate	uniquePspsGOid	DR1
StackObject* (2 tables)	uniquePspsSTid	DR1
StackApFlx* (4 tables)	uniquePspsSTid	DR1
StackModelFit* (4 tables)	uniquePspsSTid	DR1
StackPetrosian	uniquePspsSTid	DR1

Table 8
Currently Defined Views within PSPS

View Name	Tables Used to Create View
DetectionObjectView	ObjectThin, MeanObject, Detection
MeanObjectView	ObjectThin, MeanObject
StackObjectView	ObjectThin, StackObjectThin, StackObjectAttributes
StackApFlxObjectView	ObjectThin, StackApFlx
StackApFlxExGalUncObjectView	ObjectThin, StackApFlxExGalUnc
StackApFlxExGalCon6ObjectView	ObjectThin, StackApFlxExGalCon6
StackApFlxExGalCon8ObjectView	ObjectThin, StackApFlxExGalCon8
StackModelObjectView	ObjectThin, StackModelFitExp, StackModelFitDeV, StackModelFitSer, StackPetrosian
StackModelFitExpObjectView	ObjectThin, StackModelFitExp
StackModelFitDeVObjectView	ObjectThin, StackModelFitDeV
StackModelFitSerObjectView	ObjectThin, StackModelFitSer
StackModelFitPetObjectView	ObjectThin, StackPetrosian
StackObjectPrimaryView	ObjectThin, StackObjectThin, StackObjectAttributes, StackApFlx
DiffDetObjectView	DiffDetObject, DiffDetection
ForcedDetObjectView	ObjectThin, ForcedWarpMeasurement
ForcedMeanObjectView	ObjectThin, ForcedMeanObject
ForcedGalaxyModelView	ObjectThin, ForcedGalaxyShape

results faster than joins. Table 8 describes the views currently in PSPS.

8. The 3π Database

The 3π Survey, described in detail in Chambers et al. (2016), covers three-quarters of the sky (decl. $> -30°$) in five bands (g_{P1}, r_{P1}, i_{P1}, z_{P1}, y_{P1}), with approximately 60 exposures per patch of sky. For various reasons, a very tiny fraction of the data does not make it into the PSPS database. Some data were intentionally skipped because of poor data quality or other

Table 9
Exposure Count for Various Stages of IPP Processing

IPP Stage	Queued	Successful
Raw exposures	388,177	...
Chip stage	381,279	375,573
Cam stage	375,573	374,521
Fake/warp (exp)	379,973	379,551
Fake/warp (skycells)		206,177
Stack	200,730	200,725
Staticsky	200,720	200,720
Skycal	200,722	200,684
Fullforce	200,684	200,684

Table 10
Batch Count for Database Ingest Stages

IPP Stage	IPP Done	DVO	IPPTOPSPS	PSPS
Cam stage	374,521	374,446		
Skycal	200,684	200,684	200,681	198,727
Fullforce	200,684	200,684	not yet	
Forced galaxy	113,665	113,665	not yet	
Object	116,252	116,252	116,252	113,350
Gaia	116,252	116,252	116,252	116,252
Forced object	113,665	113,665	106,579	

problems; some data failed to process due to glitches or software bugs, some of which may be addressed in a future reanalysis (PV4 or other). We present here the different causes (of which we are aware) for data to be skipped or missed. This section lists the numbers of exposures, skycells, or batches that were processed in each stage, including counts for what were expected and as well as counts for known faults and quality issues (see also Tables 9 and 10).

8.0.1. IPP Processing Stages

All of the 3π data were reprocessed in a consistent way with the same version of the IPP code, internally called Processing Version 3 (PV3) and described in Paper II.

Raw Exposure: A total of 388,177 raw exposures were taken between 2009 June 3 and 2015 February 25 as part of the 3π Survey. However, only 381,279 (98.2%) of these were queued for the first stage of processing, the CHIP stage. Exposures were excluded because they did not meet various requirements: they were flagged as invalid by the observers, or they failed to be processed by nightly science processing because of bad seeing, camera issues, or other observational or telescope conditions that can ruin an exposure.

Chip Stage: Of the 381,279 exposures queued for CHIP processing, 375,573 (98.5%) completed PV3 processing with good quality: no issues detected while detrending or finding sources and performing photometry.

Camera Stage: The CAMERA stage started with these 375,573 exposures, of which 374,521 (99.7%) completed processing. The other exposures failed due to insufficient stars for the astrometric analysis, failure of single chip astrometry to converge, or failure of mosaic astrometry, usually too many failed chips.

Warp Stage: The WARP stages started off with a larger number of exposures than expected: 379,973 instead of 374,521. This was due from some challenges in managing the remote processing on the clusters at Los Alamos National Laboratory and the University of Hawai'i computer cluster (see Paper II). Data transfer failures between the remote clusters and the IPP main cluster required requeuing and rerunning the analysis for some warps in a way that resulted in temporary double counting. Of the 379,973 exposures processed, 374,339 (98.5%) are unique, and 1234 are duplicates. Of the 379,973 exposures, 379,551 (99.9%) have good quality. The WARP stage is the first stage that repartitions the exposures into the skycell tessellation, and because all later stages process on a skycell level rather than an exposure level, we note that the WARP stage yields 206,177 distinct skycells, with multiple warp skycell images from the different exposures for each skycell.

Stack to Skycal Stages: The STACK stage operates on 200,730 distinct skycells with up to five filter images per skycell. A total of 200,725 stack skycells have good quality. There are fewer stack skycells than the 206,177 warp skycells listed above because stacks are not generated for skycells with decl. $< -30°$. Stacks generated below this decl. limit would have significantly poorer coverage and are of limited utility. A total of 200,720 distinct skycells were processed by the static sky stage, and all have good quality. The SKYCAL stage processed 200,722 skycells, of which 2 were essentially duplicate STACKS (same inputs, same skycells) and 200,684 completed with good quality.

The STACK stages have a couple of additional inconsistencies. First, of the 200,684 STACKS that completed through SKYCAL, 409 STACKS (0.2%) include duplicate exposures, i.e., the same exposure appears in a STACK twice. Second, 130 STACKS unintentionally include test exposures (short exposures, 1 s, which were mislabeled as 3π data), which slightly degrade the stack. These artifacts were discovered during the IPPTOPSPS and PSPS phases and are thus present in the database. In addition, the two STACK duplicates mentioned above (i.e., two STACKS for the same filter and skycell) are also present in the PSPS.

Forced Warp Stage: Forced warps are queued by skycell and filter. The 994,890 queued FORCED WARP skycell sets resulted in 19,266,450 cmf files (one per exposure per skycell) from 373,743 exposures and 199,151 distinct skycells, consistent with expectations. There are slightly fewer distinct forced warp skycells than for the stack stages due to the varying coverage at the survey limit of $-30°$: skycells with insufficient numbers of fully filled warps were not queued for forced photometry processing.

8.1. Building the 3π DVO Database

The 3π database was built in stages, with many checks to verify all of the data was included. Full details of the construction and final calibration are in Magnier et al. (2020c). The 3π database contains the following counts of data for various processing stages, ordered by how they were ingested into the database:

Stack/skycal cmf: The end product from the skycal stage produces one cmf file per stack skycell per filter. There are one to five cmfs per skycell, corresponding to different filters. All 998,101 skycal cmfs, in 200,684 distinct skycells, were successfully ingested into the DVO.

Camera smfs: The camera stage produces one smf file per exposure, with extensions for each of the 60 chips. Of the 374,521 available camera stage smf files, 374,446 were

ingested with no faults. The remaining 75 failed to be ingested in the DVO either due to bad data quality (poor astrometry) or in a few cases data corruption in the disk file. These smfs will not be included in the PSPS.

Forced warp cmfs: The forced warp photometry stage produces many cmf files: each of the exposures that are within a given skycell will produce a cmf that is ingested into the database. There are 19,266,450 of these cmf files; they come from 373,743 exposures and are in 994,890 skycells.

Forced warp summary cmfs: The forced warp photometry stage also produces a summary cmf of the mean properties for a given skycell and filter, based on the forced photometry results for all of the included exposures that are within a given skycell. There are 994,890 of these cmfs, in 199,151 distinct skycells. There are one to five cmfs per skycell, corresponding to different filters.

Very tiny amounts of data were not ingested due to quality issues, and there are very minor duplicate issues with processing resulting in some duplicate files being ingested. It is possible to remove those duplicates, but then the mean properties must be recalculated. There are a small number of duplicates that were discovered in IPPTOPSPS and PSPS, and it was not possible to remove and recalibrate them at this time.

8.1.1. Polar Astrometry Issues

After delivery of the DR2 data to STScI, internal consistency tests revealed some problems for data in the vicinity of the celestial north pole. This issue is described in some detail in Paper IV. In short, the on-the-fly astrometric calibration performed during the PV3 analysis (Section 5.1.2) relied on an astrometric reference catalog generated from the PV2 analysis of the PS1 data set, which contained some errors. In that earlier analysis, some exposures were poorly calibrated due to large rotator errors near the pole, but the failures were not recognized. These poorly calibrated images were included in the reference database, providing a set of invalid reference stars. In the PV3 analysis, exposures in the vicinity of these problem areas sometimes latch onto the invalid stars resulting in poorly calibrated images. Individual chips may have solutions with offsets of up to $2''$.

These astrometry failures cause errors with the mean astrometry for objects in this region. They also result in misaligned warp images and therefore stacks with smeared or doubled stellar images. The photometry for warps and stacks are also corrupted. We identified the warps and stack skycells affected by this issue and provide warnings to users who attempt to download these images from MAST. Stack properties from the affected images are set to `NULL` as these values cannot be trusted. A list of the affected skycells is provided at MAST, and users are advised to be cautious of measurements from these regions. The problem skycells are almost entirely north of decl. $= 80°$, comprising roughly 21 of the 313 square degrees in this region. A reprocessing of the polar regions north of decl. $= 70°$ is underway and will be released to users in the future.

8.2. IPPTOPSPS Stage

IPPTOPSPS generates batches that includes all of the smf/cmf files categorized by stage of processing and generates batches corresponding to each DVO file. The relationship between PSPS items and the source of the data (DVO, cmf/smf files, or from the IppToPsps code) is described in Tables E1–E3. It is straightforward to verify that all the data are accounted for and have been processed through IPPTOPSP, and easy to regenerate missing batches. This section describes the batch types and expected numbers.

Stacks: IPPTOPSPS is expected to generate 200,684 STACK batches. It initially created 200,681 batches for DR1, and two of the missing batches were created and added after the original DR1 date. For DR2, it generated 200,683 batches. The one missing stack batch ended up being unsuitable data quality for the database.

ObjectThin/MeanObject: IPPTOPSPS generated all of the expected 116,252 batches for DR1, and 111,505 for DR2. There are fewer batches for DR2 because it explicitly avoids the ragged edge of the survey and excludes those with decl. < -30.

GaiaFrameCoordinate: IPPTOPSPS generated all of the expected 116,252 batches for DR1. This batch type was not relevant for DR2.

Forced Mean Objects: IPPTOPSPS generated all of the expected 113,665 *Forced Object* batches for DR1, and 113,167 batches for DR2. There are fewer of these batches than for ObjectThin because it explicitly avoids the ragged edge of the survey at decl. $= -30°$.

Detection Table: We expect 374,446 *Detection* batches, and we generated 374,344. The 102 missing batches were incorrectly marked as good exposures but in fact are not of sufficient quality and will not be added into the database.

ForcedWarp Tables: We expect 994,890 *Forced Warp* batches, and we generated 994,826.

Forced Galaxy Objects: We expect 57,758 *Forced Galaxy Objects*, and we generated 57758 *Forced Galaxy Object* batches. Not all areas of the sky will have forced galaxy objects measured, so although the batches are subdivided in the sky in the same way as for *ObjectThin/MeanObject* and *ForcedMeanObject*, we should expect a smaller number (57,758) than for the other Object types (typically $> 110{,}000$).

8.3. Loading into PSPS

The PSPS loaded the tables for DR1 and DR2; however, there are a few inconsistencies discovered:

IPPTOPSPS is expected to generate 200,684 STACK batches. It initially created 200,681 batches (missing 3); of those that are expected, 1940 partially loaded, and 14 failed to load into PSPS by the DR1 deadline. These missing batches (1957) were not included in the initial DR1 release but were added over the months after the initial release. Similar gaps were present in the initial DR2 release and largely been filled in as of this time. However, users should be cautious of possible gaps in the database and consult the MAST website.

8.3.1. Queries to Find Holes

It is possible to use the PSPS database to verify data and to check that there are no missing data. The table *GaiaFrameCoordinate* is complete and has no missing data. It can be used to do quick integrity checks on other tables within PSPS. Finding missing objects from *ObjectThin* is straightforward: do a `FULL OUTER JOIN` for *GaiaFrameCoordinate* and *ObjectThin* using *objID*. Objects with a `NULL` *ObjectThin.batchID* are missing. Missing objects from *ForcedMeanObject* can be found in a similar way to those in *ObjectThin*. Do a

FULL OUTER JOIN between *GaiaFrameCoordinate* and *ForcedMeanObject*. Objects with a NULL *ForcedMeanObject.batchID* are missing. Finding missing objects in *StackObjectThin* is trickier, because not all objects have STACK photometry. This requires a FULL OUTER JOIN on *StackObjectThin* to *ObjectThin* to *GaiaFrameCoordinate*. Missing STACKS will have valid *ObjectThin.raStack* and *ObjectThin.decStack* and NULL *StackObjectThin.objID*.

9. Conclusion

The Pan-STARRS database contains 10,723,304,629 objects. It is the largest data release from the largest digital sky survey to date, distilling the information from 1.6 PB of images and tables into a form that is accessible to the astronomical community through MAST. Nevertheless, sifting through such a large database can prove daunting, and this work is intended to describe the primary tables and quantities within the database, together with example queries. Data from Pan-STARRS have been used for myriad purposes, including detecting moving objects within the solar system (and in the case of 1I/2017 U1 ('Oumuamua), from outside it!), the analysis of tens of thousands of high-energy transient events, mapping the 3D structure of dust within our Galaxy, and studies of the large-scale structure of our universe. Yet these only scratch the surface, and it is likely that mining the database will lead to discoveries that were missed and correlations that were overlooked. As we enter the era of multimessenger astrophysics, the Pan-STARRS data products will be essential to identifying the host galaxies and electromagnetic counterparts of events detected by gravitational wave, high-energy particle, neutrino, and radio observatories. While we have provided various tools to work with this data release, we anticipate that it will spur the development of new interfaces and ways of working with high-dimensional data sets. This work will be critical to science with future surveys such as LSST. Combining this Pan-STARRS data release with other large catalogs such as GALEX, 2MASSm and Gaia will provide a rich, high-dimensional data set that will enable new scientific studies and may yield astronomical treasures that we have not even begun to imagine.

The Pan-STARRS1 Surveys (PS1) have been made possible through contributions of the Institute for Astronomy, the University of Hawai'i, the Pan-STARRS Project Office, the Max-Planck Society and its participating institutes, the Max Planck Institute for Astronomy, Heidelberg, and the Max Planck Institute for Extraterrestrial Physics, Garching, The Johns Hopkins University, Durham University, the University of Edinburgh, Queen's University Belfast, the Harvard-Smithsonian Center for Astrophysics, the Las Cumbres Observatory Global Telescope Network Incorporated, the National Central University of Taiwan, the Space Telescope Science Institute, the National Aeronautics and Space Administration under grant No. NNX08AR22G issued through the Planetary Science Division of the NASA Science Mission Directorate, the National Science Foundation under grant No. AST-1238877, the University of Maryland, Eötvös Loránd University (ELTE), the Los Alamos National Laboratory, and the Gordon and Betty Moore foundation.

This work has made use of data from the European Space Agency (ESA) mission Gaia (http://www.cosmos.esa.int/gaia), processed by the Gaia Data Processing and Analysis Consortium (DPAC, http://www.cosmos.esa.int/web/gaia/dpac/consortium). Funding for the DPAC has been provided by national institutions, in particular the institutions participating in the Gaia Multilateral Agreement.

H.F. would especially like to thank G. Hasinger for extensive LATEX help, G. Narayan for magical LATEX ninja skills, and S. Isani (Ministry of Fonts) for checking LATEX for typos (he disagrees with my font choice).

Facility: PS1 (GPC1).

Appendix A
Query Examples

This section shows example queries for the Pan-STARRS1 DR2 database. The progression will be from simple queries to more complicated queries. SQL has no requirements on case. We adopt the standard convention of using CAPITAL LETTERS for SQL-reserved words and functions and CamelCase for the tables and columns within the PSPS database schema. The queries given below may all be run from the CasJobs tab on the MAST website using the context "PanSTARRS_DR2." Note the some of the later queries rely on myDB tables generated in the earlier queries. The names for these output tables are surrounded by square brackets in the examples. These brackets are always allowed but are required if the table name includes spaces or reserved words (see https://docs.microsoft.com/en-us/sql/relational-databases/databases/database-identifiers). Also beware that cutting and pasting in some browsers can convert the underscore characters to space.

1. *Counting the number of rows in a large table.*
   This is an example of a simple query; it needs to be run in the slow queue. The difference between COUNT_BIG() and COUNT() is that COUNT_BIG() returns a BIGINT, while COUNT() returns an INT. The PSPS tables are so large that COUNT(), which goes up to 2.14 billion, is too small of a number. Users should choose the method of counting rows that is appropriate for their data ranges. Unless it involves large tables and large areas of sky, COUNT() is recommended. However, if the result is too large, using COUNT() will result in an arithmetic overflow exception.
   ```
   SELECT COUNT_BIG(objID) FROM ObjectThin.
   ```
2. *Return mean PSF magnitudes and errors for all filters (grizy) for a rectangular patch of sky.*
   ```
   SELECT ObjectThin.objID, nDetections, raMean, decMean,
   gMeanPSFMag, gMeanPSFMagErr, rMeanPSFMag, rMeanPSFMagErr,
   iMeanPSFMag, iMeanPSFMagErr, zMeanPSFMag, zMeanPSFMagErr,
   yMeanPSFMag, yMeanPSFMagErr
   FROM ObjectThin
   INNER JOIN MeanObject ON ObjectThin.objID = MeanObject.objID
   WHERE
   raMean > 100.0 AND
   raMean < 100.1
   AND decMean > 0.0
   AND decMean < 0.1.
   ```

This returns 3868 objects. The majority of these objects have only been detected once.

3. *Make a simple text histogram of ObjectThin.nDetections for a rectangular patch of sky*. It is possible to save queries into your own personal MyDB as well as to make queries on your MyDB. Do the query from above, but save it to your MyDB as "MyDBtest." Run the following query on your MyDB (MyDB context) to make a histogram of *nDetections*.

   `SELECT nDetections, COUNT(nDetections) FROM MyDBtest GROUP BY nDetections ORDER BY nDetections.`

   The results are ordered by *nDetections*, and it is apparent that most of the objects have zero to two detections. The *nDetections* column refers to the number of times something is detected from the the individual exposures. Objects that have zero detections are so faint that they are not visible in the individual exposures but are detected in the stacks. Objects with one to two (or a few) detections might be spurious detections, moving objects, or faint objects. If the user is interested in objects that are more likely to be well measured in several epochs and also of astrophysical nature, it is best to add a restriction on *nDetections*. If the user is interested in the static sky and in STACK photometry, it is best to do a `JOIN` on *StackObjectThin*. See the next two queries for examples of each of those types of queries.

4. *Select mean PSF magnitudes and errors for filters griyz and for a rectangular patch of sky, with a restriction of >10 nDetections.* This is an example of a query to get mean PSF magnitudes and errors for all filters in a rectangular patch of sky, for objects with >10 *nDetections*. The reason we chose 10 detections is somewhat arbitrary and can be adjusted, but is used primarily to cut out objects for which there are only a few detections. Objects with very few detections might not be astrophysical or they might be too faint to be seen multiple times.

```
SELECT ObjectThin.objID, raMean,decMean,
gMeanPSFMag, gMeanPSFMagErr, rMeanPSFMag, rMeanPSFMagErr,
iMeanPSFMag, iMeanPSFMagErr, zMeanPSFMag, zMeanPSFMagErr,
yMeanPSFMag, yMeanPSFMagErr
FROM ObjectThin
INNER JOIN MeanObject ON ObjectThin.objID = MeanObject.objID
WHER
nDetections > 10
 AND raMean > 100.0
 AND raMean < 100.1
AND decMean > 0.0
 AND decMean < 0.1
```

   . This returns 748 objects, a significant reduction from the 3867 returned in query # 2.

5. *Select* STACK *PSF magnitudes for all filters for a rectangular patch of sky*.

   This is an example of a query to get STACK PSF magnitudes for the same rectangular patch of sky. No restrictions on *nDetections* are necessary; the expectation is that sources on STACKS are more likely to be astrophysical.

```
SELECT ObjectThin.objID, raStack, decStack,
gPSFMag, gPSFMagErr, rPSFMag, rPSFMagErr,iPSFMag, iPSFMagErr,
zPSFMag, zPSFMagErr, yPSFMag, yPSFMagErr
FROM ObjectThin
INNER JOIN StackObjectThin ON ObjectThin.objID = StackObjectThin.objID
WHERE raMean > 100.0
 AND raMean < 100.1
 AND decMean > 0.0
AND decMean < 0.1
```

   . This returns 1806 objects.

6. *An example of finding rows with NULL values, using TOP to limit results.* The PSPS uses `−999` to denote `NULL` values. The following query returns some objects that are detected in single exposures but not in the stacks. The numbers are limited by TOP to return the first 10 rows.

```
SELECT TOP 10
objectThin.objID, raMean, decMean, raStack, decStack,
nDetections, ng, nr, ni, nz, ny, imeanpsfmag
FROM objectThin
JOIN MeanObject on objectThin.objID = meanObject.objid
WHERE raStack = −999.
```

7. *Basic search using BETWEEN to limit ranges*.

   Similar to query # 5, except uses `BETWEEN` to limit R.A. and decl. ranges as well as iPSFMag ranges.

```
SELECT ObjectThin.objID, raStack, decStack,
gPSFMag, gPSFMagErr, rPSFMag, rPSFMagErr,iPSFMag, iPSFMagErr,
zPSFMag, zPSFMagErr, yPSFMag, yPSFMagErr
FROM ObjectThin
INNER JOIN StackObjectThin ON ObjectThin.objID = StackObjectThin.objID
WHERE raMean BETWEEN 100.0 AND 100.1
AND decMean BETWEEN 0.0 AND 0.1
 AND iPSFMag BETWEEN 18.0 AND 21.0.
```

8. *Using built-in functions to do a box search.*

   ObjectThin contains Hierarchical triangular mesh information, making it possible to use the built-in function dbo.fGetObjFromRectEq(minra, mindec, maxra, maxdec) to do a rectangular search. Tables that have htm, cx,cy, cz can use this built-in function.

```
SELECT o.objID, o.raMean, o.decMean
FROM ObjectThin o, dbo.fGetObjFromRectEq(56.65, 23.92, 57.05, 24.32) AS r
WHERE o.objID = r.objID.
```

9. *Using built-in functions to do a cone search.* ObjectThin contains Hierarchical triangular mesh information, making it possible to use the built-in function dbo. fGetNearbyObjEq(ra, dec, conesize(arcmin)) to do a radial search for objects near a given ra and dec (cone search). Tables that have htm, cx, cy, cz can use this built-in function. The query below returns the objects

within 0 ′.2 of the coordinate 56.85, 24.12. Note that only one of these objects was detected in a g_{P1}-band image and thus has a valid value for the g_{P1}-magnitude.

```
SELECT o.objID, raMean, decMean, gMeanPSFMag, gMeanPSFMagErr
FROM ObjectThin AS o
JOIN MeanObject AS m ON o.objID = m.objID
JOIN dbo.fGetNearbyObjEq(56.85, 24.12, 0.2) AS n
ON o.objID = n.objID.
```

10. *Cone search of high-fidelity stellar-like objects*. We want to get all objects with *R* degrees of a given position that are high-fidelity stellar-like objects. We get all objects within 0.°2 of R.A. = 334.0 and decl. = 0.0 which have mean magnitudes in *griz* (i.e., at least one detection in each band that can be used for the mean mag). In addition, we require QfPerfect >0.85 in all bands. We select stars with a small (<0.05) difference between Kron and PSF magnitudes.

```
SELECT o.objID, o.raMean, o.decMean, o.raMeanErr, o.decMeanErr, o.qualityFlag, o.gMeanPSFMag, o.gMeanPSFMagErr, o.gMeanPSFMagNpt, o.rMeanPSFMag, o.rMeanPSFMagErr, o.rMeanPSFMagNpt, o.iMeanPSFMag, o.iMeanPSFMagErr, o.iMeanPSFMagNpt, o.zMeanPSFMag, o.zMeanPSFMagErr, o.zMeanPSFMagNpt, o.yMeanPSFMag, o.yMeanPSFMagErr, o.yMeanPSFMagNpt, o.rMeanKronMag, o.rMeanKronMagErr, o.nDetections, o.ng, o.nr, o.ni, o.nz,o.ny, o.gFlags, o.gQfPerfect, o.rFlags, o.rQfPerfect, o.iFlags, o.iQfPerfect, o.zFlags, o.zQfPerfect, o.yFlags, o.yQfPerfect, soa.primaryDetection, soa.bestDetection INTO mydb.[HighFidelityStarsDR2] FROM dbo.fGetNearbyObjEq(334, 0.0, 0.2*60.0) as x JOIN MeanObjectView o on o.objID = x.ObjId LEFT JOIN StackObjectAttributes AS soa ON soa.objID = x.objID WHERE o.nDetections > 5 AND soa.primaryDetection > 0 AND o.gQfPerfect > 0.85 and o.rQfPerfect > 0.85 and o.iQfPerfect > 0.85 and o.zQfPerfect > 0.85 AND (o.rmeanpsfmag—o.rmeankronmag < 0.05).
```

11. *Galaxy Candidates for the K2 SN Search*.

The Kepler Extra-Galactic Survey (KEGS) is a program using the Kepler telescope to search for supernovae, active galactic nuclei, and other transients in galaxies. We identify galaxies in a suitable redshift range ($z \leqslant 0.12$) a priori, which will be monitored by K2. Here is an example to select galaxies for Campaign 14. We only select objects with $r \leqslant 19.5$, and we make a cut on (rmeanpsfmag – rmeankronmag) $\geqslant 0.05$ in order to remove stars. We only want to use objects for which the majority of pixels were not masked, thus the cut on QFperfect $\geqslant 0.95$. We also obtain the Petrosian radii in order to be able to select galaxies by size.

```
SELECT o.objID, ot.raStack, ot.decStack, ot.raMean, ot.decMean, ot.ng, o.gMeanPSFMag,o.gMeanPSFMagErr,o.gMeanKronMag,o.gMeanKronMagErr, ot.nr, o.rMeanPSFMag,o.rMeanPSFMagErr,o.rMeanKronMag,o.rMeanKronMagErr, ot.ni, o.iMeanPSFMag,o.iMeanPSFMagErr,o.iMeanKronMag,o.iMeanKronMagErr, ot.nz, o.zMeanPSFMag,o.zMeanPSFMagErr,o.zMeanKronMag,o.zMeanKronMagErr, ot.ny, o.yMeanPSFMag,o.yMeanPSFMagErr,o.yMeanKronMag,o.yMeanKronMagErr, o.gQfPerfect, o.rQfPerfect, o.iQfPerfect, o.zQfPerfect, o.yQfPerfect, ot.qualityFlag, ot.objInfoFlag, sp.gpetRadius, sp.rpetRadius, sp.ipetRadius, sp.zpetRadius, sp.ypetRadius, sp.gpetR50, sp.rpetR50, sp.ipetR50, sp.zpetR50, sp.ypetR50, soa.primaryDetection, soa.bestDetection INTO mydb.[C14] FROM MeanObject AS o JOIN fgetNearbyObjEq (160.68333, 6.85167 , 8.5*60.0) cone ON cone.objid = o.objID JOIN ObjectThin AS ot ON ot.objID = o.objID LEFT JOIN StackPetrosian AS sp ON sp.objID = o.objID LEFT JOIN StackObjectAttributes AS soa ON soa.objID = o.objID WHERE ot.ni >= 3 AND ot.ng >= 3 AND ot.nr >= 3 AND soa.primaryDetection > 0 AND (o.rMeanKronMag > 0 AND o.rMeanKronMag < = 19.5) AND (o.gQfPerfect >= 0.95) AND (o.rQfPerfect >= 0.95) AND (o.iQfPerfect >= 0.95) AND (o.zQfPerfect >= 0.95) AND (o.rmeanpsfmag—o.rmeankronmag > 0.05).
```

12. *Find the objID of a single object.* Star CSS J030521.9 +013231 (Catalina Sky Survey), 584630948352256 (GAIA) is an RR Lyrae with period = 0.55547 days and coordinates R.A. = 46.341468915923 and decl. = 1.54199810825252 (ref. GAIA DR2, 2018yCat.1345....0G). In the following, we obtain the PSF and aperture photometry light curves, both forced and unforced, for this star. (See Figure 11.)

First, we generate a MyDB table containing the Gaia information for this source by running the following query against the Gaia DR2 database at MAST:

```
SELECT source_id AS ID_GAIA, ra AS RA_GAIA, dec AS DEC_GAIA, phot_g_mean_mag AS Gmag INTO mydb.[RRL_584630948352256] FROM gaia_source WHERE source_id = 584630948352256
```

. Now we run the following query to extract the Pan-STARRS DR2 information:

```
SELECT d.ID_GAIA, d.RA_GAIA as GAIARA, d.DEC_GAIA as GAIADec, d.Gmag, o.objID, o.raMean, o.decMean, o.raMeanErr, o.decMeanErr, o.qualityFlag, o.gMeanPSFMag, o.gMeanPSFMagErr, o.gMeanPSFMagNpt, o.rMeanPSFMag, o.rMeanPSFMagErr, o.rMeanPSFMagNpt, o.iMeanPSFMag, o.iMeanPSFMagErr, o.iMeanPSFMagNpt, o.zMeanPSFMag, o.zMeanPSFMagErr, o.zMeanPSFMagNpt, o.yMeanPSFMag, o.yMeanPSFMagErr, o.yMeanPSFMagNpt, o.rMeanKronMag, o.rMeanKronMagErr, o.nDetections, o.ng,
```

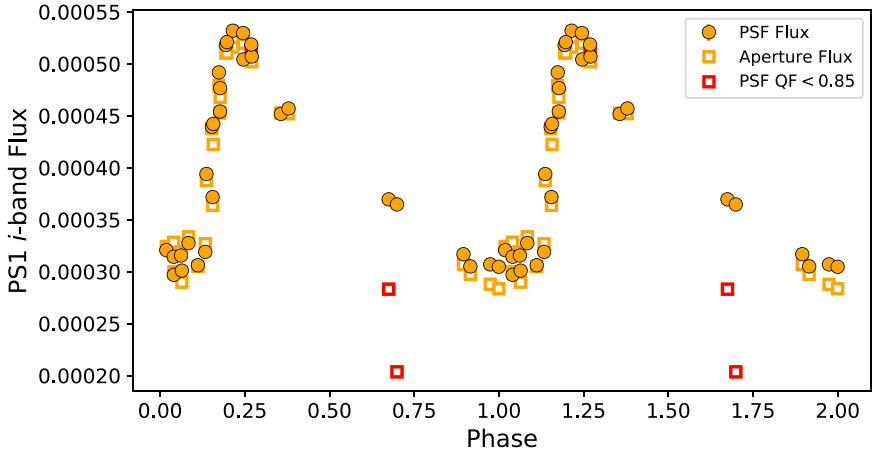

Figure 11. A key feature of this data release is the inclusion of the individual detections, allowing time-resolved studies, illustrated by the *i*-band phase curve of one of the PS1 RR Lyrae. The IPP aperture and PSF fluxes are in good agreement, and either can be used for studies of the hundreds of thousands of variable and transient sources within PS1. Users are encouraged to check the provided flags for various bits documented in this work, as these may indicate suboptimal photometry. We highlight two such measurements in red. Uncertainties are typically smaller than the marker size.

```
o.nr, o.ni, o.nz, o.ny, o.gFlags, o.
gQfPerfect, o.rFlags, o.rQfPerfect, o.
iFlags, o.iQfPerfect, o.zFlags, o.
zQfPerfect, o.yFlags, o.yQfPerfect,
soa.primaryDetection, soa.bestDetection
INTO mydb.[RRL_584630948352256_PS1] FROM
mydb.[RRL_584630948352256] d CROSS APPLY
dbo.fGetNearbyObjEq(46.341468915923,
1.54199810825252, 1.0/60.0) as x JOIN
MeanObjectView o on o.objID = x.ObjId
LEFT JOIN StackObjectAttributes AS soa
ON soa.objID = x.objID WHERE o.nDetec-
tions > 8 AND soa.primaryDetection > 0
AND o.gQfPerfect > 0.85 and o.rQfPer-
fect > 0.85 and o.iQfPerfect > 0.85 and
o.zQfPerfect > 0.85 AND (o.rmeanpsfmag—
o.rmeankronmag < 0.05).
```

13. *Obtain the lightcurve for a given object (Detections).* The query above gives an objID of 109850463414820867 for that RR Lyrae star. Knowing the objID, it is possible to query to get the lightcurve.

```
SELECT o.ID_GAIA, o.GAIARA, o.GAIA-
Dec, o.Gmag, o.objID, o.raMean, o.dec-
Mean, d.ra, d.dec, d.raErr, d.decErr, d.
detectID, d.obstime, d.exptime, d.air-
mass, d.psfflux, d.psffluxErr, d.psfQf, d.
psfQfPerfect, d.psfLikelihood, d.
psfChiSq, d.extNSigma, d.zp, d.apFlux,
d.apFluxErr, d.imageID, d.filterID, d.
sky, d.skyerr, d.infoflag, d.infoflag2, d.
infoflag3, o.qualityFlag, o.gMeanPSFMag,
o.gMeanPSFMagErr, o.gMeanPSFMagNpt, o.
rMeanPSFMag, o.rMeanPSFMagErr, o.
rMeanPSFMagNpt, o.iMeanPSFMag, o.
iMeanPSFMagErr, o.iMeanPSFMagNpt, o.
zMeanPSFMag, o.zMeanPSFMagErr, o.
zMeanPSFMagNpt, o.yMeanPSFMag, o.
yMeanPSFMagErr, o.yMeanPSFMagNpt, o.
rMeanKronMag, o.rMeanKronMagErr, o.nDe-
tections, o.ng, o.nr, o.ni, o.nz, o.ny, o.
gFlags, o.gQfPerfect, o.rFlags, o.
rQfPerfect, o.iFlags, o.iQfPerfect, o.
zFlags, o.zQfPerfect, o.yFlags, o.yQf-
Perfect, o.primaryDetection, o.bestDe-
tection INTO mydb.
[RRL_584630948352256_PS1det] FROM mydb.
[RRL_584630948352256_PS1] o JOIN Detec-
tion d on d.objID = o.objID
```

14. *Obtain the lightcurve for a given object (Forced photometry).* Similar to the query above, except this one provides the forced photometry for the star with objID = 109850463414820867.

```
SELECT o.ID_GAIA,o.GAIARA, o.GAIA-
Dec, o.Gmag, o.objID, o.raMean, o.dec-
Mean, fwm.detectID, fwm.obstime, fwm.
exptime, fwm.airmass, fwm.Fpsfflux, fwm.
FpsffluxErr, fwm.FpsfQf, fwm.FpsfQfPer-
fect, fwm.FpsfChiSq, fwm.zp, fwm.Fap-
Flux, fwm.FapFluxErr, fwm.forcedWarpID,
fwm.filterID, fwm.Fsky, fwm.Fskyerr, fwm.
Finfoflag, fwm.Finfoflag2, fwm.Finfoflag3,
o.qualityFlag, o.gMeanPSFMag, o.
gMeanPSFMagErr, o.gMeanPSFMagNpt, o.
rMeanPSFMag, o.rMeanPSFMagErr, o.
rMeanPSFMagNpt, o.iMeanPSFMag, o.
iMeanPSFMagErr, o.iMeanPSFMagNpt, o.
zMeanPSFMag, o.zMeanPSFMagErr, o.
zMeanPSFMagNpt, o.yMeanPSFMag, o.
yMeanPSFMagErr, o.yMeanPSFMagNpt, o.
rMeanKronMag, o.rMeanKronMagErr, o.nDe-
tections, o.ng, o.nr, o.ni, o.nz,o.ny, o.
gFlags, o.gQfPerfect, o.rFlags, o.
rQfPerfect, o.iFlags, o.iQfPerfect, o.
zFlags, o.zQfPerfect, o.yFlags, o.yQf-
Perfect, o.primaryDetection, o.bestDe-
tection INTO mydb.
[RRL_584630948352256_PS1forced] FROM
mydb.[RRL_584630948352256_PS1] o JOIN
ForcedWarpMeasurement fwm on fwm.
objID = o.objID.
```

Appendix B
Abbreviations and Acronyms

3pi or 3π: Three Pi Survey. This survey covers 3π steradians of the sky (three-quarters of the sky), everything with decl. greater than −30°.

DR1: Data Release 1. Covers the 3π data release for ObjectThin, MeanObject, Stack*, ForcedMean*, and related metadata tables. Covers the static sky.

DR2: Data Release 2. 3π data release of time domain tables, including Detection, ForcedWarp*, Diff*, and related metadata.

DVO: Desktop Virtual Observatory—written by Eugene Mangier, IPP uses this to store and manipulate catalog data.

GPC1: Gigapixel Camera 1. This is the name of the camera that is part of the Pan-STARRS1 telescope. 1.4 gigapixels and sees 7 deg^2 per exposure. It is made up of 60 OTA, each with 64 cells per OTA.

IPP: Image Processing Pipeline. Code developed to process and manage all aspects of Pan-STARRS1 processing, starting from downloading the images to the summit to generating data in the final database schema form.

MD: Short for Medium-Deep fields. A set of 10 fields, each of which is 7 deg^2, observed at a high cadence, primarily to be used for searches for transient objects. These will be released at a later time.

MOPS: Short for Moving Object Processing System. The Pan-STARRS subsystem responsible for linking detections from the IPP into discoveries of asteroids or other solar system objects.

OTA: Orthogonal transfer array, the name of the devices that make up the GPC1 camera

PSI: Science interface. The interface used by consortium members to access earlier versions of the data.

PSPS: Published Science Products Subsystem—the Pan-STARRS1 databases

PV3: Processing Version 3, refers to the processing/code iteration; this is the processing version of the first public Pan-STARRS1 data release (covers DR1–DR2).

Appendix C
Flag Tables

There are eight different classes of Flag tables for the database schema. This section lists the different flags as well as their descriptions. See Section 7.2.1 for more details on flags and bitmasks, and Appendix A for some example queries.

Appendix D
Schema

In this section, we present the contents of all DR2 tables, along with the expected DIFF tables for DR3. These listings were automatically generated from the XML code used to define the PSPS tables, with light editing to clean up the formatting for some of the units and equations.

D.1. Object/Mean Object Tables

Table D1
ObjectInfoFlags

Name	Hexadecimal	Value	Description
DEFAULT	0x00000000	0	Initial value; resets all bits.
FEW	0x00000001	1	Used within relphot; skip star.
POOR	0x00000002	2	Used within relphot; skip star.
ICRF_QSO	0x00000004	4	Object IDed with known ICRF quasar (may have ICRF position measurement)
HERN_QSO_P60	0x00000008	8	Identified as a likely QSO (Hernitschek et al. 2016); P_QSO $\geq$ 0.60
HERN_QSO_P05	0x00000010	16	Identified as a possible QSO (Hernitschek et al. 2016), P_QSO $\geq$ 0.05
HERN_RRL_P60	0x00000020	32	Identified as a likely RR Lyra (Hernitschek et al. 2016), P_RRLyra $\geq$ 0.60
HERN_RRL_P05	0x00000040	64	Identified as a possible RR Lyra (Hernitschek et al. 2016), P_RRLyra $\geq$ 0.05
HERN_VARIABLE	0x00000080	128	Identified as a variable based on ChiSq? (Hernitschek et al. 2016)
TRANSIENT	0x00000100	256	Identified as a nonperiodic (stationary) transient
HAS_SOLSYS_DET	0x00000200	512	At least one detection identified with a known solar system object (asteroid or other)
MOST_SOLSYS_DET	0x00000400	1024	Most detections identified with a known solar system object (asteroid or other)
LARGE_PM	0x00000800	2048	Star with large proper motion
RAW_AVE	0x00001000	4096	Simple weighted average position was used (no IRLS fitting)
FIT_AVE	0x00002000	8192	Average position was fitted
FIT_PM	0x00004000	16384	Proper motion model was fitted
FIT_PAR	0x00008000	32768	Parallax model was fitted
USE_AVE	0x00010000	65536	Average position used (not PM or PAR)
USE_PM	0x00020000	131072	Proper motion used (not AVE or PAR)
USE_PAR	0x00040000	262144	Parallax used (not AVE or PM)
NO_MEAN_ASTROM	0x00080000	524288	Mean astrometry could not be measured
STACK_FOR_MEAN	0x00100000	1048576	Stack position used for mean astrometry
MEAN_FOR_STACK	0x00200000	2097152	Mean astrometry used for STACK position
BAD_PM	0x00400000	4194304	Failure to measure proper motion model
EXT	0x00800000	8388608	Extended in our data (eg; PS)
EXT_ALT	0x01000000	16777216	Extended in external data (e.g., 2MASS)
GOOD	0x02000000	33554432	Good-quality measurement in our data (e.g., PS)
GOOD_ALT	0x04000000	67108864	Good-quality measurement in external data (e.g., 2MASS)
GOOD_STACK	0x08000000	134217728	Good-quality object in the STACK (>1 good stack measurement)
BEST_STACK	0x10000000	268435456	The primary STACK measurements are the best measurements
SUSPECT_STACK	0x20000000	536870912	Suspect object in the STACK (no more than one good measurement, two or more suspect or good stack measurement)
BAD_STACK	0x40000000	1073741824	Poor-quality STACK object (no more than one good or suspect measurement)

Table D2
ObjectQualityFlags

Name	Hexadecimal	Value	Description
DEFAULT	0x00000000	0	Initial value; resets all bits.
QF_OBJ_EXT	0x00000001	1	Extended in our data (e.g., PS).
QF_OBJ_EXT_ALT	0x00000002	2	Extended in external data (e.g., 2MASS).
QF_OBJ_GOOD	0x00000004	4	Good-quality measurement in our data (e.g., PS).
QF_OBJ_GOOD_ALT	0x00000008	8	Good-quality measurement in external data (e.g., 2MASS).
QF_OBJ_GOOD_STACK	0x00000010	16	Good-quality object in the STACK (>1 good stack measurement).
QF_OBJ_BEST_STACK	0x00000020	32	The primary stack measurements are the best measurements.
QF_OBJ_SUSPECT_STACK	0x00000040	64	Suspect object in the STACK (no more than one good measurement, two or more suspect or good stack measurement).
QF_OBJ_BAD_STACK	0x00000080	128	Poor-quality STACK object (no more than one good or suspect measurement).

Table D3
ObjectFilterFlags

Name	Hexadecimal	Value	Description
DEFAULT	0x00000000	0	Initial value; resets all bits.
SECF_STAR_FEW	0x00000001	1	Used within relphot: skip star.
SECF_STAR_POOR	0x00000002	2	Used within relphot: skip star.
SECF_USE_SYNTH	0x00000004	4	Synthetic photometry used in average measurement.
SECF_USE_UBERCAL	0x00000008	8	Ubercal photometry used in average measurement.
SECF_HAS_PS1	0x00000010	16	PS1 photometry used in average measurement.
SECF_HAS_PS1_STACK	0x00000020	32	PS1 STACK photometry exists.
SECF_HAS_TYCHO	0x00000040	64	Tycho photometry used for synthetic magnitudes.
SECF_FIX_SYNTH	0x00000080	128	Synthetic magnitudes repaired with zero-point map.
SECF_RANK_0	0x00000100	256	Average magnitude calculated in zeroth pass.
SECF_RANK_1	0x00000200	512	Average magnitude calculated in first pass.
SECF_RANK_2	0x00000400	1024	Average magnitude calculated in second pass.
SECF_RANK_3	0x00000800	2048	Average magnitude calculated in third pass.
SECF_RANK_4	0x00001000	4096	Average magnitude calculated in fourth pass.
SECF_STACK_PRIMARY	0x00004000	16384	PS1 STACK photometry comes from primary skycell.
SECF_STACK_BESTDET	0x00008000	32768	PS1 STACK best measurement is a detection (not forced).
SECF_STACK_PRIMDET	0x00010000	65536	PS1 stack primary measurement is a detection (not forced).
SECF_STACK_PRIMARY_MULTIPLE	0x00020000	131072	PS1 stack object has multiple primary measurements (DR2).
SECF_HAS_SDSS	0x00100000	1048576	This photcode has SDSS photometry.
SECF_HAS_HSC	0x00200000	2097152	This photcode has HSC photometry.
SECF_HAS_CFH	0x00400000	4194304	This photcode has CFH photometry (mostly megacam).
SECF_HAS_DES	0x00800000	8388608	This photcode has DES photometry.
SECF_OBJ_EXT	0x01000000	16777216	Extended in this band.

Table D4
ImageFlags

Name	Hexadecimal	Value	Description
NEW	0x00000000	0	No relphot/relastro attempted.
PHOTOM_NOCAL	0x00000001	1	Used within relphot to mean "do not apply fit."
PHOTOM_POOR	0x00000002	2	Relphot says image is bad (dMcal $>$ limit).
PHOTOM_SKIP	0x00000004	4	External information image has bad photometry.
PHOTOM_FEW	0x00000008	8	Currently too few measurements for good value for photometry.
ASTROM_NOCAL	0x00000010	16	User-set value used within relastro: ignore.
ASTROM_POOR	0x00000020	32	Relastro says image is bad (dR, dD $>$ limit).
ASTROM_FAIL	0x00000040	64	Relastro fit diverged, fit not applied.
ASTROM_SKIP	0x00000080	128	External information image has bad astrometry.
ASTROM_FEW	0x00000100	256	Currently too few measurements for good value for astrometry.
PHOTOM_UBERCAL	0x00000200	512	Externally supplied photometry zero point from ubercal analysis.
ASTROM_GMM	0x00000400	1024	Image was fitted to positions corrected by the galaxy motion model.

Table D5
ForcedGalaxyShapeFlags

Name	Hexadecimal	Value	Description
NO_ERROR	0x00000000	0	No error condition raised.
FAIL_FIT	0x00000001	1	Fit failed to converge or was degenerate
TOO_FEW	0x00000002	2	Not enough points to fit the model
OUT_OF_RANGE	0x00000004	4	Fit minimum too far outside data range
BAD_ERROR	0x00000008	8	Invalid size error (nan or inf)

Table D6
DetectionFlags

Name	Hexadecimal	Value	Description
DEFAULT	0x00000000	0	Initial value; resets all bits.
PSFMODEL	0x00000001	1	Source fitted with a PSF model (linear or nonlinear).
EXTMODEL	0x00000002	2	Source fitted with an extended source model.
FITTED	0x00000004	4	Source fitted with a nonlinear model (PSF or EXT; good or bad).
FAIL	0x00000008	8	Fit (nonlinear) failed (nonconverge; off edge; run to zero).
POOR	0x00000010	16	Fit succeeds, but low signal-to-noise ratio, high-Chisq, or large (for PSF—drop?).
PAIR	0x00000020	32	Source fitted with a double PSF.
PSFSTAR	0x00000040	64	Source used to define PSF model.
SATSTAR	0x00000080	128	Source model peak is above saturation.
BLEND	0x00000100	256	Source is a blend with other sources.
EXTERNAL	0x00000200	512	Source based on supplied input position.
BADPSF	0x00000400	1024	Failed to get good estimate of object's PSF.
DEFECT	0x00000800	2048	Source is thought to be a defect.
SATURATED	0x00001000	4096	Source is thought to be saturated pixels (bleed trail).
CR_LIMIT	0x00002000	8192	Source has crNsigma above limit.
EXT_LIMIT	0x00004000	16384	Source has extNsigma above limit.
MOMENTS_FAILURE	0x00008000	32768	Could not measure the moments.
SKY_FAILURE	0x00010000	65536	Could not measure the local sky.
SKYVAR_FAILURE	0x00020000	131072	Could not measure the local sky variance.
BELOW_MOMENTS_SN	0x00040000	262144	Moments not measured due to low signal-to-noise ratio.
UNDEF_1	0x00080000	524288	Unused bit value.
BIG_RADIUS	0x00100000	1048576	Poor moments for small radius; try large radius.
AP_MAGS	0x00200000	2097152	Source has an aperture magnitude.
BLEND_FIT	0x00400000	4194304	Source was fitted as a blend.
EXTENDED_FIT	0x00800000	8388608	Full extended fit was used.
EXTENDED_STATS	0x01000000	16777216	Extended aperture stats calculated.
LINEAR_FIT	0x02000000	33554432	Source fitted with the linear fit.
NONLINEAR_FIT	0x04000000	67108864	Source fitted with the nonlinear fit.
RADIAL_FLUX	0x08000000	134217728	Radial flux measurements calculated.
SIZE_SKIPPED	0x10000000	268435456	Size could not be determined.
PEAK_ON_SPIKE	0x20000000	536870912	Peak lands on diffraction spike.
PEAK_ON_GHOST	0x40000000	1073741824	Peak lands on ghost or glint.
PEAK_OFF_CHIP	0x80000000	2147483648	Peak lands off edge of chip.

Table D7
DetectionFlags2

Name	Hexadecimal	Value	Description
DEFAULT	0x00000000	0	Initial value; resets all bits.
DIFF_WITH_SINGLE	0x00000001	1	Difference source matched to a single positive detection.
DIFF_WITH_DOUBLE	0x00000002	2	Difference source matched to positive detections in both images.
MATCHED	0x00000004	4	Source generated based on another image (forced photometry at source location).
ON_SPIKE	0x00000008	8	More than 25% of (PSF-weighted) pixels land on a diffraction spike.
ON_STARCORE	0x00000010	16	More than 25% of (PSF-weighted) pixels land on star core.
ON_BURNTOOL	0x00000020	32	More than 25% of (PSF-weighted) pixels land on burntool.
ON_CONVPOOR	0x00000040	64	More than 25% of (PSF-weighted) pixels land on convpoor.
PASS1_SRC	0x00000080	128	Source detected in first pass analysis
HAS_BRIGHTER_NEIGHBOR	0x00000100	256	Peak is not the brightest in its footprint
BRIGHT_NEIGHBOR_1	0x00000200	512	Flux_negative/(r^2 flux_positive) > 1.
BRIGHT_NEIGHBOR_10	0x00000400	1024	Flux_negative/(r^2 flux_positive) > 10.
DIFF_SELF_MATCH	0x00000800	2048	Positive detection match is probably this source.
SATSTAR_PROFILE	0x00001000	4096	Saturated source is modeled with a radial profile.
ECONTOUR_FEW_PTS	0x00002000	8192	Too few points to measure the elliptical contour.
RADBIN_NAN_CENTER	0x00004000	16384	Radial bins failed with too many NaN center bin.
PETRO_NAN_CENTER	0x00008000	32768	Petrosian (1976) radial bins failed with too many NaN center bin.
PETRO_NO_PROFILE	0x00010000	65536	Petrosian (1976) not built because radial bins missing.
PETRO_INSIG_RATIO	0x00020000	131072	Insignificant measurement of Petrosian (1976) ratio.
PETRO_RATIO_ZEROBIN	0x00040000	262144	Petrosian (1976) ratio in the zeroth bin (likely bad).
EXT_FITS_RUN	0x00080000	524288	Attempted to run extended fits on this source.
EXT_FITS_FAIL	0x00100000	1048576	At least one of the model fits failed.
EXT_FITS_RETRY	0x00200000	2097152	One of the model fits was retried with new window.
EXT_FITS_NONE	0x00400000	4194304	All of the model fits failed.

Table D8
DetectionFlags3

Name	Hexadecimal	Value	Description
DEFAULT	0x00000000	0	Initial value; resets all bits.
NOCAL	0x00000001	1	Detection ignored for this analysis (photcode; time range)—internal only.
POOR_PHOTOM	0x00000002	2	Detection is photometry outlier.
SKIP_PHOTOM	0x00000004	4	Detection was ignored for photometry measurement.
AREA	0x00000008	8	Detection near image edge.
POOR_ASTROM	0x00000010	16	Detection is astrometry outlier.
SKIP_ASTROM	0x00000020	32	Detection was ignored for astrometry measurement.
USED_OBJ	0x00000040	64	Detection was used during update objects
USED_CHIP	0x00000080	128	Detection was used during update chips to measure astrometry with IRLS fit.
BLEND_MEAS	0x00000100	256	Detection is within radius of multiple objects.
BLEND_OBJ	0x00000200	512	Multiple detections within radius of object.
WARP_USED	0x00000400	1024	Measurement used to find mean WARP photometry.
UNMASKED_ASTRO	0x00000800	2048	Detection was unmasked in update chips to determine astrometry parameter errors.
BLEND_MEAS_X	0x00001000	4096	Detection is within radius of multiple objects across catalogs.
ARTIFACT	0x00002000	8192	Detection is thought to be nonastronomical.
SYNTH_MAG	0x00004000	16384	Magnitude is synthetic.
PHOTOM_UBERCAL	0x00008000	32768	Externally supplied zero point from ubercal analysis.
STACK_PRIMARY	0x00010000	65536	This STACK measurement is in the primary skycell.
STACK_PHOT_SRC	0x00020000	131072	This measurement supplied the STACK photometry.
ICRF_QSO	0x00040000	262144	This measurement is an ICRF reference position.
IMAGE_EPOCH	0x00080000	524288	This measurement is registered to the image epoch (not tied to the reference catalog epoch).
PHOTOM_PSF	0x00100000	1048576	This measurement is used for the mean PSF magnitude.
PHOTOM_APER	0x00200000	2097152	This measurement is used for the mean aperture magnitude.
PHOTOM_KRON	0x00400000	4194304	This measurement is used for the mean Kron (1980) magnitude.
MASKED_PSF	0x01000000	16777216	This measurement is masked based on IRLS weights for the mean PSF magnitude.
MASKED_APER	0x02000000	33554432	This measurement is masked based on IRLS weights for the mean aperture magnitude.
MASKED_KRON	0x04000000	67108864	This measurement is masked based on IRLS weights for the mean Kron (1980) magnitude.
OBJECT_HAS_2MASS	0x10000000	268435456	This measurement comes from an object with 2MASS data.
OBJECT_HAS_GAIA	0x20000000	536870912	This measurement comes from an object with Gaia data.
OBJECT_HAS_TYCHO	0x40000000	1073741824	This measurement comes from an object with Tycho data.

D.2. Single Exposure Detection Tables

Table D9
ObjectThin: Contains the Positional Information for Objects in a Number of Coordinate Systems

Column Name	Units	Data Type	Default	Description
objName	···	VARCHAR(32)	NA	IAU name for this object.
objNameHMS	···	VARCHAR(32)	NA	Alternate sexigesimal name for this object (DR2 only).
objPSOName	···	VARCHAR(32)	NA	Alternate Pan-STARRS name for this object (DR1 only).
objAltName1	···	VARCHAR(32)	NA	Alternate name for this object.
objAltName2	···	VARCHAR(32)		Alternate name for this object.
objAltName3	···	VARCHAR(32)		Alternate name for this object.
objPopularName	···	VARCHAR(140)		Well-known name for this object.
objID	···	BIGINT	NA	Unique object identifier.
uniquePspsOBid	···	BIGINT	NA	Unique internal PSPS object identifier.
ippObjID	···	BIGINT	NA	IPP internal object identifier.
surveyID	···	TINYINT	NA	Survey identifier. Details in the Survey table.
htmID	···	BIGINT	NA	Hierarchical triangular mesh (Szalay et al. 2007) index.
zoneID	···	INT	NA	Local zone index, found by dividing the sky into bands of decl. 1/2 arcminute in height: zoneID = floor((90+decl.)/0.0083333).
tessID	···	TINYINT	0	Tessellation identifier. Details in the TessellationType table.
projectionID	···	SMALLINT	−1	Projection cell identifier.
skyCellID	···	TINYINT	255	Skycell region identifier.
randomID	···	FLOAT	NA	Random value drawn from the interval between zero and one.
batchID	···	BIGINT	NA	Internal database batch identifier.
dvoRegionID	···	INT	−1	Internal DVO region identifier.
processingVersion	···	TINYINT	NA	Data release version.
objInfoFlag	···	INT	0	Information flag bitmask indicating details of the photometry. Values listed in ObjectInfoFlags.
qualityFlag	···	TINYINT	0	Subset of objInfoFlag denoting whether this object is real or a likely false positive. Values listed in ObjectQualityFlags.
raStack	degrees	FLOAT	−999	Right ascension from STACK detections, weighted mean value across filters, in equinox J2000. See StackObjectThin for STACK epoch information.
decStack	degrees	FLOAT	−999	Decl. from STACK detections, weighted mean value across filters, in equinox J2000. See StackObjectThin for STACK epoch information.
raStackErr	arcsec	REAL	−999	Right ascension standard deviation from STACK detections.
decStackErr	arcsec	REAL	−999	Decl. standard deviation from STACK detections.
raMean	degrees	FLOAT	−999	Right ascension from single-epoch detections (weighted mean) in equinox J2000 at the mean epoch given by epochMean.
decMean	degrees	FLOAT	−999	Decl. from single-epoch detections (weighted mean) in equinox J2000 at the mean epoch given by epochMean.
raMeanErr	arcsec	REAL	−999	Right ascension standard deviation from single-epoch detections.
decMeanErr	arcsec	REAL	−999	Decl. standard deviation from single-epoch detections.
epochMean	days	FLOAT	−999	Modified Julian Date of the mean epoch corresponding to raMean, decMean (equinox J2000).
posMeanChisq	···	REAL	−999	Reduced chi-squared value of mean position.
cx	···	FLOAT	NA	Cartesian x on a unit sphere.
cy	···	FLOAT	NA	Cartesian y on a unit sphere.
cz	···	FLOAT	NA	Cartesian z on a unit sphere.
lambda	degrees	FLOAT	−999	Ecliptic longitude.
beta	degrees	FLOAT	−999	Ecliptic latitude.
l	degrees	FLOAT	−999	Galactic longitude.
b	degrees	FLOAT	−999	Galactic latitude.
nStackObjectRows	···	SMALLINT	−999	No. of independent StackObjectThin rows associated with this object.
nStackDetections	···	SMALLINT	−999	Number of STACK detections.
nDetections	···	SMALLINT	−999	Number of single-epoch detections in all filters.
ng	···	SMALLINT	−999	Number of single-epoch detections in the g filter.
nr	···	SMALLINT	−999	Number of single-epoch detections in the r filter.
ni	···	SMALLINT	−999	Number of single-epoch detections in the i filter.
nz	···	SMALLINT	−999	Number of single-epoch detections in the z filter.
ny	···	SMALLINT	−999	Number of single-epoch detections in the y filter.

Note. The objects associate single-epoch detections and the stacked detections within a 1″ radius. The mean position from the single-epoch data is used as the basis for coordinates when available, or the position of an object in the STACK when it is not. The R.A. and decl. for both the STACK and single-epoch mean are provided. The number of detections in each filter from single-epoch data is listed, along with which filters the object has a STACK detection (Szalay et al. 2007).

Table D10
MeanObject: Contains the Mean Photometric Information for Objects Based on the Single-epoch Data, Calculated as Described in Magnier et al. (2013)

Column Name	Units	Data Type	Default	Description
objID	⋯	BIGINT	NA	Unique object identifier.
uniquePspsOBid	⋯	BIGINT	NA	Unique internal PSPS object identifier.
gQfPerfect	⋯	REAL	−999	Maximum PSF-weighted fraction of pixels totally unmasked from *g*-filter detections.
gMeanPSFMag	AB	REAL	−999	Mean PSF magnitude from *g*-filter detections.
gMeanPSFMagErr	AB	REAL	−999	Error in mean PSF magnitude from *g*-filter detections.
gMeanPSFMagStd	AB	REAL	−999	Standard deviation of PSF magnitudes from *g*-filter detections.
gMeanPSFMagNpt	⋯	SMALLINT	−999	Number of measurements included in the mean PSF magnitude from *g*-filter detections.
gMeanPSFMagMin	AB	REAL	−999	Minimum PSF magnitude from *g*-filter detections.
gMeanPSFMagMax	AB	REAL	−999	Maximum PSF magnitude from *g*-filter detections.
gMeanKronMag	AB	REAL	−999	Mean Kron (1980) magnitude from *g*-filter detections.
gMeanKronMagErr	AB	REAL	−999	Error in mean Kron (1980) magnitude from *g*-filter detections.
gMeanKronMagStd	AB	REAL	−999	Standard deviation of Kron (1980) magnitudes from *g*-filter detections.
gMeanKronMagNpt	⋯	SMALLINT	−999	Number of measurements included in mean Kron (1980) magnitude from *g*-filter detections.
gMeanApMag	AB	REAL	−999	Mean aperture magnitude from *g*-filter detections.
gMeanApMagErr	AB	REAL	−999	Error in mean aperture magnitude from *g*-filter detections.
gMeanApMagStd	AB	REAL	−999	Standard deviation of aperture magnitudes from *g*-filter detections.
gMeanApMagNpt	⋯	SMALLINT	−999	Number of measurements included in the mean aperture magnitude from *g*-filter detections.
gFlags	⋯	INT	0	Information flag bitmask for mean object from *g*-filter detections. Values listed in ObjectFilterFlags.
rQfPerfect ... yFlags				Same entries repeated for the *r*, *i*, *z*, and *y* filters

Note. To be included in this table, an object must be bright enough to have been detected at least once in an individual exposure. PSF, Kron (1980), and aperture magnitudes and statistics are listed for all filters.

Table D11
GaiaFrameCoordinate: PSPS Objects Calibrated Against Gaia Astrometry

Column Name	Units	Data Type	Default	Description
objID	⋯	BIGINT	NA	Unique object identifier.
uniquePspsGOid	⋯	BIGINT	NA	Unique internal PSPS object identifier.
ippObjID	⋯	BIGINT	NA	IPP internal object identifier.
batchID	⋯	BIGINT	NA	Internal database batch identifier.
gaiaFlag	⋯	INT		Information flag bitmask.
ra	degrees	FLOAT	−999	Right ascension from single-epoch detections (weighted mean) in equinox J2000 at the mean epoch given by epochMean and calibrated against Gaia.
dec	degrees	FLOAT	−999	Decl. from single-epoch detections (weighted mean) in equinox J2000 at the mean epoch given by epochMean and calibrated against Gaia.
raErr	arcsec	REAL	−999	Right ascension standard deviation from single-epoch detections.
decErr	arcsec	REAL	−999	Decl. standard deviation from single-epoch detections.

Table D12
FrameMeta: Contains Metadata Related to an Individual Exposure

Column Name	Units	Data Type	Default	Description
frameID	⋯	INT	NA	Unique frame/exposure identifier.
frameName	⋯	VARCHAR(32)	NA	Frame/exposure name provided by the camera software.
surveyID	⋯	TINYINT	NA	Survey identifier. Details in the Survey table.
filterID	⋯	TINYINT	NA	Filter identifier. Details in the Filter table.
ippChipID	⋯	INT	NA	IPP chipRun identifier.
ippCamID	⋯	INT	NA	IPP camRun identifier.
ippWarpID	⋯	INT	NA	IPP warpRun identifier.
cameraID	⋯	SMALLINT	NA	Camera identifier. Details in the CameraConfig table.
cameraConfigID	⋯	SMALLINT	NA	Camera configuration identifier. Details in the CameraConfig table.
telescopeID	⋯	SMALLINT	NA	Telescope identifier.
analysisVer	⋯	VARCHAR(100)		IPP software analysis release version.
md5sum	⋯	VARCHAR(100)		IPP MD5 Checksum.
nOTA	⋯	SMALLINT	−999	Number of valid OTA images in this frame/exposure.
photoScat	magnitudes	REAL	−999	Photometric scatter relative to reference catalog across the full FOV.
nPhotoRef	⋯	INT	−999	Number of photometric reference sources.
expStart	days	FLOAT	−999	Modified Julian Date at the start of the exposure.
expTime	seconds	REAL	−999	Exposure time of the frame/exposure. Necessary for converting listed fluxes and magnitudes back to measured ADU counts.
airmass	⋯	REAL	0	Airmass at midpoint of the exposure. Necessary for converting listed fluxes and magnitudes back to measured ADU counts.
raBore	degrees	FLOAT	−999	Right ascension of telescope boresight.
decBore	degrees	FLOAT	−999	Decl. of telescope boresight.
ctype1	⋯	VARCHAR(100)		Name of astrometric projection in R.A.
ctype2	⋯	VARCHAR(100)		Name of astrometric projection in decl.
crval1	degrees	FLOAT	−999	Right ascension corresponding to reference pixel.
crval2	degrees	FLOAT	−999	Decl. corresponding to reference pixel.
crpix1	pixels	FLOAT	−999	Reference pixel for R.A.
crpix2	pixels	FLOAT	−999	Reference pixel for decl.
cdelt1	degrees/pixel	FLOAT	−999	Pixel scale in R.A.
cdelt2	degrees/pixel	FLOAT	−999	Pixel scale in decl.
pc001001	⋯	FLOAT	−999	Linear transformation matrix element between focal plane pixel L and R.A.
pc001002	⋯	FLOAT	−999	Linear transformation matrix element between focal plane pixel M and R.A.
pc002001	⋯	FLOAT	−999	Linear transformation matrix element between focal plane pixel L and decl.
pc002002	⋯	FLOAT	−999	Linear transformation matrix element between focal plane pixel M and decl.
polyOrder	⋯	TINYINT	255	Polynomial order of astrometric fit between detector focal plane and sky.
pca1x3y0	⋯	FLOAT	−999	Polynomial coefficient for the astrometric fit component (x^3 y^0) for R.A.
pca1x2y1	⋯	FLOAT	−999	Polynomial coefficient for the astrometric fit component (x^2 y^1) for R.A.
pca1x1y2	⋯	FLOAT	−999	Polynomial coefficient for the astrometric fit component (x^1 y^2) for R.A.
pca1x0y3	⋯	FLOAT	−999	Polynomial coefficient for the astrometric fit component (x^0 y^3) for R.A.
pca1x2y0	⋯	FLOAT	−999	Polynomial coefficient for the astrometric fit component (x^2 y^0) for R.A.
pca1x1y1	⋯	FLOAT	−999	Polynomial coefficient for the astrometric fit component (x^1 y^1) for R.A.
pca1x0y2	⋯	FLOAT	−999	Polynomial coefficient for the astrometric fit component (x^0 y^2) for R.A.
pca2x3y0	⋯	FLOAT	−999	Polynomial coefficient for the astrometric fit component (x^3 y^0) for decl.
pca2x2y1	⋯	FLOAT	−999	Polynomial coefficient for the astrometric fit component (x^2 y^1) for decl.
pca2x1y2	⋯	FLOAT	−999	Polynomial coefficient for the astrometric fit component (x^1 y^2) for decl.
pca2x0y3	⋯	FLOAT	−999	Polynomial coefficient for the astrometric fit component (x^0 y^3) for decl.
pca2x2y0	⋯	FLOAT	−999	Polynomial coefficient for the astrometric fit component (x^2 y^0) for decl.
pca2x1y1	⋯	FLOAT	−999	Polynomial coefficient for the astrometric fit component (x^1 y^1) for decl.
pca2x0y2	⋯	FLOAT	−999	Polynomial coefficient for the astrometric fit component (x^0 y^2) for decl.
batchID	⋯	BIGINT	NA	Internal database batch identifier.
processingVersion	⋯	TINYINT	NA	Data release version.

Note. A "Frame" refers to the collection of all images obtained by the 60 OTA devices in the camera in a single exposure. The camera configuration, telescope pointing, observation time, and astrometric solution from the detector focal plane (L, M) to the sky (R.A., decl.) are provided.

Table D13
ImageMeta: Contains Metadata Related to an Individual OTA Image That Comprises a Portion of the Full Exposure

Column Name	Units	Data Type	Default	Description
imageID	⋯	BIGINT	NA	Unique image identifier. Constructed as (100 × frameID + ccdID).
frameID	⋯	INT	NA	Unique frame/exposure identifier.
ccdID	⋯	SMALLINT	NA	OTA identifier based on location in the focal plane, specific to an individual device.
photoCalID	⋯	INT	NA	Photometric calibration identifier. Details in the PhotoCal table.
filterID	⋯	TINYINT	NA	Filter identifier. Details in the Filter table.
bias	adu	REAL	−999	OTA bias level.
biasScat	adu	REAL	−999	Scatter in bias level.
sky	Jy arcsec^{-2}	REAL	−999	Mean sky brightness.
skyScat	Jy arcsec^{-2}	REAL	−999	Scatter in mean sky brightness.
nDetect	⋯	INT	−999	Number of detections in this image.
detectionThreshold	magnitudes	REAL	−999	Reference magnitude for detection efficiency calculation.
astroScat	arcseconds	REAL	−999	Measurement of the calibration (not astrometric error) defined to be the sum in quadrature of the standard deviations in the X and Y directions.
photoScat	magnitudes	REAL	−999	Photometric scatter relative to reference catalog.
nAstroRef	⋯	INT	−999	Number of astrometric reference sources.
nPhotoRef	⋯	INT	−999	Number of photometric reference sources.
recalAstroScatX	arcseconds	REAL	−999	Measurement of the recalibration (not astrometric error) in the X direction.
recalAstroScatY	arcseconds	REAL	−999	Measurement of the recalibration (not astrometric error) in the Y direction.
recalNAstroStars	⋯	INT	−999	Number of astrometric reference sources used in recalibration.
recalphotoScat	magnitudes	REAL	−999	Photometric scatter relative to reference catalog.
recalNPhotoStars	⋯	INT	−999	Number of astrometric reference sources used in recalibration.
nAxis1	pixels	SMALLINT	−999	Image dimension in x.
nAxis2	pixels	SMALLINT	−999	Image dimension in y.
psfModelID	⋯	INT	−999	PSF model identifier.
psfFWHM	arcseconds	REAL	−999	Mean PSF FWHM at image center.
psfWidMajor	arcseconds	REAL	−999	PSF major axis FWHM at image center.
psfWidMinor	arcseconds	REAL	−999	PSF minor axis FWHM at image center.
psfTheta	degrees	REAL	−999	PSF major axis orientation at image center.
momentMajor	arcseconds	REAL	−999	PSF major axis second moment.
momentMinor	arcseconds	REAL	−999	PSF minor axis second moment.
momentM2C	arcsec^2	REAL	−999	Moment $M2C = M_{xx} - M_{yy}$.
momentM2S	arcsec^2	REAL	−999	Moment $M2S = 2M_{xy}$.
momentM3	arcsec^2	REAL	−999	Trefoil second moment $= \sqrt{(M_{xxx} - 3M_{xyy})^2 + (3M_{xxy} - M_{yyy})^2}$.
momentM4	arcsec^2	REAL	−999	Quadrupole second moment $= \sqrt{(M_{xxxx} - 6M_{xxyy} + M_{yyyy})^2 + (4M_{xxxy} - 4M_{xyyy})^2}$.
apResid	magnitudes	REAL	−999	Residual of aperture corrections.
dapResid	magnitudes	REAL	−999	Scatter of aperture corrections.
detectorID	⋯	VARCHAR (100)		Identifier for each individual OTA detector device.
qaFlags	⋯	BIGINT	−999	Q/A flags for this image. Values listed in ImageFlags.
detrend1	⋯	VARCHAR (100)		Identifier for detrend image 1, the static mask.
detrend2	⋯	VARCHAR (100)		Identifier for detrend image 2, the dark model.
detrend3	⋯	VARCHAR (100)		Identifier for detrend image 3, the flat.
detrend4	⋯	VARCHAR (100)		Identifier for detrend image 4, the fringe.
detrend5	⋯	VARCHAR (100)		Identifier for detrend image 5, the noise map.
detrend6	⋯	VARCHAR (100)		Identifier for detrend image 6, the nonlinearity correction.
detrend7	⋯	VARCHAR (100)		Identifier for detrend image 7, the video dark model.
detrend8	⋯	VARCHAR (100)		Identifier for detrend image 8.
photoZero	magnitudes	REAL	−999	Locally derived photometric zero point for this image.
ctype1	⋯	VARCHAR (100)		Name of astrometric projection in focal plane L.
ctype2	⋯	VARCHAR (100)		Name of astrometric projection in focal plane M.
crval1	focal plane pixels	FLOAT	−999	Focal plane L corresponding to reference pixel.
crval2	focal plane pixels	FLOAT	−999	Focal plane M corresponding to reference pixel.

Table D13
(Continued)

Column Name	Units	Data Type	Default	Description
crpix1	raw pixels	FLOAT	−999	Reference pixel for focal plane *L*.
crpix2	raw pixels	FLOAT	−999	Reference pixel for focal plane *M*.
cdelt1	focal plane pixels/ raw pixel	FLOAT	−999	Pixel scale in focal plane *x*.
cdelt2	focal plane pixels/ raw pixel	FLOAT	−999	Pixel scale in focal plane *y*.
pc001001	⋯	FLOAT	−999	Linear transformation matrix element between image pixel *x* and focal plane pixel *L*.
pc001002	⋯	FLOAT	−999	Linear transformation matrix element between image pixel *y* and focal plane pixel *L*.
pc002001	⋯	FLOAT	−999	Linear transformation matrix element between image pixel *x* and focal plane pixel *M*.
pc002002	⋯	FLOAT	−999	Linear transformation matrix element between image pixel *y* and focal plane pixel *M*.
polyOrder	⋯	TINYINT	255	Polynomial order of astrometric fit between the image pixels and the detector focal plane.
pca1x3y0	⋯	FLOAT	−999	Polynomial coefficient for the astrometric fit component (x^3 y^0) for focal plane *L*.
pca1x2y1	⋯	FLOAT	−999	Polynomial coefficient for the astrometric fit component (x^2 y^1) for focal plane *L*.
pca1x1y2	⋯	FLOAT	−999	Polynomial coefficient for the astrometric fit component (x^1 y^2) for focal plane *L*.
pca1x0y3	⋯	FLOAT	−999	Polynomial coefficient for the astrometric fit component (x^0 y^3) for focal plane *L*.
pca1x2y0	⋯	FLOAT	−999	Polynomial coefficient for the astrometric fit component (x^2 y^0) for focal plane *L*.
pca1x1y1	⋯	FLOAT	−999	Polynomial coefficient for the astrometric fit component (x^1 y^1) for focal plane *L*.
pca1x0y2	⋯	FLOAT	−999	Polynomial coefficient for the astrometric fit component (x^0 y^2) for focal plane *L*.
pca2x3y0	⋯	FLOAT	−999	Polynomial coefficient for the astrometric fit component (x^3 y^0) for focal plane *M*.
pca2x2y1	⋯	FLOAT	−999	Polynomial coefficient for the astrometric fit component (x^2 y^1) for focal plane *M*.
pca2x1y2	⋯	FLOAT	−999	Polynomial coefficient for the astrometric fit component (x^1 y^2) for focal plane *M*.
pca2x0y3	⋯	FLOAT	−999	Polynomial coefficient for the astrometric fit component (x^0 y^3) for focal plane *M*.
pca2x2y0	⋯	FLOAT	−999	Polynomial coefficient for the astrometric fit component (x^2 y^0) for focal plane *M*.
pca2x1y1	⋯	FLOAT	−999	Polynomial coefficient for the astrometric fit component (x^1 y^1) for focal plane *M*.
pca2x0y2	⋯	FLOAT	−999	Polynomial coefficient for the astrometric fit component (x^0 y^2) for focal plane *M*.
processingVersion	⋯	TINYINT	NA	Data release version.

Note. The characterization of the image quality, the detrends applied, and the astrometric solution from the raw pixels (*X*, *Y*) to the detector focal plane (*L*, *M*) are provided.

Table D14
Detection: Contains Single-epoch Photometry of Individual Detections from a Single Exposure

Column Name	Units	Data Type	Default	Description
objID	⋯	BIGINT	NA	Unique object identifier.
uniquePspsP2id	⋯	BIGINT	NA	Unique internal PSPS detection identifier.
detectID	⋯	BIGINT	NA	Unique detection identifier.
ippObjID	⋯	BIGINT	NA	IPP internal object identifier.
ippDetectID	⋯	BIGINT	NA	IPP internal detection identifier.
filterID	⋯	TINYINT	NA	Filter identifier. Details in the Filter table.
surveyID	⋯	TINYINT	NA	Survey identifier. Details in the Survey table.
imageID	⋯	BIGINT	NA	Unique image identifier. Constructed as (100 × frameID + ccdID).
randomDetID	⋯	FLOAT	NA	Random value drawn from the interval between zero and one.
dvoRegionID	⋯	INT	−1	Internal DVO region identifier.
obsTime	days	FLOAT	−999	Modified Julian Date at the midpoint of the observation.
xPos	raw pixels	REAL	−999	PSF *x*-center location.
yPos	raw pixels	REAL	−999	PSF *y*-center location.
xPosErr	raw pixels	REAL	−999	Error in the PSF *x* -center location.
yPosErr	raw pixels	REAL	−999	Error in the PSF *y*-center location.
pltScale	arcseconds/pixel	REAL	−999	Local plate scale at this location.
posAngle	degrees	REAL	−999	Position angle (sky-to-chip) at this location.
ra	degrees	FLOAT	−999	Right ascension.
dec	degrees	FLOAT	−999	Declination.
raErr	arcseconds	REAL	−999	Right ascension error.
decErr	arcseconds	REAL	−999	Declination error.
extNSigma	⋯	REAL	0	An extendedness measure based on the deviation between PSF and Kron magnitudes, normalized by the PSF magnitude uncertainty.
zp	magnitudes	REAL	0	Photometric zero point. Necessary for converting listed fluxes and magnitudes back to measured ADU counts.
telluricExt	magnitudes	REAL	NA	Estimated Telluric extinction due to nonphotometric observing conditions. Necessary for converting listed fluxes and magnitudes back to measured ADU counts.
expTime	seconds	REAL	−999	Exposure time of the frame/exposure. Necessary for converting listed fluxes and magnitudes back to measured ADU counts.
airMass	⋯	REAL	0	Airmass at midpoint of the exposure. Necessary for converting listed fluxes and magnitudes back to measured ADU counts.
psfFlux	Jy	REAL	−999	Flux from PSF fit.
psfFluxErr	Jy	REAL	−999	Error on flux from PSF fit.
psfMajorFWHM	arcsec	REAL	−999	PSF major axis FWHM.
psfMinorFWHM	arcsec	REAL	−999	PSF minor axis FWHM.
psfTheta	degrees	REAL	−999	PSF major axis orientation.
psfCore	⋯	REAL	−999	PSF core parameter k, where $F = F0/(1 + kr^2 + r^{3.33})$.
psfQf	⋯	REAL	−999	PSF coverage factor.
psfQfPerfect	⋯	REAL	−999	PSF weighted fraction of pixels totally unmasked.
psfChiSq	⋯	REAL	−999	Reduced chi-squared value of the PSF model fit.
psfLikelihood	⋯	REAL	−999	Likelihood that this detection is best fit by a PSF.
momentXX	arcsec^2	REAL	−999	Second moment M_{xx}.
momentXY	arcsec^2	REAL	−999	Second moment M_{xy}.
momentYY	arcsec^2	REAL	−999	Second moment M_{yy}.
momentR1	arcsec	REAL	−999	First radial moment.
momentRH	$\mathrm{arcsec}^{0.5}$	REAL	−999	Half-radial moment ($r^{0.5}$ weighting).
momentM3C	arcsec^2	REAL	−999	Cosine of trefoil second moment term: $r^2\cos(3\theta) = M_{xxx} - 3M_{xyy}$.
momentM3S	arcsec^2	REAL	−999	Sine of trefoil second moment: $r^2\sin(3\theta) = 3M_{xxy} - M_{yyy}$.
momentM4C	arcsec^2	REAL	−999	Cosine of quadrupole second moment: $r^2\cos(4\theta) = M_{xxxx} - 6M_{xxyy} + M_{yyyy}$.
momentM4S	arcsec^2	REAL	−999	Sine of quadrupole second moment: $r^2\sin(4\theta) = 4M_{xxxy} - 4M_{xyyy}$.
apFlux	Jy	REAL	−999	Flux in seeing-dependent aperture.
apFluxErr	Jy	REAL	−999	Error on flux in seeing-dependent aperture.
apFillF	⋯	REAL	−999	Aperture fill factor.
apRadius	arcsec	REAL	−999	Aperture radius.
kronFlux	Jy	REAL	−999	Kron (1980) flux.
kronFluxErr	Jy	REAL	−999	Error on Kron (1980) flux.
kronRad	arcsec	REAL	−999	Kron (1980) radius.
sky	Jy arcsec^{-2}	REAL	−999	Background sky level.
skyErr	Jy arcsec^{-2}	REAL	−999	Error in background sky level.
infoFlag	⋯	BIGINT	0	Information flag bitmask indicating details of the photometry. Values listed in DetectionFlags.
infoFlag2	⋯	INT	0	Information flag bitmask indicating details of the photometry. Values listed in DetectionFlags2.

Table D14
(Continued)

Column Name	Units	Data Type	Default	Description
infoFlag3	···	INT	0	Information flag bitmask indicating details of the photometry. Values listed in DetectionFlags3.
processingVersion	···	TINYINT	NA	Data release version.

Note. The identifiers connecting the detection back to the original image and to the object association are provided. PSF, aperture, and Kron (1980) photometry are included, along with sky and detector coordinate positions.

Table D15
ImageDetEffMeta: Contains the Detection Efficiency Information for a Given Individual OTA Image

Column Name	Units	Data Type	Default	Description
imageID	···	BIGINT	NA	Unique image identifier. Constructed as (100 × frameID + ccdID).
frameID	···	INT	NA	Unique frame/exposure identifier.
magref	magnitudes	REAL	NA	Detection efficiency reference magnitude.
nInjected	···	INT	NA	Number of fake sources injected in each magnitude bin.
offset01	magnitudes	REAL	NA	Detection efficiency magnitude offset for bin 1.
counts01	···	REAL	NA	Detection efficiency count of recovered sources in bin 1.
diffMean01	magnitudes	REAL	NA	Detection efficiency mean magnitude difference in bin 1.
diffStdev01	magnitudes	REAL	NA	Detection efficiency standard deviation of magnitude differences in bin 1.
errMean01	magnitudes	REAL	NA	Detection efficiency mean magnitude error in bin 1.
offset02	magnitudes	REAL	NA	Detection efficiency magnitude offset for bin 2.
counts02	···	REAL	NA	Detection efficiency count of recovered sources in bin 2.
diffMean02	magnitudes	REAL	NA	Detection efficiency mean magnitude difference in bin 2.
diffStdev02	magnitudes	REAL	NA	Detection efficiency standard deviation of magnitude differences in bin 2.
errMean02	magnitudes	REAL	NA	Detection efficiency mean magnitude error in bin 2.
offset03	magnitudes	REAL	NA	Detection efficiency magnitude offset for bin 3.
counts03	···	REAL	NA	Detection efficiency count of recovered sources in bin 3.
diffMean03	magnitudes	REAL	NA	Detection efficiency mean magnitude difference in bin 3.
diffStdev03	magnitudes	REAL	NA	Detection efficiency standard deviation of magnitude differences in bin 3.
errMean03	magnitudes	REAL	NA	Detection efficiency mean magnitude error in bin 3.
...				
offset13	magnitudes	REAL	NA	Detection efficiency magnitude offset for bin 13.
counts13	···	REAL	NA	Detection efficiency count of recovered sources in bin 13.
diffMean13	magnitudes	REAL	NA	Detection efficiency mean magnitude difference in bin 13.
diffStdev13	magnitudes	REAL	NA	Detection efficiency standard deviation of magnitude differences in bin 13.
errMean13	magnitudes	REAL	NA	Detection efficiency mean magnitude error in bin 13.

Note. Provides the number of recovered sources out of 500 injected fake sources and statistics about the magnitudes of the recovered sources for a range of magnitude offsets.

D.3. Stack Tables

Table D16
StackMeta: Contains the Metadata Describing the Stacked Image Produced from the Combination of a Set of Single-epoch Exposures

Column Name	Units	Data Type	Default	Description
stackImageID	⋯	BIGINT	NA	Unique STACK identifier.
batchID	⋯	BIGINT	NA	Internal database batch identifier.
surveyID	⋯	TINYINT	NA	Survey identifier. Details in the Survey table.
filterID	⋯	TINYINT	NA	Filter identifier. Details in the Filter table.
stackTypeID	⋯	TINYINT	0	Stack-type identifier. Details in the StackType table.
tessID	⋯	TINYINT	0	Tessellation identifier. Details in the TessellationType table.
projectionID	⋯	SMALLINT	−1	Projection cell identifier.
skyCellID	⋯	TINYINT	255	Skycell region identifier.
photoCalID	⋯	INT	NA	Photometric calibration identifier. Details in the PhotoCal table.
analysisVer	⋯	VARCHAR(100)		IPP software analysis release version.
md5sum	⋯	VARCHAR(100)		IPP MD5 Checksum.
expTime	seconds	REAL	−999	Exposure time of the stack. Necessary for converting listed fluxes and magnitudes back to measured ADU counts.
nP2Images	⋯	SMALLINT	−999	Number of input exposures/frames contributing to this stack.
detectionThreshold	magnitudes	REAL	−999	Reference magnitude for detection efficiency calculation.
astroScat	⋯	REAL	−999	Measurement of the calibration (not astrometric error) defined to be the sum in quadrature of the standard deviations in the *X* and *Y* directions.
photoScat	⋯	REAL	−999	Photometric scatter relative to the reference catalog.
nAstroRef	⋯	INT	−999	Number of astrometric reference sources.
nPhotoRef	⋯	INT	−999	Number of photometric reference sources.
recalAstroScatX	arcsec	REAL	−999	Measurement of the recalibration (not astrometric error) in the *X* direction.
recalAstroScatY	arcsec	REAL	−999	Measurement of the recalibration (not astrometric error) in the *Y* direction.
recalNAstroStars	⋯	INT	−999	Number of astrometric reference sources used in recalibration.
recalphotoScat	magnitudes	REAL	−999	Photometric scatter relative to reference catalog.
recalNPhotoStars	⋯	INT	−999	Number of astrometric reference sources used in recalibration.
psfModelID	⋯	INT	−999	PSF model identifier.
psfFWHM	arcsec	REAL	−999	Mean PSF FWHM at image center.
psfWidMajor	arcsec	REAL	−999	PSF major axis FWHM at image center.
psfWidMinor	arcsec	REAL	−999	PSF minor axis FWHM at image center.
psfTheta	degrees	REAL	−999	PSF major axis orientation at image center.
photoZero	magnitudes	REAL	−999	Locally derived photometric zero point for this stack.
photoZeroAperture	magnitudes	REAL	−999	Locally derived photometric zero point for this stack (aperture-like measurements only; DR2).
ctype1	⋯	VARCHAR(100)		Name of astrometric projection in R.A.
ctype2	⋯	VARCHAR(100)		Name of astrometric projection in decl.
crval1	degrees	FLOAT	−999	R.A. corresponding to reference pixel.
crval2	degrees	FLOAT	−999	Decl. corresponding to reference pixel.
crpix1	sky pixels	FLOAT	−999	Reference pixel for R.A.
crpix2	sky pixels	FLOAT	−999	Reference pixel for decl.
cdelt1	degrees/pixel	FLOAT	−999	Pixel scale in R.A.
cdelt2	degrees/pixel	FLOAT	−999	Pixel scale in decl.
pc001001	⋯	FLOAT	−999	Linear transformation matrix element between image pixel *x* and R.A.
pc001002	⋯	FLOAT	−999	Linear transformation matrix element between image pixel *y* and R.A.
pc002001	⋯	FLOAT	−999	Linear transformation matrix element between image pixel *x* and decl.
pc002002	⋯	FLOAT	−999	Linear transformation matrix element between image pixel *y* and decl.
processingVersion	⋯	TINYINT	NA	Data release version.

Note. The nature of the STACK is given by the StackTypeID. The astrometric and photometric calibration of the stacked image are listed.

Table D17
StackObjectThin: Contains the Positional and Photometric Information for Point-source Photometry of STACK Detections

Column Name	Units	Data Type	Default	Description
objID	⋯	BIGINT	NA	Unique object identifier.
uniquePspsSTid	⋯	BIGINT	NA	Unique internal PSPS STACK identifier.
ippObjID	⋯	BIGINT	NA	IPP internal object identifier.
surveyID	⋯	TINYINT	NA	Survey identifier. Details in the Survey table.
tessID	⋯	TINYINT	0	Tessellation identifier. Details in the TessellationType table.
projectionID	⋯	SMALLINT	−1	Projection cell identifier.
skyCellID	⋯	TINYINT	255	Skycell region identifier.
randomStackObjID	⋯	FLOAT	NA	Random value drawn from the interval between zero and one.
primaryDetection	⋯	TINYINT	255	Identifies if this row is the primary STACK detection (incorrectly set in DR1 and DR2).
bestDetection	⋯	TINYINT	255	Identifies if this row is the best detection (incorrectly set in DR1 and DR2).
dvoRegionID	⋯	INT	−1	Internal DVO region identifier.
processingVersion	⋯	TINYINT	NA	Data release version.
gippDetectID	⋯	BIGINT	NA	IPP internal detection identifier.
gstackDetectID	⋯	BIGINT	NA	Unique STACK detection identifier.
gstackImageID	⋯	BIGINT	NA	Unique STACK identifier for *g*-filter detection.
gra	degrees	FLOAT	−999	Right ascension from *g*-filter STACK detection.
gdec	degrees	FLOAT	−999	Decl. from *g*-filter STACK detection.
graErr	arcseconds	REAL	−999	Right ascension error from *g*-filter STACK detection.
gdecErr	arcsec	REAL	−999	Decl. error from *g*-filter STACK detection.
gEpoch	days	FLOAT	−999	Modified Julian Date of the mean epoch of images contributing to the *g*-band STACK (equinox J2000).
gPSFMag	AB	REAL	−999	PSF magnitude from the *g*-filter STACK detection.
gPSFMagErr	AB	REAL	−999	Error in the PSF magnitude from the *g*-filter STACK detection.
gApMag	AB	REAL	−999	Aperture magnitude from the *g*-filter STACK detection.
gApMagErr	AB	REAL	−999	Error in the aperture magnitude from the *g*-filter STACK detection.
gKronMag	AB	REAL	−999	Kron (1980) magnitude from the *g*-filter STACK detection.
gKronMagErr	AB	REAL	−999	Error in the Kron (1980) magnitude from the *g*- filter STACK detection.
ginfoFlag	⋯	BIGINT	0	Information flag bitmask indicating details of the *g*-filter STACK photometry. Values listed in DetectionFlags.
ginfoFlag2	⋯	INT	0	Information flag bitmask indicating details of the *g*-filter STACK photometry. Values listed in DetectionFlags2.
ginfoFlag3	⋯	INT	0	Information flag bitmask indicating details of the *g*-filter STACK photometry. Values listed in DetectionFlags3.
ginfoFlag4	⋯	INT	0	Information flag bitmask indicating details of the *g* filter stack photometry. Values listed in ObjectFilterFlags. (DR2)
gnFrames	⋯	INT	−999	Number of input frames/exposures contributing to the *g*-filter STACK detection.
rippDetectID ... ynFrames				Same entries repeated for the *r*, *i*, *z*, and *y* filters

Note. The information for all filters are joined into a single row, with metadata indicating if this STACK object represents the primary detection. Due to overlaps in the STACK tessellations, an object may appear in multiple STACK images. The primary detection is the unique detection from the STACK image that provides the best coverage with minimal projection stretching. All other detections of the object in that filter are secondary, regardless of their properties. The detection flagged as best is the primary detection if that detection has a psfQf value greater than 0.98; if that is not met, then any of the primary or secondary detections with the highest psfQf value is flagged as best.

Table D18
StackObjectAttributes: Contains the PSF, Kron (1980), and Aperture Fluxes for All Filters in a Single Row, along with Point-source Object Shape Parameters

Column Name	Units	Data Type	Default	Description
objID	⋯	BIGINT	NA	Unique object identifier.
uniquePspsSTid	⋯	BIGINT	NA	Unique internal PSPS STACK identifier.
ippObjID	⋯	BIGINT	NA	IPP internal object identifier.
randomStackObjID	⋯	FLOAT	NA	Random value drawn from the interval between zero and one.
primaryDetection	⋯	TINYINT	255	Identifies if this row is the primary STACK detection.
bestDetection	⋯	TINYINT	255	Identifies if this row is the best detection.
gippDetectID	⋯	BIGINT	NA	IPP internal detection identifier.
gstackDetectID	⋯	BIGINT	NA	Unique STACK detection identifier.
gstackImageID	⋯	BIGINT	NA	Unique STACK identifier for *g*-filter detection.
gxPos	sky pixels	REAL	−999	PSF *x*-center location from *g*-filter STACK detection.
gyPos	sky pixels	REAL	−999	PSF *y*-center location from *g*-filter STACK detection.
gxPosErr	sky pixels	REAL	−999	Error in PSF *x*-center location from *g*-filter STACK detection.
gyPosErr	sky pixels	REAL	−999	Error in PSF *y*-center location from *g*-filter STACK detection.
gpsfMajorFWHM	arcseconds	REAL	−999	PSF major axis FWHM from *g*-filter STACK detection.
gpsfMinorFWHM	arcseconds	REAL	−999	PSF minor axis FWHM from *g*-filter STACK detection.
gpsfTheta	degrees	REAL	−999	PSF major axis orientation from *g*-filter STACK detection.
gpsfCore	⋯	REAL	−999	PSF core parameter k from *g*-filter STACK detection, where $F = F0/(1 + kr^2 + r^{3.33})$.
gpsfLikelihood	⋯	REAL	−999	Likelihood that this *g*-filter STACK detection is best fit by a PSF.
gpsfQf	⋯	REAL	−999	PSF coverage factor for *g*-filter STACK detection.
gpsfQfPerfect	⋯	REAL	−999	PSF-weighted fraction of pixels totally unmasked for *g*-filter STACK detection.
gpsfChiSq	⋯	REAL	−999	Reduced chi-squared value of the PSF model fit for *g*-filter STACK detection.
gmomentXX	arcsec^2	REAL	−999	Second moment M_{xx} for the *g*-filter STACK detection.
gmomentXY	arcsec^2	REAL	−999	Second moment M_{xy} for the *g*-filter STACK detection.
gmomentYY	arcsec^2	REAL	−999	Second moment M_{yy} for the *g*-filter STACK detection.
gmomentR1	arcseconds	REAL	−999	First radial moment for the *g*-filter STACK detection.
gmomentRH	$\mathrm{arcsec}^{0.5}$	REAL	−999	Half-radial moment ($r^{0.5}$ weighting) for the *g*-filter STACK detection.
gPSFFlux	Jansky	REAL	−999	PSF flux from the *g*-filter STACK detection.
gPSFFluxErr	Jansky	REAL	−999	Error in PSF flux from the *g*-filter STACK detection.
gApFlux	Jansky	REAL	−999	Aperture flux from the *g*-filter STACK detection.
gApFluxErr	Jansky	REAL	−999	Error in aperture flux from the *g*-filter STACK detection.
gApFillFac	⋯	REAL	−999	Aperture fill factor from the *g*-filter STACK detection.
gApRadius	arcseconds	REAL	−999	Aperture radius for the *g*-filter STACK detection.
gKronFlux	Jansky	REAL	−999	Kron (1980) flux from *g*-filter STACK detection.
gKronFluxErr	Jansky	REAL	−999	Error in Kron (1980) flux from the *g*-filter STACK detection.
gKronRad	arcseconds	REAL	−999	Kron (1980) radius from *g*-filter STACK detection.
gexpTime	seconds	REAL	−999	Exposure time of the *g*-filter stack. Necessary for converting listed fluxes and magnitudes back to measured ADU counts.
gExtNSigma	⋯	REAL	−999	An extendedness measure for the *g*-filter STACK detection based on the deviation between the PSF and Kron (1980) magnitudes, normalized by the PSF magnitude uncertainty.
gsky	$\mathrm{Jy\ arcsec}^{-2}$	REAL	−999	Residual background sky level at the *g*-filter STACK detection.
gskyErr	$\mathrm{Jy\ arcsec}^{-2}$	REAL	−999	Error in the residual background sky level at the *g*-filter STACK detection.
gzp	magnitudes	REAL	0	Photometric zero point for the *g*-filter stack. Necessary for converting listed fluxes and magnitudes back to measured ADU counts.
gzpAPER	magnitudes	REAL	0	Photometric zero point for the *g*-filter stack (APERTURE-like magnitudes only). Needed to convert fluxes or magnitudes back to measured ADU counts. (DR2).
gPlateScale	arcsec/pixel	REAL	0	Local plate scale for the *g*-filter stack.
rippDetectID				
...				Same entries repeated for the *r*, *i*, *z*, and *y* filters
yPlateScale				

Note. See *StackObjectThin* table for discussion of primary, secondary, and best detections.

Table D19

StackApFlx: Contains the Unconvolved Fluxes within the SDSS R5 ($r = 3\farcs00$), R6 ($r = 4\farcs63$), and R7 ($r = 7\farcs43$) Apertures (Stoughton et al. 2002)

Column Name	Units	Data Type	Default	Description
objID	⋯	BIGINT	NA	Unique object identifier.
uniquePspsSTid	⋯	BIGINT	NA	Unique internal PSPS STACK identifier.
ippObjID	⋯	BIGINT	NA	IPP internal object identifier.
randomStackObjID	⋯	FLOAT	NA	Random value drawn from the interval between zero and one.
primaryDetection	⋯	TINYINT	255	Identifies if this row is the primary STACK detection.
bestDetection	⋯	TINYINT	255	Identifies if this row is the best detection.
gstackDetectID	⋯	BIGINT	NA	Unique STACK detection identifier.
gstackImageID	⋯	BIGINT	NA	Unique STACK identifier for g-filter detection.
gippDetectID	⋯	BIGINT	NA	IPP internal detection identifier.
gflxR5	Jy	REAL	−999	Flux from g-filter detection within an aperture of radius $r = 3\farcs00$.
gflxR5Err	Jy	REAL	−999	Error in the flux from the g-filter detection within an aperture of radius $r = 3\farcs00$.
gflxR5Std	Jy	REAL	−999	Standard deviation of the g-filter flux within an aperture of radius $r = 3\farcs00$.
gflxR5Fill	⋯	REAL	−999	Aperture fill factor for the g-filter detection within an aperture of radius $r = 3\farcs00$.
gflxR6	Jy	REAL	−999	Flux from the g-filter detection within an aperture of radius $r = 4\farcs63$.
gflxR6Err	Jy	REAL	−999	Error in the flux from the g-filter detection within an aperture of radius $r = 4\farcs63$.
gflxR6Std	Jy	REAL	−999	Standard deviation of the g-filter flux within an aperture of radius $r = 4\farcs63$.
gflxR6Fill	⋯	REAL	−999	Aperture fill factor for the g-filter detection within an aperture of radius $r = 4\farcs63$.
gflxR7	Jy	REAL	−999	Flux from the g-filter detection within an aperture of radius $r = 7\farcs43$.
gflxR7Err	Jy	REAL	−999	Error in the flux from the g-filter detection within an aperture of radius $r = 7\farcs43$.
gflxR7Std	Jy	REAL	−999	Standard deviation of the g-filter flux within an aperture of radius $r = 7\farcs43$.
gflxR7Fill	⋯	REAL	−999	Aperture fill factor for the g-filter detection within an aperture of radius $r = 7\farcs43$.
gc6flxR5	Jy	REAL	−999	Flux from the g-filter detection convolved to a target of 6 sky pixels ($1\farcs5$) within an aperture of radius $r = 3\farcs00$.
gc6flxR5Err	Jy	REAL	−999	Error in the flux from the g-filter detection convolved to a target of 6 sky pixels ($1\farcs5$) within an aperture of radius $r = 3\farcs00$.
gc6flxR5Std	Jy	REAL	−999	Standard deviation of the flux from the g-filter detection convolved to a target of 6 sky pixels ($1\farcs5$) within an aperture of radius $r = 3\farcs00$.
gc6flxR5Fill	⋯	REAL	−999	Aperture fill factor for the g-filter detection convolved to a target of 6 sky pixels ($1\farcs5$) within an aperture of radius $r = 3\farcs00$.
gc6flxR6	Jy	REAL	−999	Flux from the g-filter detection convolved to a target of 6 sky pixels ($1\farcs5$) within an aperture of radius $r = 4\farcs63$.
gc6flxR6Err	Jy	REAL	−999	Error in the flux from the g-filter detection convolved to a target of 6 sky pixels ($1\farcs5$) within an aperture of radius $r = 4\farcs63$.
gc6flxR6Std	Jy	REAL	−999	Standard deviation of the flux from the g-filter detection convolved to a target of 6 sky pixels ($1\farcs5$) within an aperture of radius $r = 4\farcs63$.
gc6flxR6Fill	⋯	REAL	−999	Aperture fill factor for the g-filter detection convolved to a target of 6 sky pixels ($1\farcs5$) within an aperture of radius $r = 4\farcs63$.
gc6flxR7	Jy	REAL	−999	Flux from the g-filter detection convolved to a target of 6 sky pixels ($1\farcs5$) within an aperture of radius $r = 7\farcs43$.
gc6flxR7Err	Jy	REAL	−999	Error in the flux from the g-filter detection convolved to a target of 6 sky pixels ($1\farcs5$) within an aperture of radius $r = 7\farcs43$.
gc6flxR7Std	Jy	REAL	−999	Standard deviation of the flux from the g-filter detection convolved to a target of 6 sky pixels ($1\farcs5$) within an aperture of radius $r = 7\farcs43$.
gc6flxR7Fill	⋯	REAL	−999	Aperture fill factor for the g-filter detection convolved to a target of 6 sky pixels ($1\farcs5$) within an aperture of radius $r = 7\farcs43$.
gc8flxR5	Jy	REAL	−999	Flux from the g-filter detection convolved to a target of 8 sky pixels ($2\farcs0$) within an aperture of radius $r = 3\farcs00$.
gc8flxR5Err	Jy	REAL	−999	Error in the flux from the g-filter detection convolved to a target of 8 sky pixels ($2\farcs0$) within an aperture of radius $r = 3\farcs00$.
gc8flxR5Std	Jy	REAL	−999	Standard deviation of the flux from the g-filter detection convolved to a target of 8 sky pixels ($2\farcs0$) within an aperture of radius $r = 3\farcs00$.
gc8flxR5Fill	⋯	REAL	−999	Aperture fill factor for the g-filter detection convolved to a target of 8 sky pixels ($2\farcs0$) within an aperture of radius $r = 3\farcs00$.
gc8flxR6	Jy	REAL	−999	Flux from the g-filter detection convolved to a target of 8 sky pixels ($2\farcs0$) within an aperture of radius $r = 4\farcs63$.
gc8flxR6Err	Jy	REAL	−999	Error in the flux from the g-filter detection convolved to a target of 8 sky pixels ($2\farcs0$) within an aperture of radius $r = 4\farcs63$.
gc8flxR6Std	Jy	REAL	−999	Standard deviation of the flux from the g-filter detection convolved to a target of 8 sky pixels ($2\farcs0$) within an aperture of radius $r = 4\farcs63$.
gc8flxR6Fill	⋯	REAL	−999	Aperture fill factor for the g-filter detection convolved to a target of 8 sky pixels ($2\farcs0$) within an aperture of radius $r = 4\farcs63$.
gc8flxR7	Jy	REAL	−999	Flux from the g-filter detection convolved to a target of 8 sky pixels ($2\farcs0$) within an aperture of radius $r = 7\farcs43$.

Table D19
(Continued)

Column Name	Units	Data Type	Default	Description
gc8flxR7Err	Jy	REAL	−999	Error in the flux from the *g*-filter detection convolved to a target 8 sky pixels (2.″0) within an aperture of radius $r = 7.''43$.
gc8flxR7Std	Jy	REAL	−999	Standard deviation of the flux from the *g*-filter detection convolved to a target of 8 sky pixels (2.″0) within an aperture of radius $r = 7.''43$.
gc8flxR7Fill	⋯	REAL	−999	Aperture fill factor for the *g*-filter detection convolved to a target of 8 sky pixels (2.″0) within an aperture of radius $r = 7.''43$.
rstackDetectID ... yc8flxR7Fill				Same entries repeated for the *r*, *i*, *z*, and *y* filters

Note. Convolved fluxes within these same apertures are also provided for images convolved to 6 sky pixels (1.″5) and 8 sky pixels (2.″0). All filters are matched into a single row. See the *StackObjectThin* table for a discussion of the primary, secondary, and best detections.

Table D20
StackModelFitExp: Contains the Exponential Fit Parameters to Extended Sources

Column Name	Units	Data Type	Default	Description
objID	⋯	BIGINT	NA	Unique object identifier.
uniquePspsSTid	⋯	BIGINT	NA	Unique internal PSPS STACK identifier.
ippObjID	⋯	BIGINT	NA	IPP internal object identifier.
randomStackObjID	⋯	FLOAT	NA	Random value drawn from the interval between zero and one.
primaryDetection	⋯	TINYINT	255	Identifies if this row is the primary STACK detection.
bestDetection	⋯	TINYINT	255	Identifies if this row is the best detection.
gippDetectID	⋯	BIGINT	NA	IPP internal detection identifier.
gstackDetectID	⋯	BIGINT	NA	Unique STACK detection identifier.
gstackImageID	⋯	BIGINT	NA	Unique STACK identifier for the *g*-filter detection.
gExpRadius	arcsec	REAL	−999	Exponential fit radius for the *g*-filter STACK detection.
gExpRadiusErr	arcsec	REAL	−999	Error in exponential fit radius for the *g*-filter STACK detection.
gExpMag	AB	REAL	−999	Exponential fit magnitude for the *g*-filter STACK detection.
gExpMagErr	AB	REAL	−999	Error in exponential fit magnitude for the *g*-filter STACK detection.
gExpAb	⋯	REAL	−999	Exponential fit axis ratio for the *g*-filter STACK detection.
gExpAbErr	⋯	REAL	−999	Error in exponential fit axis ratio for the *g*-filter STACK detection.
gExpPhi	degrees	REAL	−999	Major axis position angle, phi, of exponential fit for the *g*-filter STACK detection.
gExpPhiErr	degrees	REAL	−999	Error in major axis position angle of exponential fit for the *g*-filter STACK detection.
gExpRa	degrees	FLOAT	−999	Right ascension of exponential fit center for the *g*-filter STACK detection.
gExpDec	degrees	FLOAT	−999	Decl. of the exponential fit center for the *g*-filter STACK detection.
gExpRaErr	arcsec	REAL	−999	Error in the R.A. of the exponential fit center for the *g*-filter STACK detection.
gExpDecErr	arcsec	REAL	−999	Error in decl. of the exponential fit center for the *g*-filter STACK detection.
gExpChisq	⋯	REAL	−999	Exponential fit reduced chi squared for the *g*-filter STACK detection.
rippDetectID ... yExpChisq				Same entries repeated for the *r*, *i*, *z*, and *y* filters

Note. See the *StackObjectThin* table for a discussion of the primary, secondary, and best detections.

Table D21
StackModelFitDeV: Contains the de Vaucouleurs (1948) Fit Parameters to Extended Sources

Column Name	Units	Data Type	Default	Description
objID	⋯	BIGINT	NA	Unique object identifier.
uniquePspsSTid	⋯	BIGINT	NA	Unique internal PSPS STACK identifier.
ippObjID	⋯	BIGINT	NA	IPP internal object identifier.
randomStackObjID	⋯	FLOAT	NA	Random value drawn from the interval between zero and one.
primaryDetection	⋯	TINYINT	255	Identifies if this row is the primary STACK detection.
bestDetection	⋯	TINYINT	255	Identifies if this row is the best detection.
gippDetectID	⋯	BIGINT	NA	IPP internal detection identifier.
gstackDetectID	⋯	BIGINT	NA	Unique STACK detection identifier.
gstackImageID	⋯	BIGINT	NA	Unique STACK identifier for *g*-filter detection.
gDeVRadius	arcsec	REAL	−999	de Vaucouleurs (1948) fit radius for the *g*-filter STACK detection.
gDeVRadiusErr	arcsec	REAL	−999	Error in the de Vaucouleurs (1948) fit radius for the *g*-filter STACK detection.
gDeVMag	AB	REAL	−999	de Vaucouleurs (1948) fit magnitude for the *g*-filter STACK detection.
gDeVMagErr	AB	REAL	−999	Error in the de Vaucouleurs (1948) fit magnitude for the *g*-filter STACK detection.
gDeVAb	⋯	REAL	−999	de Vaucouleurs (1948) fit axis ratio for the *g*-filter STACK detection.
gDeVAbErr	⋯	REAL	−999	Error in de Vaucouleurs (1948) fit axis ratio for *g*-filter STACK detection.
gDeVPhi	degrees	REAL	−999	Major axis position angle, phi, of the de Vaucouleurs (1948) fit for the *g*-filter STACK detection.
gDeVPhiErr	degrees	REAL	−999	Error in the major axis position angle of the de Vaucouleurs (1948) fit for the *g*-filter STACK detection.
gDeVRa	degrees	FLOAT	−999	Right ascension of the de Vaucouleurs (1948) fit center for the *g*-filter STACK detection.
gDeVDec	degrees	FLOAT	−999	Decl. of the de Vaucouleurs (1948) fit center for the *g*-filter STACK detection.
gDeVRaErr	arcsec	REAL	−999	Error in the R.A. of the de Vaucouleurs (1948) fit center for the *g*-filter STACK detection.
gDeVDecErr	arcsec	REAL	−999	Error in the decl. of the de Vaucouleurs (1948) fit center for the *g*-filter STACK detection.
gDeVChisq	⋯	REAL	−999	de Vaucouleurs (1948) fit reduced chi squared for the *g*-filter STACK detection.
rippDetectID				
...				Same entries repeated for the *r*, *i*, *z*, and *y* filters
yDeVChisq				

Note. See the *StackObjectThin* table for a discussion of the primary, secondary, and best detections.

Table D22
StackModelFitSer: Contains the Sérsic (1963) Fit Parameters to Extended Sources

Column Name	Units	Data Type	Default	Description
objID	⋯	BIGINT	NA	Unique object identifier.
uniquePspsSTid	⋯	BIGINT	NA	Unique internal PSPS STACK identifier.
ippObjID	⋯	BIGINT	NA	IPP internal object identifier.
randomStackObjID	⋯	FLOAT	NA	Random value drawn from the interval between zero and one.
primaryDetection	⋯	TINYINT	255	Identifies if this row is the primary STACK detection.
bestDetection	⋯	TINYINT	255	Identifies if this row is the best detection.
gippDetectID	⋯	BIGINT	NA	IPP internal detection identifier.
gstackDetectID	⋯	BIGINT	NA	Unique STACK detection identifier.
gstackImageID	⋯	BIGINT	NA	Unique STACK identifier for the *g*-filter detection.
gSerRadius	arcsec	REAL	−999	Sérsic (1963) fit radius for the *g*-filter STACK detection.
gSerRadiusErr	arcsec	REAL	−999	Error in the Sérsic (1963) fit radius for the *g*-filter STACK detection.
gSerMag	AB	REAL	−999	Sérsic (1963) fit magnitude for the *g*-filter STACK detection.
gSerMagErr	AB	REAL	−999	Error in the Sérsic (1963) fit magnitude for the *g*-filter STACK detection.
gSerAb	⋯	REAL	−999	Sérsic (1963) fit axis ratio for the *g*-filter STACK detection.
gSerAbErr	⋯	REAL	−999	Error in the Sérsic (1963) fit axis ratio for the *g*-filter STACK detection.
gSerNu	⋯	REAL	−999	Sérsic (1963) fit index for the *g*-filter STACK detection.
gSerNuErr	⋯	REAL	−999	Error in the Sérsic (1963) fit index for *g*-filter STACK detection.
gSerPhi	degrees	REAL	−999	Major axis position angle, phi, of the Sérsic (1963) fit for the *g*-filter STACK detection.
gSerPhiErr	degrees	REAL	−999	Error in the major axis position angle of Sérsic (1963) fit for the *g*-filter STACK detection.
gSerRa	degrees	FLOAT	−999	Right ascension of the Sérsic (1963) fit center for the *g*-filter STACK detection.
gSerDec	degrees	FLOAT	−999	Decl. of the Sérsic (1963) fit center for *g*-filter STACK detection.
gSerRaErr	arcsec	REAL	−999	Error in the R.A. of the Sérsic (1963) fit center for the *g*-filter STACK detection.
gSerDecErr	arcsec	REAL	−999	Error in the decl. of the Sérsic (1963) fit center for the *g*-filter STACK detection.
gSerChisq	⋯	REAL	−999	Sérsic (1963) fit reduced chi squared for the *g*-filter STACK detection.
rippDetectID				
...				Same entries repeated for the *r*, *i*, *z*, and *y* filters
ySerChisq				

Note. See the *StackObjectThin* table for a discussion of the primary, secondary, and best detections (Sérsic 1963).

Table D23
StackApFlxExGalUnc: Contains the Unconvolved Fluxes within the SDSS R3 ($r = 1\farcs03$), R4 ($r = 1\farcs76$), R5 ($r = 3\farcs00$), R6 ($r = 4\farcs63$), R7 ($r = 7\farcs43$), R8 ($r = 11\farcs42$), R9 ($r = 18\farcs20$), R10 ($r = 28\farcs20$), and R11 ($r = 44\farcs21$) Apertures (Stoughton et al. 2002) for Extended Sources

Column Name	Units	Data Type	Default	Description
objID	⋯	BIGINT	NA	Unique object identifier.
uniquePspsSTid	⋯	BIGINT	NA	Unique internal PSPS STACK identifier.
ippObjID	⋯	BIGINT	NA	IPP internal object identifier.
randomStackObjID	⋯	FLOAT	NA	Random value drawn from the interval between zero and one.
primaryDetection	⋯	TINYINT	255	Identifies if this row is the primary STACK detection.
bestDetection	⋯	TINYINT	255	Identifies if this row is the best detection.
gippDetectID	⋯	BIGINT	NA	IPP internal detection identifier.
gstackDetectID	⋯	BIGINT	NA	Unique STACK detection identifier.
gstackImageID	⋯	BIGINT	NA	Unique STACK identifier for the *g*-filter detection.
gflxR3	Jy	REAL	−999	Flux from the *g*-filter detection within an aperture of radius $r = 1\farcs03$.
gflxR3Err	Jy	REAL	−999	Error in the flux from the *g*-filter detection within an aperture of radius $r = 1\farcs03$.
gflxR3Std	Jy	REAL	−999	Standard deviation of the flux from the *g*-filter detection within an aperture of radius $r = 1\farcs03$.
gflxR3Fill	⋯	REAL	−999	Aperture fill factor for the *g*-filter detection within an aperture of radius $r = 1\farcs03$.
gflxR4	Jy	REAL	−999	Flux from the *g*-filter detection within an aperture of radius $r = 1\farcs76$.
gflxR4Err	Jy	REAL	−999	Error in flux from the *g*-filter detection within an aperture of radius $r = 1\farcs76$.
gflxR4Std	Jy	REAL	−999	Standard deviation of the flux from the *g*-filter detection within an aperture of radius $r = 1\farcs76$.
gflxR4Fill	⋯	REAL	−999	Aperture fill factor for the *g*-filter detection within an aperture of radius $r = 1\farcs76$.
gflxR5	Jy	REAL	−999	Flux from the *g*-filter detection within an aperture of radius $r = 3\farcs00$.
gflxR5Err	Jy	REAL	−999	Error in the flux from the *g*-filter detection within an aperture of radius $r = 3\farcs00$.
gflxR5Std	Jy	REAL	−999	Standard deviation of the flux from the *g*-filter detection within an aperture of radius $r = 3\farcs00$.
gflxR5Fill	⋯	REAL	−999	Aperture fill factor for the *g*-filter detection within an aperture of radius $r = 3\farcs00$.
gflxR6	Jy	REAL	−999	Flux from the *g*-filter detection within an aperture of radius $r = 4\farcs63$.
gflxR6Err	Jy	REAL	−999	Error in the flux from the *g*-filter detection within an aperture of radius $r = 4\farcs63$.
gflxR6Std	Jy	REAL	−999	Standard deviation of the flux from the *g*-filter detection within an aperture of radius $r = 4\farcs63$.
gflxR6Fill	⋯	REAL	−999	Aperture fill factor for the *g*-filter detection within an aperture of radius $r = 4\farcs63$.
gflxR7	Jy	REAL	−999	Flux from the *g*-filter detection within an aperture of radius $r = 7\farcs43$.
gflxR7Err	Jy	REAL	−999	Error in the flux from the *g*-filter detection within an aperture of radius $r = 7\farcs43$.
gflxR7Std	Jy	REAL	−999	Standard deviation of the flux from the *g*-filter detection within an aperture of radius $r = 7\farcs43$.
gflxR7Fill	⋯	REAL	−999	Aperture fill factor for the *g*-filter detection within an aperture of radius $r = 7\farcs43$.
gflxR8	Jy	REAL	−999	Flux from the *g*-filter detection within an aperture of radius $r = 11\farcs42$.
gflxR8Err	Jy	REAL	−999	Error in the flux from the *g*-filter detection within an aperture of radius $r = 11\farcs42$.
gflxR8Std	Jy	REAL	−999	Standard deviation of the flux from the *g*-filter detection within an aperture of radius $r = 11\farcs42$.
gflxR8Fill	⋯	REAL	−999	Aperture fill factor for the *g*-filter detection within an aperture of radius $r = 11\farcs42$.
gflxR9	Jy	REAL	−999	Flux from the *g*-filter detection within an aperture of radius $r = 18\farcs20$.
gflxR9Err	Jy	REAL	−999	Error in the flux from the *g*-filter detection within an aperture of radius $r = 18\farcs20$.
gflxR9Std	Jy	REAL	−999	Standard deviation of flux from the *g*-filter detection within an aperture of radius $r = 18\farcs20$.
gflxR9Fill	⋯	REAL	−999	Aperture fill factor for the *g*-filter detection within an aperture of radius $r = 18\farcs20$.
gflxR10	Jy	REAL	−999	Flux from the *g*-filter detection within an aperture of radius $r = 28\farcs20$.
gflxR10Err	Jy	REAL	−999	Error in the flux from the *g*-filter detection within an aperture of radius $r = 28\farcs20$.
gflxR10Std	Jy	REAL	−999	Standard deviation of the flux from the *g*-filter detection within an aperture of radius $r = 28\farcs20$.
gflxR10Fill	⋯	REAL	−999	Aperture fill factor for the *g*-filter detection within an aperture of radius $r = 28\farcs20$.
gflxR11	Jy	REAL	−999	Flux from the *g*-filter detection within an aperture of radius $r = 44\farcs21$.
gflxR11Err	Jy	REAL	−999	Error in the flux from the *g*-filter detection within an aperture of radius $r = 44\farcs21$.
gflxR11Std	Jy	REAL	−999	Standard deviation of the flux from the *g*-filter detection within an aperture of radius $r = 44\farcs21$.
gflxR11Fill	⋯	REAL	−999	Aperture fill factor for the *g*-filter detection within an aperture of radius $r = 44\farcs21$.
rippDetectID ... yflxR11Fill				Same entries repeated for the *r*, *i*, *z*, and *y* filters

Note. These measurements are only provided for objects in the extragalactic sky, i.e., they are not provided for objects in the Galactic plane because they are not useful in crowded areas. See the *StackObjectThin* table for a discussion of the primary, secondary, and best detections.

Table D24

StackApFlxExGalCon6: Contains the Fluxes within the SDSS R3 ($r = 1\farcs03$), R4 ($r = 1\farcs76$), R5 ($r = 3\farcs00$), R6 ($r = 4\farcs63$), R7 ($r = 7\farcs43$), R8 ($r = 11\farcs42$), R9 ($r = 18\farcs20$), R10 ($r = 28\farcs20$), and R11 ($r = 44\farcs21$) Apertures (Stoughton et al. 2002) for Extended Sources after the Images Have Been Convolved to a Target of 6 Sky Pixels ($1\farcs5$)

Column Name	Units	Data Type	Default	Description
objID	⋯	BIGINT	NA	Unique object identifier.
uniquePspsSTid	⋯	BIGINT	NA	Unique internal PSPS STACK identifier.
ippObjID	⋯	BIGINT	NA	IPP internal object identifier.
randomStackObjID	⋯	FLOAT	NA	Random value drawn from the interval between zero and one.
primaryDetection	⋯	TINYINT	255	Identifies if this row is the primary STACK detection.
bestDetection	⋯	TINYINT	255	Identifies if this row is the best detection.
gippDetectID	⋯	BIGINT	NA	IPP internal detection identifier.
gstackDetectID	⋯	BIGINT	NA	Unique STACK detection identifier.
gstackImageID	⋯	BIGINT	NA	Unique STACK identifier for the *g*-filter detection.
gc6flxR3	Jy	REAL	−999	Flux from the *g*-filter detection convolved to a target of 6 sky pixels ($1\farcs5$) within an aperture of radius $r = 1\farcs03$.
gc6flxR3Err	Jy	REAL	−999	Error in the flux from the *g*-filter detection convolved to a target of 6 sky pixels ($1\farcs5$) within an aperture of radius $r = 1\farcs03$.
gc6flxR3Std	Jy	REAL	−999	Standard deviation of the flux from the *g*-filter detection convolved to a target of 6 sky pixels ($1\farcs5$) within an aperture of radius $r = 1\farcs03$.
gc6flxR3Fill	⋯	REAL	−999	Aperture fill factor for the *g*-filter detection convolved to a target of 6 sky pixels ($1\farcs5$) within an aperture of radius $r = 1\farcs03$.
...				gc6flxR3 ... gc6flxR3Fill columns repeated for R4 ($r = 1\farcs76$).
...				repeated for R5 ($r = 3\farcs00$).
...				repeated for R6 ($r = 4\farcs63$).
...				repeated for R7 ($r = 7\farcs43$).
...				repeated for R8($r = 11\farcs42$).
...				repeated for R9 ($r = 18\farcs20$).
...				repeated for R10 ($r = 28\farcs20$).
gc6flxR11	Jy	REAL	−999	Flux from the *g*-filter detection convolved to a target of 6 sky pixels ($1\farcs5$) within an aperture of radius $r = 44\farcs21$.
gc6flxR11Err	Jy	REAL	−999	Error in the flux from the *g*-filter detection convolved to a target of 6 sky pixels ($1\farcs5$) within an aperture of radius $r = 44\farcs21$.
gc6flxR11Std	Jy	REAL	−999	Standard deviation of the flux from the *g*-filter detection convolved to a target of 6 sky pixels ($1\farcs5$) within an aperture of radius $r = 44\farcs21$.
gc6flxR11Fill	⋯	REAL	−999	Aperture fill factor for the *g*-filter detection convolved to a target of 6 sky pixels ($1\farcs5$) within an aperture of radius $r = 44\farcs21$.
rippDetectID				
...				Same entries repeated for *r*, *i*, *z*, and *y* filters
yc6flxR11Fill				

Note. These measurements are only provided for objects in the extragalactic sky, i.e., they are not provided for objects in the Galactic plane because they are not useful in crowded areas. See the *StackObjectThin* table for a discussion of primary, secondary, and best detections.

Table D25

StackApFlxExGalCon8: Contains the Fluxes within the SDSS R3 ($r = 1\farcs03$), R4 ($r = 1\farcs76$), R5 ($r = 3\farcs00$), R6 ($r = 4\farcs63$), R7 ($r = 7\farcs43$), R8 ($r = 11\farcs42$), R9 ($r = 18\farcs20$), R10 ($r = 28\farcs20$), and R11 ($r = 44\farcs21$) Apertures (Stoughton et al. 2002) for Extended Sources after the Images Have Been Convolved to a Target of 8 Sky Pixels ($2\farcs0$)

Column Name	Units	Data Type	Default	Description
objID	⋯	BIGINT	NA	Unique object identifier.
uniquePspsSTid	⋯	BIGINT	NA	Unique internal PSPS STACK identifier.
ippObjID	⋯	BIGINT	NA	IPP internal object identifier.
randomStackObjID	⋯	FLOAT	NA	Random value drawn from the interval between zero and one.
primaryDetection	⋯	TINYINT	255	Identifies if this row is the primary STACK detection.
bestDetection	⋯	TINYINT	255	Identifies if this row is the best detection.
gippDetectID	⋯	BIGINT	NA	IPP internal detection identifier.
gstackDetectID	⋯	BIGINT	NA	Unique STACK detection identifier.
gstackImageID	⋯	BIGINT	NA	Unique STACK identifier for the *g*-filter detection.
gc8flxR3	Jy	REAL	−999	Flux from the *g*-filter detection convolved to a target of 8 sky pixels ($2\farcs0$) within an aperture of radius $r = 1\farcs03$.
gc8flxR3Err	Jy	REAL	−999	Error in the flux from the *g*-filter detection convolved to a target of 8 sky pixels ($2\farcs0$) within an aperture of radius $r = 1\farcs03$.
gc8flxR3Std	Jy	REAL	−999	Standard deviation of the flux from the *g*-filter detection convolved to a target of 8 sky pixels ($2\farcs0$) within an aperture of radius $r = 1\farcs03$.
gc8flxR3Fill	⋯	REAL	−999	Aperture fill factor for the *g*-filter detection convolved to a target of 8 sky pixels ($2\farcs0$) within an aperture of radius $r = 1\farcs03$.
...				gc8flxR3 ... gc8flxR3Fill columns repeated for R4 ($r = 1\farcs76$).
...				repeated for R5 ($r = 3\farcs00$).
...				repeated for R6 ($r = 4\farcs63$).
...				repeated for R7 ($r = 7\farcs43$).
...				repeated for R8($r = 11\farcs42$).
...				repeated for R9 ($r = 18\farcs20$).
...				repeated for R10 ($r = 28\farcs20$).
gc8flxR11	Jy	REAL	−999	Flux from the *g*-filter detection convolved to a target of 8 sky pixels ($2\farcs0$) within an aperture of radius $r = 44\farcs21$.
gc8flxR11Err	Jy	REAL	−999	Error in the flux from the *g*-filter detection convolved to a target of 8 sky pixels ($2\farcs0$) within an aperture of radius $r = 44\farcs21$.
gc8flxR11Std	Jy	REAL	−999	Standard deviation of the flux from the *g*-filter detection convolved to a target of 8 sky pixels ($2\farcs0$) within an aperture of radius $r = 44\farcs21$.
gc8flxR11Fill	⋯	REAL	−999	Aperture fill factor for the *g*-filter detection convolved to a target of 8 sky pixels ($2\farcs0$) within an aperture of radius $r = 44\farcs21$.
rippDetectID				
...				Same entries repeated for the *r*, *i*, *z*, and *y* filters
yc8flxR11Fill				

Note. These measurements are only provided for objects in the extragalactic sky, i.e., they are not provided for objects in the Galactic plane because they are not useful in crowded areas. See the *StackObjectThin* table for a discussion of the primary, secondary, and best detections.

Table D26
StackPetrosian: Contains the Petrosian (1976) Magnitudes and Radii for Extended Sources

Column Name	Units	Data Type	Default	Description
objID	⋯	BIGINT	NA	Unique object identifier.
uniquePspsSTid	⋯	BIGINT	NA	Unique internal PSPS STACK identifier.
ippObjID	⋯	BIGINT	NA	IPP internal object identifier.
randomStackObjID	⋯	FLOAT	NA	Random value drawn from the interval between zero and one.
primaryDetection	⋯	TINYINT	255	Identifies if this row is the primary STACK detection.
bestDetection	⋯	TINYINT	255	Identifies if this row is the best detection.
gippDetectID	⋯	BIGINT	NA	IPP internal detection identifier.
gstackDetectID	⋯	BIGINT	NA	Unique STACK detection identifier.
gstackImageID	⋯	BIGINT	NA	Unique STACK identifier for the *g*-filter detection.
gpetRadius	arcsec	REAL	−999	Petrosian (1976) fit radius for the *g*-filter STACK detection.
gpetRadiusErr	arcsec	REAL	−999	Error in the Petrosian (1976) fit radius for the *g*-filter STACK detection.
gpetMag	AB	REAL	−999	Petrosian (1976) magnitude from the *g*-filter STACK detection.
gpetMagErr	AB	REAL	−999	Error in the Petrosian (1976) magnitude from the *g*-filter STACK detection.
gpetR50	arcsec	REAL	−999	Petrosian (1976) fit radius for the *g*-filter STACK detection at 50% light
gpetR50Err	arcsec	REAL	−999	Error in the Petrosian (1976) fit radius for the *g*-filter STACK detection at 50% light
gpetR90	arcsec	REAL	−999	Petrosian (1976) fit radius for the *g*-filter STACK detection at 90% light
gpetR90Err	arcsec	REAL	−999	Error in the Petrosian (1976) fit radius for the *g*-filter STACK detection at 90% light
gpetCf	⋯	REAL	−999	Petrosian (1976) fit coverage factor for the *g*-filter STACK detection.
rippDetectID				
...				Same entries repeated for the *r*, *i*, *z*, and *y* filters
ypetCf				

Note. See the *StackObjectThin* table for a discussion of the primary, secondary, and best detections.

Table D27
StackToImage: Contains the Mapping of Which Input Images Were Used to Construct a Particular Stack

Column Name	Units	Data Type	Default	Description
stackImageID	⋯	BIGINT	NA	Unique STACK identifier.
imageID	⋯	BIGINT	NA	Unique image identifier. Constructed as (100 × frameID + ccdID).

Table D28
StackToFrame: Contains the Mapping of Input Frames Used to Construct a Particular STACK along with Processing Statistics

Column Name	Units	Data Type	Default	Description
stackImageID	⋯	BIGINT	NA	Unique STACK identifier.
frameID	⋯	INT	NA	Unique frame/exposure identifier.
scaleFactor	⋯	REAL	0	normalization factor applied to input image before stacking.
zp	magnitudes	REAL	0	Photometric zero point. Necessary for converting listed fluxes and magnitudes back to measured ADU counts.
expTime	seconds	REAL	−999	Exposure time of the frame/exposure. Necessary for converting listed fluxes and magnitudes back to measured ADU counts.
airMass	⋯	REAL	0	Airmass at midpoint of the exposure. Necessary for converting listed fluxes and magnitudes back to measured ADU counts.

Table D29
StackDetEffMeta: Contains the Detection Efficiency Information for a Given Stacked Image

Column Name	Units	Data Type	Default	Description
stackImageID	⋯	BIGINT	NA	Unique stack identifier.
magref	magnitudes	REAL	NA	Detection efficiency reference magnitude.
nInjected	⋯	INT	NA	Number of fake sources injected in each magnitude bin.
offset01	magnitudes	REAL	NA	Detection efficiency magnitude offset for bin 1.
counts01	⋯	REAL	NA	Detection efficiency count of recovered sources in bin 1.
diffMean01	magnitudes	REAL	NA	Detection efficiency mean magnitude difference in bin 1.
diffStdev01	magnitudes	REAL	NA	Detection efficiency standard deviation of magnitude differences in bin 1.
errMean01	magnitudes	REAL	NA	Detection efficiency mean magnitude error in bin 1.
offset02	magnitudes	REAL	NA	Detection efficiency magnitude offset for bin 2.
counts02	⋯	REAL	NA	Detection efficiency count of recovered sources in bin 2.
diffMean02	magnitudes	REAL	NA	Detection efficiency mean magnitude difference in bin 2.
diffStdev02	magnitudes	REAL	NA	Detection efficiency standard deviation of magnitude differences in bin 2.
errMean02	magnitudes	REAL	NA	Detection efficiency mean magnitude error in bin 2.
offset03	magnitudes	REAL	NA	Detection efficiency magnitude offset for bin 3.
counts03	⋯	REAL	NA	Detection efficiency count of recovered sources in bin 3.
diffMean03	magnitudes	REAL	NA	Detection efficiency mean magnitude difference in bin 3.
diffStdev03	magnitudes	REAL	NA	Detection efficiency standard deviation of magnitude differences in bin 3.
errMean03	magnitudes	REAL	NA	Detection efficiency mean magnitude error in bin 3.
...				
offset13	magnitudes	REAL	NA	Detection efficiency magnitude offset for bin 13.
counts13	⋯	REAL	NA	Detection efficiency count of recovered sources in bin 13.
diffMean13	magnitudes	REAL	NA	Detection efficiency mean magnitude difference in bin 13.
diffStdev13	magnitudes	REAL	NA	Detection efficiency standard deviation of magnitude differences in bin 13.
errMean13	magnitudes	REAL	NA	Detection efficiency mean magnitude error in bin 13.

Note. Provides the number of recovered sources out of 500 injected sources for each magnitude bin and statistics about the magnitudes of the recovered sources for a range of magnitude offsets.

D.4. Forced Warp Tables

Table D30
ForcedMeanObject: Contains the Mean of Single-epoch Photometric Information for Sources Detected in the Stacked Data, Calculated as Described in Magnier et al. (2013)

Column Name	Units	Data Type	Default	Description
objID	⋯	BIGINT	NA	Unique object identifier.
uniquePspsFOid	⋯	BIGINT	NA	Unique internal PSPS forced object identifier.
ippObjID	⋯	BIGINT	NA	IPP internal object identifier.
randomForcedObjID	⋯	FLOAT	NA	Random value drawn from the interval between zero and one.
nDetections	⋯	SMALLINT	−999	Number of single-epoch detections in all filters.
batchID	⋯	BIGINT	NA	Internal database batch identifier.
processingVersion	⋯	TINYINT	NA	Data release version.
gnTotal	⋯	SMALLINT	−999	Number of forced single-epoch detections in the g filter.
gnIncPSFFlux	⋯	SMALLINT	−999	Number of forced single-epoch detections in the PSF flux mean in the g filter.
gnIncKronFlux	⋯	SMALLINT	−999	Number of forced single-epoch detections in the Kron (1980) flux mean in the g filter.
gnIncApFlux	⋯	SMALLINT	−999	Number of forced single-epoch detections in the aperture flux mean in the g filter.
gnIncR5	⋯	SMALLINT	−999	Number of forced single-epoch detections in the R5 ($r = 3\farcs00$) aperture flux mean in the g filter.
gnIncR6	⋯	SMALLINT	−999	Number of forced single-epoch detections in the R6 ($r = 4\farcs63$) aperture flux mean in the g filter.
gnIncR7	⋯	SMALLINT	−999	Number of forced single-epoch detections in the R7 ($r = 7\farcs43$) aperture flux mean in the g filter.
gFPSFFlux	Jy	REAL	−999	Mean PSF flux from forced single-epoch g-filter detections.
gFPSFFluxErr	Jy	REAL	−999	Error in the mean PSF flux from forced single-epoch g-filter detections.
gFPSFFluxStd	Jy	REAL	−999	Standard deviation of PSF fluxes from forced single-epoch g-filter detections.
gFPSFMag	AB	REAL	−999	Magnitude from mean PSF flux from forced single-epoch g-filter detections.
gFPSFMagErr	AB	REAL	−999	Error in magnitude from the mean PSF flux from forced single-epoch g-filter detections.
gFKronFlux	Jy	REAL	−999	Mean Kron (1980) flux from forced single-epoch g-filter detections.
gFKronFluxErr	Jy	REAL	−999	Error in mean Kron (1980) flux from forced single-epoch g-filter detections.
gFKronFluxStd	Jy	REAL	−999	Standard deviation of Kron (1980) fluxes from forced single-epoch g-filter detections.
gFKronMag	AB	REAL	−999	Magnitude from thhe mean Kron (1980) flux from forced single-epoch g-filter detections.
gFKronMagErr	AB	REAL	−999	Error in magnitude from the mean Kron (1980) flux from forced single-epoch g-filter detections.
gFApFlux	Jy	REAL	−999	Mean aperture flux from forced single-epoch g-filter detections.
gFApFluxErr	Jy	REAL	−999	Error in the mean aperture flux from forced single-epoch g-filter detections.
gFApFluxStd	Jy	REAL	−999	Standard deviation of aperture fluxes from forced single-epoch g-filter detections.
gFApMag	AB	REAL	−999	Magnitude from the mean aperture flux from forced single-epoch g-filter detections.
gFApMagErr	AB	REAL	−999	Error in magnitude from the mean aperture flux from forced single-epoch g-filter detections.
gFmeanflxR5	Jy	REAL	−999	Mean flux from forced single-epoch g-filter detections within an aperture of radius $r = 3\farcs00$.
gFmeanflxR5Err	Jy	REAL	−999	Error in mean flux from forced single-epoch g-filter detections within an aperture of radius $r = 3\farcs00$.
gFmeanflxR5Std	Jy	REAL	−999	Standard deviation of forced single-epoch g-filter detection fluxes within an aperture of radius $r = 3\farcs00$.
gFmeanflxR5Fill	⋯	REAL	−999	Aperture fill factor for forced single-epoch g-filter detections within an aperture of radius $r = 3\farcs00$.
gFmeanMagR5	AB	REAL	−999	Magnitude from the mean flux from forced single-epoch g-filter detections within an aperture of radius $r = 3\farcs00$.
gFmeanMagR5Err	AB	REAL	−999	Error in magnitude from the mean flux from forced single-epoch g-filter detections within an aperture of radius $r = 3\farcs00$.
gFmeanflxR6	Jy	REAL	−999	Mean flux from the forced single-epoch g-filter detections within an aperture of radius $r = 4\farcs63$.
gFmeanflxR6Err	Jy	REAL	−999	Error in the mean flux from forced single-epoch g-filter detections within an aperture of radius $r = 4\farcs63$.
gFmeanflxR6Std	Jy	REAL	−999	Standard deviation of forced single-epoch g-filter detection fluxes within an aperture of radius $r = 4\farcs63$.
gFmeanflxR6Fill	⋯	REAL	−999	Aperture fill factor for forced single-epoch g-filter detections within an aperture of radius $r = 4\farcs63$.
gFmeanMagR6	AB	REAL	−999	Magnitude from the mean flux from forced single-epoch g-filter detections within an aperture of radius $r = 4\farcs63$.
gFmeanMagR6Err	AB	REAL	−999	Error in the magnitude from the mean flux from forced single-epoch g-filter detections within an aperture of radius $r = 4\farcs63$.
gFmeanflxR7	Jy	REAL	−999	Mean flux from forced single-epoch g-filter detections within an aperture of radius $r = 7\farcs43$.
gFmeanflxR7Err	Jy	REAL	−999	Error in the mean flux from forced single-epoch g-filter detections within an aperture of radius $r = 7\farcs43$.
gFmeanflxR7Std	Jy	REAL	−999	Standard deviation of forced single-epoch g-filter

Table D30
(Continued)

Column Name	Units	Data Type	Default	Description
				detection fluxes within an aperture of radius $r = 7\farcs43$.
gFmeanflxR7Fill	⋯	REAL	−999	Aperture fill factor for forced single-epoch g-filter detections within an aperture of radius $r = 7\farcs43$.
gFmeanMagR7	AB	REAL	−999	Magnitude from the mean flux from forced single-epoch g-filter detections within an aperture of radius $r = 7\farcs43$.
gFmeanMagR7Err	AB	REAL	−999	Error in the magnitude from the mean flux from forced single-epoch g-filter detections within an aperture of radius $r = 7\farcs43$.
gFlags	⋯	INT	0	Information flag bitmask indicating details of the photometry from forced single-epoch g-filter detections. Values listed in ObjectInfoFlags.
gE1	⋯	REAL	−999	Kaiser et al. (1995) polarization parameter $e1 = (M_{xx} - M_{yy})/(M_{xx} + M_{yy})$ from forced single-epoch g-filter detections.
gE2	⋯	REAL	−999	Kaiser et al. (1995) polarization parameter $e2 = (2M_{xy})/(M_{xx} + M_{yy})$ from forced single-epoch g-filter detections.
rnTotal				
...				Same entries repeated for the r, i, z, and y filters
yE2				

Note. The mean is calculated for detections associated into objects within a $1''$ correlation radius. PSF, Kron (1980), and SDSS aperture R5 ($r = 3\farcs00$), R6 ($r = 4\farcs63$), and R7 ($r = 7\farcs43$) aperture (Stoughton et al. 2002) magnitudes and statistics are listed for all filters. See also Kaiser et al. (1995).

Table D31
ForcedMeanLensing: Contains the Mean Kaiser et al. (1995, K95) Lensing Parameters Measured from the Forced Photometry of Objects Detected in Stacked Images on the Individual Single-epoch Data

Column Name	Units	Data Type	Default	Description
objID	⋯	BIGINT	NA	Unique object identifier.
uniquePspsFOid	⋯	BIGINT	NA	Unique internal PSPS forced object identifier.
ippObjID	⋯	BIGINT	NA	IPP internal object identifier.
randomForcedObjID	⋯	FLOAT	NA	Random value drawn from the interval between zero and one.
nDetections	⋯	SMALLINT	−999	Number of single-epoch detections in all filters.
batchID	⋯	BIGINT	NA	Internal database batch identifier.
processingVersion	⋯	TINYINT	NA	Data release version.
gLensObjSmearX11	arcsec^{-2}	REAL	−999	K95 Equation (A11) smear polarizability X11 term from forced g-filter detections.
gLensObjSmearX12	arcsec^{-2}	REAL	−999	K95 Equation (A11) smear polarizability X12 term from forced g-filter detections.
gLensObjSmearX22	arcsec^{-2}	REAL	−999	K95 Equation (A11) smear polarizability X22 term from forced g-filter detections.
gLensObjSmearE1	arcsec^{-2}	REAL	−999	K95 Equation (A12) smear polarizability e1 term from forced g-filter detections.
gLensObjSmearE2	arcsec^{-2}	REAL	−999	K95 Equation (A12) smear polarizability e2 term from forced g-filter detections.
gLensObjShearX11	⋯	REAL	−999	K95 Equation (B11) shear polarizability X11 term from forced g-filter detections.
gLensObjShearX12	⋯	REAL	−999	K95 Equation (B11) shear polarizability X12 term from forced g-filter detections.
gLensObjShearX22	⋯	REAL	−999	K95 Equation (B11) shear polarizability X22 term from forced g-filter detections.
gLensObjShearE1	⋯	REAL	−999	K95 Equation (B12) shear polarizability e1 term from forced g-filter detections.
gLensObjShearE2	⋯	REAL	−999	K95 Equation (B12) shear polarizability e2 term from forced g-filter detections.
gLensPSFSmearX11	arcsec^{-2}	REAL	−999	K95 Equation (A11) smear polarizability X11 term from the PSF model for forced g-filter detections.
gLensPSFSmearX12	arcsec^{-2}	REAL	−999	K95 Equation (A11) smear polarizability X12 term from the PSF model for forced g-filter detections.
gLensPSFSmearX22	arcsec^{-2}	REAL	−999	K95 Equation (A11) smear polarizability X22 term from the PSF model for forced g-filter detections.
gLensPSFSmearE1	arcsec^{-2}	REAL	−999	K95 Equation (A12) smear polarizability e1 term from the PSF model for forced g-filter detections.
gLensPSFSmearE2	arcsec^{-2}	REAL	−999	K95 Equation (A12) smear polarizability e2 term from the PSF model for forced g-filter detections.
gLensPSFShearX11	⋯	REAL	−999	K95 Equation (B11) shear polarizability X11 term from the PSF model for forced g-filter detections.
gLensPSFShearX12	⋯	REAL	−999	K95 Equation (B11) shear polarizability X12 term from the PSF model for forced g-filter detections.
gLensPSFShearX22	⋯	REAL	−999	K95 Equation (B11) shear polarizability X22 term from the PSF model for forced g-filter detections.
gLensPSFShearE1	⋯	REAL	−999	K95 Equation (B12) shear polarizability e1 term from the PSF model for forced g-filter detections.
gLensPSFShearE2	⋯	REAL	−999	K95 Equation (B12) shear polarizability e2 term from the PSF model for forced g-filter detections.
rlensObjSmearX11				
...				same entries repeated for r, i, z, and y filters
ylensPSFShearE2				

Table D32
ForcedWarpMeta: Contains the Metadata Related to a Sky-aligned Distortion-corrected WARP Image, Upon Which Forced Photometry Is Performed

Column Name	Units	Data Type	Default	Description
forcedWarpID	⋯	BIGINT	NA	Unique forced WARP identifier.
batchID	⋯	BIGINT	NA	Internal database batch identifier.
surveyID	⋯	TINYINT	NA	Survey identifier. Details in the Survey table.
filterID	⋯	TINYINT	NA	Filter identifier. Details in the Filter table.
frameID	⋯	INT	NA	Frame/exposure identifier of the Frame associated with this warp.
ippSkycalID	⋯	INT	NA	IPP skycal identifier for the run that generated the positions for forced photometry.
stackMetaID	⋯	INT	NA	Identifier for the STACK that yielded the positions for forced photometry.
tessID	⋯	TINYINT	0	Tessellation identifier. Details in the TessellationType table.
projectionID	⋯	SMALLINT	−1	Projection cell identifier.
skyCellID	⋯	TINYINT	255	Skycell region identifier.
photoCalID	⋯	INT	NA	Photometric calibration identifier. Details in the PhotoCal table.
analysisVer	⋯	VARCHAR(100)		IPP software analysis release version.
md5sum	⋯	VARCHAR(100)		IPP MD5 Checksum.
expTime	seconds	REAL	−999	Exposure time of the source frame/exposure for this WARP image. Necessary for converting listed fluxes and magnitudes back to measured ADU counts.
recalAstroScatX	arcsec	REAL	−999	Measurement of the recalibration (not astrometric error) in the *X* direction.
recalAstroScatY	arcsec	REAL	−999	Measurement of the recalibration (not astrometric error) in the *Y* direction.
recalNAstroStars	⋯	INT	−999	Number of astrometric reference sources used in recalibration.
recalphotoScat	magnitudes	REAL	−999	Photometric scatter relative to reference catalog.
recalNPhotoStars	⋯	INT	−999	Number of astrometric reference sources used in recalibration.
psfModelID	⋯	INT	−999	PSF model identifier.
psfFWHM	arcsec	REAL	−999	Mean PSF FWHM at image center.
psfWidMajor	arcsec	REAL	−999	PSF major axis FWHM at image center.
psfWidMinor	arcsec	REAL	−999	PSF minor axis FWHM at image center.
psfTheta	degrees	REAL	−999	PSF major axis orientation at image center.
photoZero	magnitudes	REAL	−999	Locally derived photometric zero point for this WARP image.
ctype1	⋯	VARCHAR(100)		Name of astrometric projection in R.A.
ctype2	⋯	VARCHAR(100)		Name of astrometric projection in decl.
crval1	degrees	FLOAT	−999	Right ascension corresponding to reference pixel.
crval2	degrees	FLOAT	−999	Decl. corresponding to reference pixel.
crpix1	sky pixels	FLOAT	−999	Reference pixel for R.A.
crpix2	sky pixels	FLOAT	−999	Reference pixel for decl.
cdelt1	degrees/pixel	FLOAT	−999	Pixel scale in R.A.
cdelt2	degrees/pixel	FLOAT	−999	Pixel scale in decl.
pc001001	⋯	FLOAT	−999	Linear transformation matrix element between image pixel *x* and R.A.
pc001002	⋯	FLOAT	−999	Linear transformation matrix element between image pixel *y* and R.A.
pc002001	⋯	FLOAT	−999	Linear transformation matrix element between image pixel *x* and decl.
pc002002	⋯	FLOAT	−999	Linear transformation matrix element between image pixel *y* and decl.
processingVersion	⋯	TINYINT	NA	Data release version.

Note. The astrometric and photometric calibrations of the WARP image are listed.

Table D33
ForcedWarpMeasurement: Contains Single-epoch Forced Photometry of Individual Measurements of Objects Detected in the Stacked Images

Column Name	Units	Data Type	Default	Description
objID	⋯	BIGINT	NA	Unique object identifier.
uniquePspsFWid	⋯	BIGINT	NA	Unique internal PSPS forced WARP identifier.
detectID	⋯	BIGINT	NA	Unique detection identifier.
ippObjID	⋯	BIGINT	NA	IPP internal object identifier.
ippDetectID	⋯	BIGINT	NA	IPP internal detection identifier.
filterID	⋯	TINYINT	NA	Filter identifier. Details in the Filter table.
surveyID	⋯	TINYINT	NA	Survey identifier. Details in the Survey table.
forcedSummaryID	⋯	BIGINT	NA	Unique forced WARP summary identifier.
forcedWarpID	⋯	BIGINT	NA	Unique forced WARP identifier.
randomWarpID	⋯	FLOAT	NA	Random value drawn from the interval between zero and one.
tessID	⋯	TINYINT	0	Tessellation identifier. Details in the TessellationType table.
projectionID	⋯	SMALLINT	−1	Projection cell identifier.
skyCellID	⋯	TINYINT	255	Skycell region identifier.
dvoRegionID	⋯	INT	−1	Internal DVO region identifier.
obsTime	days	FLOAT	−999	Modified Julian Date at the midpoint of the observation.
zp	magnitudes	REAL	0	Photometric zero point. Necessary for converting listed fluxes and magnitudes back to measured ADU counts.
telluricExt	magnitudes	REAL	NA	Estimated telluric extinction due to nonphotometric observing conditions. Necessary for converting listed fluxes and magnitudes back to measured ADU counts.
expTime	seconds	REAL	−999	Exposure time of the frame/exposure. Necessary for converting listed fluxes and magnitudes back to measured ADU counts.
airMass	⋯	REAL	0	Airmass at midpoint of the exposure. Necessary for converting listed fluxes and magnitudes back to measured ADU counts.
FpsfFlux	Jy	REAL	−999	PSF flux.
FpsfFluxErr	Jy	REAL	−999	Error in PSF flux.
xPosChip	raw pixels	REAL	−999	PSF x position in original chip pixels.
yPosChip	raw pixels	REAL	−999	PSF y position in original chip pixels.
FccdID	⋯	SMALLINT	−999	OTA identifier of original chip (see ImageMeta).
FpsfMajorFWHM	arcsec	REAL	−999	PSF major axis FWHM.
FpsfMinorFWHM	arcsec	REAL	−999	PSF minor axis FWHM.
FpsfTheta	degrees	REAL	−999	PSF major axis orientation.
FpsfCore	⋯	REAL	−999	PSF core parameter k, where $F = F0/(1 + kr^2 + r^{3.33})$.
FpsfQf	⋯	REAL	−999	PSF coverage factor.
FpsfQfPerfect	⋯	REAL	−999	PSF weighted fraction of pixels totally unmasked.
FpsfChiSq	⋯	REAL	−999	Reduced chi-squared value of the PSF model fit.
FmomentXX	arcsec^2	REAL	−999	Second moment M_{xx}.
FmomentXY	arcsec^2	REAL	−999	Second moment M_{xy}.
FmomentYY	arcsec^2	REAL	−999	Second moment M_{yy}.
FmomentR1	arcsec	REAL	−999	First radial moment.
FmomentRH	arcsec$^{0.5}$	REAL	−999	Half-radial moment ($r^{0.5}$ weighting).
FmomentM3C	arcsec^2	REAL	−999	Cosine of trefoil second moment term: $r^2\cos(3\theta) = M_{xxx} - 3M_{xyy}$.
FmomentM3S	arcsec^2	REAL	−999	Sine of trefoil second moment: $r^2\sin(3\theta) = 3M_{xxy} - M_{yyy}$.
FmomentM4C	arcsec^2	REAL	−999	Cosine of quadrupole second moment: $r^2\cos(4\theta) = M_{xxxx} - 6M_{xxyy} + M_{yyyy}$.
FmomentM4S	arcsec^2	REAL	−999	Sine of quadrupole second moment: $r^2\sin(4\theta) = 4M_{xxxy} - 4M_{xyyy}$.
FapFlux	Jy	REAL	−999	Aperture flux.
FapFluxErr	Jy	REAL	−999	Error in aperture flux.
FapFillF	⋯	REAL	−999	Aperture fill factor.
FapRadius	arcsec	REAL	−999	Aperture radius for forced WARP detection.
FkronFlux	Jy	REAL	−999	Kron (1980) flux.
FkronFluxErr	Jy	REAL	−999	Error in Kron (1980) flux.
FkronRad	arcsec	REAL	−999	Kron (1980) radius.
Fsky	Jy arcsec^{-2}	REAL	−999	Background sky level.
FskyErr	Jy arcsec^{-2}	REAL	−999	Error in background sky level.
FinfoFlag	⋯	BIGINT	0	Information flag bitmask indicating details of the photometry. Values listed in DetectionFlags.
FinfoFlag2	⋯	INT	0	Information flag bitmask indicating details of the photometry. Values listed in DetectionFlags2.
FinfoFlag3	⋯	INT	0	Information flag bitmask indicating details of the photometry. Values listed in DetectionFlags3.
processingVersion	⋯	TINYINT	NA	Data release version.

Note. The identifiers connecting the measurement back to the original image and to the object association are provided. PSF, aperture, and Kron (1980) photometry are included, along with sky and detector coordinate positions.

Table D34
ForcedWarpMasked: Contains an Entry for Objects Detected in the Stacked Images Which Were in the Footprint of a Single-epoch Exposure, but for Which There Are No Unmasked Pixels at that Epoch

Column Name	Units	Data Type	Default	Description
objID	⋯	BIGINT	NA	Unique object identifier.
uniquePspsFWid	⋯	BIGINT	NA	Unique internal PSPS forced WARP identifier.
ippObjID	⋯	BIGINT	NA	IPP internal object identifier.
ippDetectID	⋯	BIGINT	NA	IPP internal detection identifier.
filterID	⋯	TINYINT	NA	Filter identifier. Details in the Filter table.
surveyID	⋯	TINYINT	NA	Survey identifier. Details in the Survey table.
forcedSummaryID	⋯	BIGINT	NA	Forced WARP summary meta identifier
forcedWarpID	⋯	BIGINT	NA	Unique forced WARP identifier.
randomWarpID	⋯	FLOAT	NA	Random value drawn from the interval between zero and one.
tessID	⋯	TINYINT	0	Tessellation identifier. Details in the TessellationType table.
projectionID	⋯	SMALLINT	−1	Projection cell identifier.
skyCellID	⋯	REAL	−999	Skycell region identifier.
dvoRegionID	⋯	REAL	−999	Internal DVO region identifier.
obsTime	days	FLOAT	−999	Modified Julian Date at the midpoint of the observation.

Table D35
ForcedWarpExtended: Contains the Single-epoch Forced Photometry Fluxes within the SDSS R5 ($r = 3\farcs00$), R6 ($r = 4\farcs63$), and R7 ($r = 7\farcs43$) Apertures (Stoughton et al. 2002) for Objects Detected in the Stacked Images

Column Name	Units	Data Type	Default	Description
objID	⋯	BIGINT	NA	Unique object identifier.
uniquePspsFWid	⋯	BIGINT	NA	Unique internal PSPS forced WARP identifier.
detectID	⋯	BIGINT	NA	Unique detection identifier.
ippObjID	⋯	BIGINT	NA	IPP internal object identifier.
ippDetectID	⋯	BIGINT	NA	IPP internal detection identifier.
filterID	⋯	TINYINT	NA	Filter identifier. Details in the Filter table.
surveyID	⋯	TINYINT	NA	Survey identifier. Details in the Survey table.
forcedWarpID	⋯	BIGINT	NA	Unique forced WARP identifier.
randomWarpID	⋯	FLOAT	NA	Random value drawn from the interval between zero and one.
tessID	⋯	TINYINT	0	Tessellation identifier. Details in the TessellationType table.
projectionID	⋯	SMALLINT	−1	Projection cell identifier.
skyCellID	⋯	TINYINT	255	Skycell region identifier.
dvoRegionID	⋯	INT	−1	Internal DVO region identifier.
obsTime	days	FLOAT	−999	Modified Julian Date at the midpoint of the observation.
flxR5	Jy	REAL	−999	Flux from forced photometry measurement within an aperture of radius $r = 3\farcs00$.
flxR5Err	Jy	REAL	−999	Error in flux from forced photometry measurement within an aperture of radius $r = 3\farcs00$.
flxR5Std	Jy	REAL	−999	Standard deviation of flux from forced photometry measurement within an aperture of radius $r = 3\farcs00$.
flxR5Fill	⋯	REAL	−999	Aperture fill factor for forced photometry measurement within an aperture of radius $r = 3\farcs00$.
flxR6	Jy	REAL	−999	Flux from forced photometry measurement within an aperture of radius $r = 4\farcs63$.
flxR6Err	Jy	REAL	−999	Error in flux from forced photometry measurement within an aperture of radius $r = 4\farcs63$.
flxR6Std	Jy	REAL	−999	Standard deviation of flux from forced photometry measurement within an aperture of radius $r = 4\farcs63$.
flxR6Fill	⋯	REAL	−999	Aperture fill factor for forced photometry measurement within an aperture of radius $r = 4\farcs63$.
flxR7	Jy	REAL	−999	Flux from forced photometry measurement within an aperture of radius $r = 7\farcs43$.
flxR7Err	Jy	REAL	−999	Error in flux from forced photometry measurement within an aperture of radius $r = 7\farcs43$.
flxR7Std	Jy	REAL	−999	Standard deviation of flux from forced photometry measurement within an aperture of radius $r = 7\farcs43$.
flxR7Fill	⋯	REAL	−999	Aperture fill factor for forced photometry measurement within an aperture of radius $r = 7\farcs43$.

Table D36
ForcedWarpLensing: Contains the Kaiser et al. (1995, K95) Lensing Parameters Measured from the Forced Photometry of Objects Detected in Stacked Images on the Individual Single-epoch Data

Column Name	Units	Data Type	Default	Description
objID	⋯	BIGINT	NA	Unique object identifier.
uniquePspsFWid	⋯	BIGINT	NA	Unique internal PSPS forced WARP identifier.
detectID	⋯	BIGINT	NA	Unique detection identifier.
ippObjID	⋯	BIGINT	NA	IPP internal object identifier.
ippDetectID	⋯	BIGINT	NA	IPP internal detection identifier.
filterID	⋯	TINYINT	NA	Filter identifier. Details in the Filter table.
surveyID	⋯	TINYINT	NA	Survey identifier. Details in the Survey table.
forcedWarpID	⋯	BIGINT	NA	Unique forced WARP identifier.
randomWarpID	⋯	FLOAT	NA	Random value drawn from the interval between zero and one.
tessID	⋯	TINYINT	0	Tessellation identifier. Details in the TessellationType table.
projectionID	⋯	SMALLINT	−1	Projection cell identifier.
skyCellID	⋯	TINYINT	255	Skycell region identifier.
dvoRegionID	⋯	INT	−1	Internal DVO region identifier.
obsTime	days	FLOAT	−999	Modified Julian Date at the midpoint of the observation.
lensObjSmearX11	arcsec^{-2}	REAL	−999	K95 Equation (A11) smear polarizability X11 term from forced photometry.
lensObjSmearX12	arcsec^{-2}	REAL	−999	K95 Equation (A11) smear polarizability X12 term from forced photometry.
lensObjSmearX22	arcsec^{-2}	REAL	−999	K95 Equation (A11) smear polarizability X22 term from forced photometry.
lensObjSmearE1	arcsec^{-2}	REAL	−999	K95 Equation (A12) smear polarizability e1 term from forced photometry.
lensObjSmearE2	arcsec^{-2}	REAL	−999	K95 Equation (A12) smear polarizability e2 term from forced photometry.
lensObjShearX11	⋯	REAL	−999	K95 Equation (B11) shear polarizability X11 term from forced photometry.
lensObjShearX12	⋯	REAL	−999	K95 Equation (B11) shear polarizability X12 term from forced photometry.
lensObjShearX22	⋯	REAL	−999	K95 Equation (B11) shear polarizability X22 term from forced photometry.
lensObjShearE1	⋯	REAL	−999	K95 Equation (B12) shear polarizability e1 term from forced photometry.
lensObjShearE2	⋯	REAL	−999	K95 Equation (B12) shear polarizability e2 term from forced photometry.
lensPSFSmearX11	arcsec^{-2}	REAL	−999	K95 Equation (A11) smear polarizability X11 term from PSF model for forced photometry.
lensPSFSmearX12	arcsec^{-2}	REAL	−999	K95 Equation (A11) smear polarizability X12 term from PSF model for forced photometry.
lensPSFSmearX22	arcsec^{-2}	REAL	−999	K95 Equation (A11) smear polarizability X22 term from PSF model for forced photometry.
lensPSFSmearE1	arcsec^{-2}	REAL	−999	K95 Equation (A12) smear polarizability e1 term from PSF model for forced photometry.
lensPSFSmearE2	arcsec^{-2}	REAL	−999	K95 Equation (A12) smear polarizability e2 term from PSF model for forced photometry.
lensPSFShearX11	⋯	REAL	−999	K95 Equation (B11) shear polarizability X11 term from PSF model for forced photometry.
lensPSFShearX12	⋯	REAL	−999	K95 Equation (B11) shear polarizability X12 term from PSF model for forced photometry.
lensPSFShearX22	⋯	REAL	−999	K95 Equation (B11) shear polarizability X22 term from PSF model for forced photometry.
lensPSFShearE1	⋯	REAL	−999	K95 Equation (B12) shear polarizability e1 term from PSF model for forced photometry.
lensPSFShearE2	⋯	REAL	−999	K95 Equation (B12) shear polarizability e2 term from PSF model for forced photometry.
psfE1	⋯	REAL	−999	K95 polarization parameter $e1 = (M_{xx} - M_{yy})/(M_{xx} + M_{yy})$ from forced photometry.
psfE2	⋯	REAL	−999	K95 polarization parameter $e2 = (2M_{xy})/(M_{xx} + M_{yy})$ from forced photometry.

Table D37
ForcedWarpToImage: Contains the Mapping of Which Input Image Comprises a Particular WARP Image Used for Forced Photometry

Column Name	Units	Data Type	Default	Description
forcedWarpID	⋯	BIGINT	NA	Unique forced WARP identifier.
imageID	⋯	BIGINT	NA	Unique image identifier. Constructed as (100 × frameID + ccdID).

Table D38
ForcedGalaxyShape: Contains the Extended Source Galaxy Shape Parameters

Column Name	Units	Data Type	Default	Description
objID	⋯	BIGINT	NA	Unique object identifier.
uniquePspsFGid	⋯	BIGINT	NA	Unique internal PSPS forced galaxy identifier.
ippObjID	⋯	BIGINT	NA	IPP internal object identifier.
surveyID	⋯	TINYINT	NA	Survey identifier. Details in the Survey table.
randomForcedGalID	⋯	FLOAT	NA	Random value drawn from the interval between zero and one.
galModelType	⋯	TINYINT	−999	Galaxy model identifier.
nFilter	⋯	TINYINT	−999	Number of filters with valid model measurements.
gippDetectID	⋯	BIGINT	NA	IPP internal detection identifier.
gstackImageID	⋯	BIGINT	NA	Unique STACK identifier for the *g*-filter STACK that was the original detection source.
gGalMajor	arcsec	REAL	−999	Galaxy major axis for the *g*-filter measurement.
gGalMajorErr	arcsec	REAL	−999	Error in the galaxy major axis for the *g*-filter measurement.
gGalMinor	arcsec	REAL	−999	Galaxy minor axis for the *g*-filter measurement.
gGalMinorErr	arcsec	REAL	−999	Error in the galaxy minor axis for the *g*-filter measurement.
gGalMag	AB	REAL	−999	Galaxy fit magnitude for the *g*-filter measurement.
gGalMagErr	AB	REAL	−999	Error in the galaxy fit magnitude for the *g*-filter measurement.
gGalPhi	degrees	REAL	−999	Major axis position angle of the model fit for the *g*-filter measurement.
gGalIndex	⋯	REAL	−999	Sérsic index of the model fit for the *g*-filter measurement.
gGalFlags	⋯	SMALLINT	−999	Analysis flags for the galaxy model chi-square fit (*g*-filter measurement, values defined in ForcedGalaxyShapeFlags).
gGalChisq	⋯	REAL	−999	Reduced chi-squared value for the *g*-filter measurement.
rippDetectID				
...				Same entries repeated for the *r*, *i*, *z*, and *y* filters
yGalChisq				

Note. All filters are matched into a single row. The positions, magnitudes, fluxes, and Sérsic indices are inherited from their parent measurement in the StackModelFit tables and are reproduced here for convenience. The major and minor axes and orientation are recalculated on a warp-by-warp basis from the best fit given these inherited properties (Sérsic 1963).

D.5. Tables Related to Difference Image Analysis

Table D39
DiffDetObject: Contains the Positional Information for Difference Detection Objects in a Number of Coordinate Systems

Column Name	Units	Data Type	Default	Description
diffObjName	⋯	VARCHAR(32)	NA	IAU name for this object.
diffObjPSOName	⋯	VARCHAR(32)	NA	Alternate Pan-STARRS name for this object.
diffObjAltName1	⋯	VARCHAR(32)		Alternate name for this object.
diffObjAltName2	⋯	VARCHAR(32)		Alternate name for this object.
diffObjAltName3	⋯	VARCHAR(32)		Alternate name for this object.
diffObjPopularName	⋯	VARCHAR(140)		Well-known name for this object.
diffObjID	⋯	BIGINT	NA	Unique difference object identifier.
uniquePspsDOid	⋯	BIGINT	NA	Unique internal PSPS difference object identifier.
ippObjID	⋯	BIGINT	NA	IPP internal object identifier.
surveyID	⋯	TINYINT	NA	Survey identifier. Details in the Survey table.
htmID	⋯	BIGINT	NA	Hierarchical triangular mesh (Szalay et al. 2007) index.
zoneID	⋯	INT	NA	Local zone index, found by dividing the sky into bands of decl. $0\farcs5$ in height: zoneID = floor((90 + decl.)/0.0083333).
randomDiffObjID	⋯	FLOAT	NA	Random value drawn from the interval between zero and one.
batchID	⋯	BIGINT	NA	Internal database batch identifier.
dvoRegionID	⋯	INT	−1	Internal DVO region identifier.
objInfoFlag	⋯	INT	0	Information flag bitmask indicating details of the photometry. Values listed in ObjectInfoFlags.
qualityFlag	⋯	TINYINT	0	Subset of objInfoFlag denoting whether this object is real or a likely false positive. Values listed in ObjectQualityFlags.
ra	degrees	FLOAT	−999	Right ascension mean.
dec	degrees	FLOAT	−999	Decl. mean.
cx	⋯	FLOAT	NA	Cartesian x on a unit sphere.
cy	⋯	FLOAT	NA	Cartesian y on a unit sphere.
cz	⋯	FLOAT	NA	Cartesian z on a unit sphere.
lambda	degrees	FLOAT	−999	Ecliptic longitude.
beta	degrees	FLOAT	−999	Ecliptic latitude.
l	degrees	FLOAT	−999	Galactic longitude.
b	degrees	FLOAT	−999	Galactic latitude.
gQfPerfect	⋯	REAL	−999	Maximum PSF weighted fraction of pixels totally unmasked from g-filter detections.
rQfPerfect	⋯	REAL	−999	Maximum PSF weighted fraction of pixels totally unmasked from r-filter detections.
iQfPerfect	⋯	REAL	−999	Maximum PSF weighted fraction of pixels totally unmasked from i-filter detections.
zQfPerfect	⋯	REAL	−999	Maximum PSF weighted fraction of pixels totally unmasked from z-filter detections.
yQfPerfect	⋯	REAL	−999	Maximum PSF weighted fraction of pixels totally unmasked from y-filter detections.
processingVersion	⋯	TINYINT	NA	Data release version.
nDetections	⋯	SMALLINT	−999	Number of difference detections in all filters.
ng	⋯	SMALLINT	−999	Number of difference detections in the g filter.
nr	⋯	SMALLINT	−999	Number of difference detections in the r filter.
ni	⋯	SMALLINT	−999	Number of difference detections in the i filter.
nz	⋯	SMALLINT	−999	Number of difference detections in the z filter.
ny	⋯	SMALLINT	−999	Number of difference detections in the y filter.

Note. The objects associate difference detections within a $1''$ radius. The number of detections in each filter from is listed, along with maximum coverage fractions (see Szalay et al. 2007).

Table D40

DiffMeta: Contains Metadata Related to a Difference Image Constructed by Subtracting a Stacked Image from a Single-epoch Image, or In the Case of the MD Survey, from a Nightly STACK (Stack Made from All Exposures in a Single Filter in a Single Night)

Column Name	Units	Data Type	Default	Description
diffImageID	⋯	BIGINT	NA	Unique difference identifier.
batchID	⋯	BIGINT	NA	Internal database batch identifier.
surveyID	⋯	TINYINT	NA	Survey identifier. Details in the Survey table.
filterID	⋯	TINYINT	NA	Filter identifier. Details in the Filter table.
diffTypeID	⋯	TINYINT	0	Difference type identifier. Details in the DiffType table.
frameID	⋯	INT	NA	Frame/exposure identifier for the positive image in warp-stack difference images.
posImageID	⋯	BIGINT	NA	Image identifier for the positive image.
negImageID	⋯	BIGINT	NA	Image identifier for the negative image.
ippDiffID	⋯	BIGINT	NA	IPP diffRun identifier.
tessID	⋯	TINYINT	0	Tessellation identifier. Details in the TessellationType table.
projectionID	⋯	SMALLINT	−1	Projection cell identifier.
skyCellID	⋯	TINYINT	255	Skycell region identifier.
photoCalID	⋯	INT	NA	Photometric calibration identifier. Details in the PhotoCal table.
analysisVer	⋯	VARCHAR(100)		IPP software analysis release version.
md5sum	⋯	VARCHAR(100)		IPP MD5 Checksum.
detectionThreshold	magnitudes	REAL	−999	Reference magnitude for detection efficiency calculation.
expTime	seconds	REAL	−999	Exposure time of positive image. Necessary for converting listed fluxes and magnitudes back to measured ADU counts.
psfModelID	⋯	INT	−999	PSF model identifier.
psfFWHM	arcsec	REAL	−999	Mean PSF FWHM at image center.
psfWidMajor	arcsec	REAL	−999	PSF major axis FWHM at image center.
psfWidMinor	arcsec	REAL	−999	PSF minor axis FWHM at image center.
psfTheta	degrees	REAL	−999	PSF major axis orientation at image center.
kernel	⋯	VARCHAR(100)		Subtraction kernel.
mode	⋯	TINYINT	0	Subtraction mode for which input to convolve.
numStamps	⋯	INT	−999	Number of stamps.
stampDevMean	⋯	REAL	−999	Mean stamp deviation.
stampDevRMS	⋯	REAL	−999	rms stamp deviation.
normalization	⋯	REAL	−999	Normalization.
convolveMax	⋯	REAL	−999	Maxiumum convolution fraction.
deconvolveMax	⋯	REAL	−999	Maximum deconvolution fraction.
ctype1	⋯	VARCHAR(100)		Name of astrometric projection in R.A.
ctype2	⋯	VARCHAR(100)		Name of astrometric projection in decl.
crval1	degrees	FLOAT	−999	Right ascension corresponding to reference pixel.
crval2	degrees	FLOAT	−999	decl. corresponding to reference pixel.
crpix1	sky pixels	FLOAT	−999	Reference pixel for R.A.
crpix2	sky pixels	FLOAT	−999	Reference pixel for decl.
cdelt1	degrees/pixel	FLOAT	−999	Pixel scale in R.A.
cdelt2	degrees/pixel	FLOAT	−999	Pixel scale in decl.
pc001001	⋯	FLOAT	−999	Linear transformation matrix element between image pixel x and R.A.
pc001002	⋯	FLOAT	−999	Linear transformation matrix element between image pixel y and R.A.
pc002001	⋯	FLOAT	−999	Linear transformation matrix element between image pixel x and decl.
pc002002	⋯	FLOAT	−999	Linear transformation matrix element between image pixel y and decl.
processingVersion	⋯	TINYINT	NA	Data release version.

Note. The astrometric calibration of the reference STACK is listed.

Table D41
DiffDetection: Contains the Photometry of Individual Detections from a Difference Image

Column Name	Units	Data Type	Default	Description
diffObjID	⋯	BIGINT	NA	Unique difference object identifier.
uniquePspsDFid	⋯	BIGINT	NA	Unique internal PSPS difference detection identifier.
diffDetID	⋯	BIGINT	NA	Unique difference detection identifier.
diffImageID	⋯	BIGINT	NA	Difference detection meta identifier.
ippObjID	⋯	BIGINT	NA	IPP internal object identifier.
ippDetectID	⋯	BIGINT	NA	IPP internal detection identifier.
fromPosImage	⋯	TINYINT	NA	Detection is from positive image (if 1) or negative image (if 0).
filterID	⋯	TINYINT	NA	Filter identifier. Details in the Filter table.
surveyID	⋯	TINYINT	NA	Survey identifier. Details in the Survey table.
randomDiffID	⋯	FLOAT	NA	Random value drawn from the interval between zero and one.
tessID	⋯	TINYINT	0	Tessellation identifier. Details in the TessellationType table.
projectionID	⋯	SMALLINT	−1	Projection cell identifier.
skyCellID	⋯	TINYINT	255	Skycell region identifier.
dvoRegionID	⋯	INT	−1	Internal DVO region identifier.
obsTime	days	FLOAT	−999	Modified Julian Date at the midpoint of the observation.
xPos	sky pixels	REAL	−999	PSF x-center location.
yPos	sky pixels	REAL	−999	PSF y-center location.
xPosErr	sky pixels	REAL	−999	Error in PSF x-center location.
yPosErr	sky pixels	REAL	−999	Error in PSF y-center location.
pltScale	arcsec/pixel	REAL	−999	Local plate scale at this location.
posAngle	degrees	REAL	−999	Position angle (sky-to-chip) at this location.
ra	degrees	FLOAT	−999	Right ascension.
dec	degrees	FLOAT	−999	Declination.
raErr	arcsec	REAL	−999	Right ascension error.
decErr	arcsec	REAL	−999	Decl. error.
zp	magnitudes	REAL	0	Photometric zero point for converting fluxes and magnitudes to measured ADU.
telluricExt	magnitudes	REAL	NA	Estimated telluric extinction due to nonphotometric observing conditions.
expTime	seconds	REAL	−999	Exposure time of the positive single-epoch image.
airMass	⋯	REAL	0	Airmass at the midpoint of the exposure to convert fluxes and magnitudes to measured ADU.
DpsfFlux	Jy	REAL	−999	Flux from PSF fit.
DpsfFluxErr	Jy	REAL	−999	Error in PSF flux.
xPosChip	raw pixels	REAL	−999	PSF x position in original chip pixels.
yPosChip	raw pixels	REAL	−999	PSF y position in original chip pixels.
ccdID	⋯	SMALLINT	−999	OTA identifier of original chip (see ImageMeta).
DpsfMajorFWHM	arcsec	REAL	−999	PSF major axis FWHM.
DpsfMinorFWHM	arcsec	REAL	−999	PSF minor axis FWHM.
DpsfTheta	degrees	REAL	−999	PSF major axis orientation.
DpsfCore	⋯	REAL	−999	PSF core parameter k, where $F = F0/(1 + kr^2 + r^{3.33})$.
DpsfQf	⋯	REAL	−999	PSF coverage factor.
DpsfQfPerfect	⋯	REAL	−999	PSF-weighted fraction of pixels totally unmasked.
DpsfChiSq	⋯	REAL	−999	Reduced chi-squared value of the PSF model fit.
DpsfLikelihood	⋯	REAL	−999	Likelihood that this detection is best fit by a PSF.
DmomentXX	arcsec^2	REAL	−999	Second moment M_{xx}.
DmomentXY	arcsec^2	REAL	−999	Second moment M_{xy}.
DmomentYY	arcsec^2	REAL	−999	Second moment M_{yy}.
DmomentR1	arcsec	REAL	−999	First radial moment.
DmomentRH	arcsec$^{0.5}$	REAL	−999	Half-radial moment ($r^{0.5}$ weighting).
DapFlux	Jy	REAL	−999	Aperture flux.
DapFluxErr	Jy	REAL	−999	Error in aperture flux.
DapFillF	⋯	REAL	−999	Aperture fill factor.
DkronFlux	Jy	REAL	−999	Kron (1980) flux.
DkronFluxErr	Jy	REAL	−999	Error in Kron (1980) flux.
DkronRad	arcsec	REAL	−999	Kron (1980) radius.
diffNPos	sky pixels	INT	−999	Number of difference pixels within the aperture that are positive.
diffFPosRatio	⋯	REAL	−999	Ratio of the sum of positive flux pixel values to the sum of the absolute value of all unmasked pixels within the aperture.
diffNPosRatio	⋯	REAL	−999	Ratio of the number of positive flux pixels to the number of unmasked pixels within the aperture.
diffNPosMask	⋯	REAL	−999	Ratio of the number of positive flux pixels to the number of positive or masked pixels within the aperture.
diffNPosAll	⋯	REAL	−999	Ratio of the number of positive flux pixels to the total number of all pixels within the aperture.
diffPosDist	sky pixels	REAL	−999	Distance to matching source in positive image.

Table D41
(Continued)

Column Name	Units	Data Type	Default	Description
diffNegDist	sky pixels	REAL	−999	Distance to matching source in negative image.
diffPosSN	···	REAL	−999	Signal to noise of matching source in positive image.
diffNegSN	···	REAL	−999	Signal to noise of matching source in negative image.
Dsky	Jy arcsec^{-2}	REAL	−999	Background sky level.
DskyErr	Jy arcsec^{-2}	REAL	−999	Error in background sky level.
DinfoFlag	···	BIGINT	0	Information flag bitmask indicating details of the photometry. see DetectionFlags.
DinfoFlag2	···	INT	0	Information flag bitmask indicating details of the photometry. See DetectionFlags2.
DinfoFlag3	···	INT	0	Information flag bitmask indicating details of the photometry. See DetectionFlags3.
processingVersion	···	TINYINT	NA	Data release version.

Note. The identifiers connecting the detection back to the difference image and to the object association are provided. PSF, aperture, and Kron (1980) photometry are included, along with sky and detector coordinate positions.

Table D42
DiffToImage: Contains the Mapping of Which Input Images Were Used to Construct a Particular Difference Image

Column Name	Units	Data Type	Default	Description
diffImageID	···	BIGINT	NA	Unique difference identifier.
imageID	···	BIGINT	NA	Unique image identifier. Constructed as (100 × frameID + ccdID).

Table D43
DiffDetEffMeta: Contains the Detection Efficiency Information for a Given Individual Difference Image

Column Name	Units	Data Type	Default	Description
diffImageID	···	BIGINT	NA	Unique difference image identifier.
magref	magnitudes	REAL	NA	Detection efficiency reference magnitude.
nInjected	···	INT	NA	Number of fake sources injected in each magnitude bin.
offset01	magnitudes	REAL	NA	Detection efficiency magnitude offset for bin 1.
counts01	···	REAL	NA	Detection efficiency count of recovered sources in bin 1.
diffMean01	magnitudes	REAL	NA	Detection efficiency mean magnitude difference in bin 1.
diffStdev01	magnitudes	REAL	NA	Detection efficiency standard deviation of magnitude differences in bin 1.
errMean01	magnitudes	REAL	NA	Detection efficiency mean magnitude error in bin 1.
offset02	magnitudes	REAL	NA	Detection efficiency magnitude offset for bin 2.
counts02	···	REAL	NA	Detection efficiency count of recovered sources in bin 2.
diffMean02	magnitudes	REAL	NA	Detection efficiency mean magnitude difference in bin 2.
diffStdev02	magnitudes	REAL	NA	Detection efficiency standard deviation of magnitude differences in bin 2.
errMean02	magnitudes	REAL	NA	Detection efficiency mean magnitude error in bin 2.
offset03	magnitudes	REAL	NA	Detection efficiency magnitude offset for bin 3.
counts03	···	REAL	NA	Detection efficiency count of recovered sources in bin 3.
diffMean03	magnitudes	REAL	NA	Detection efficiency mean magnitude difference in bin 3.
diffStdev03	magnitudes	REAL	NA	Detection efficiency standard deviation of magnitude differences in bin 3.
errMean03	magnitudes	REAL	NA	Detection efficiency mean magnitude error in bin 3.
...				
offset13	magnitudes	REAL	NA	Detection efficiency magnitude offset for bin 13.
counts13	···	REAL	NA	Detection efficiency count of recovered sources in bin 13.
diffMean13	magnitudes	REAL	NA	Detection efficiency mean magnitude difference in bin 13.
diffStdev13	magnitudes	REAL	NA	Detection efficiency standard deviation of magnitude differences in bin 13.
errMean13	magnitudes	REAL	NA	Detection efficiency mean magnitude error in bin 13.

Note. Provides the number of recovered sources out of 500 injected sources and statistics about the magnitudes of the recovered sources for a range of magnitude offsets.

Appendix E
IppToPsps Translation Tables

The tables in this section describe the relationship between fields in the PSPS database and their immediate source. In some cases, the values are calculated by the IPP processing and extracted by the IPPTOPSPS system from the output catalog files (e.g., the cmf or smf files). In other cases, the values are calculated within the DVO system during the construction of that database or during the calibration. Some values are calculated directly by the PSPS ingest software from other information (e.g., the *cx*, *cy*, *cz* coordinate system for objects).

Table E1
ObjectThin: This Describes the Sources for Each of the Columns within ippdbtableObjectThin as Well as the Formula to Generate the Data within the Column, If It Is Not Just Copying Directly

Column Name	Source	Notes
objName	DVO cpt IAUNAME /IPPTOPSPS	
objPSOName	DVO cpt PSO_NAME	
objAltName1	not set	
objAltName2	not set	
objAltName3	not set	
objPopularName	not set	
objID	DVO cpt EXT_ID	
uniquePspsOBid	IPPTOPSPS	uniquePspsOBid = (batchID * 1000000000) + row number)
ippObjID	DVO cpt OBJ_ID and CAT_ID	OBJ_ID + (CAT_ID $\ll$ 32)
surveyID	IPPTOPSPS	set to 0 for 3π
htmID	PSPS	calculated and filled in PSPS (Szalay et al. 2007)
zoneID	PSPS	calculated and filled in PSPS
tessID	DVO cpt TESS_ID	
projectionID	DVO cpt PROJECTION_ID	
skyCellID	DVO cpt SKYCELL_ID	
randomID	IPPTOPSPS	random is seeded with RAND(batchID)
batchID	IPPTOPSPS	sequentially ncreases as batches are made
dvoRegionID	DVO cpt CAT_ID	
processingVersion	IPPTOPSPS	set to 3 for this data release, for PV3
objInfoFlag	DVO cpt FLAGS	
qualityFlag	DVO cpt FLAGS	FLAGS $\gg$ 23 & 0xFF
raStack	DVO cpt RA_STK	
decStack	DVO cpt DEC_STK	
raStackErr	DVO cpt RA_STK_ERR	
decStackErr	DVO cpt DEC_STK_ERR	
raMean	DVO cpt RA_MEAN	
decMean	DVO cpt DEC_MEAN	
raMeanErr	DVO cpt RA_ERR	
decMeanErr	DVO cpt DEC_ERR	
epochMean	DVO cpt EPOCH_MEAN	
posMeanChisq	DVO cpt CHISQ_POS	
cx	PSPS	set to 0 initially; calculated and filled by PSPS
cy	PSPS	set to 0 initially; calculated and filled by PSPS
cz	PSPS	set to 0 initially; calculated and filled by PSPS
lambda	PSPS set to 0; calculated and filled by PSPS	
beta	PSPS set to 0; calculated and filled by PSPS	
l	PSPS	set to 0; calculated and filled by PSPS
b	PSPS	set to 0; calculated and filled by PSPS
nStackObjectRows	IPPTOPSPS	set to -999 for 3π
nStackDetections	DVO cpt NSTACK_DET	sum of NSTACK_DET for all 5 filters
nDetections	IPPTOPSPS	sum of non-null ng + nr + ni +nz + ny
ng	DVO cpt NCODE	
nr	DVO cpt NCODE	
ni	DVO cpt NCODE	
nz	DVO cpt NCODE	
ny	DVO cpt NCODE	

Note. For this table, DVO cpt NAME shows that this comes from the cpt files in the DVO database and has a column of NAME. The sources for this table include the DVO cpt files, IPPTOPSPS, PSPS, as well as a few columns that are not currently being used.

Table E2
MeanObject: This Describes the Sources for Each of the Columns within MeanObject as Well as the Formula to Generate the Data within the Column, If It Is Not Just Copying Directly

Column Name	Source	Notes
objID	IPPTOPSPSobjectThin.objID	
uniquePspsOBid	IPPTOPSPSobjectThin. uniquePspsOBid	
gQfPerfect	DVO cps PSF_QF_PERF_MAX	
gMeanPSFMag	DVO cps MAG	
gMeanPSFMagErr	DVO cps MAG_ERR	
gMeanPSFMagStd	DVO cps MAG_STDEV	
gMeanPSFMagNpt	DVO cps NUSED	
gMeanPSFMagMin	DVO cps MAG_MIN	
gMeanPSFMagMax	DVO cps MAG_MAX	
gMeanKronMag	DVO cps MAG_KRON	
gMeanKronMagErr	DVO cps MAG_KRON_ERR	
gMeanKronMagStd	DVO cps MAG_KRON_STDEV	
gMeanKronMagNpt	DVO cps NUSED_KRON	
gMeanApMag	DVO cps MAG_AP	
gMeanApMagErr	DVO cps MAG_AP_ERR	
gMeanApMagStd	DVO cps MAG_AP_STDEV	
gMeanApMagNpt	DVO cps NUSED_AP	
gFlags	DVO cps FLAGS	
rQfPerfect		
...		Same entries repeated for the *r*, *i*, *z*, and *y* filters
yFlags		

Note. For this table, DVO cps NAME shows that this comes from the cps files in the DVO database and has a column of NAME. The sources for this table include the DVO cps files and IPPTOPSPS.

Table E3
StackObjectThin: This Describes the Sources for Each of the Columns within StackObjectThin as Well as the Formula to Generate the Data within the Column, If It Is Not Just Copying Directly

Column Name	Source	Notes
objID	DVO cpt	average.extID
uniquePspsSTid	IPPTOPSPS	(batchID $*$ 1000000000) + row number)
ippObjID	DVO cpt	OBJ_ID + (CAT_ID $\ll$ 32)
surveyID	IPPTOPSPS	set to 0 for 3π
tessID	cmf file	from header: TESS_ID
projectionID	cmf file	from header, first 4 numbers in SKYCELL
skyCellID	cmf file	from header, last 4 numbers in SKYCELL
randomStackObjID	ipptopsps	random number generated in ipptopsps, seeded with batch_id
primaryDetection	DVO cpm	(dvo.measure.flags & 0x10000) $\gg$ 16
bestDetection	DVO cpt	(dvo.average.objflags & 0x8000) $\gg$ 15)
dvoRegionID	DVO cpt	dvo.measure.catID
processingVersion	ipptopsps	set to 3 for this data release, for PV3
gippDetectID	DVO cpm	dvo.measure.detID
gstackDetectID	DVO cpm	dvo.measure.extID
gstackImageID	gpc1 database	internal stack ID for this stack
gra	DVO cpm	dvo.average.ra
gdec	DVO cpm	dvo.average.dec
graErr	cmf file	*X_PSF$_S$IG $*$ PLTSCALE*
gdecErr	cmf file	*Y_PSF$_S$IG $*$ PLTSCALE*
gEpoch	cmf file	from header, MJD-OBS
gPSFMag	DVO cpm	dvo.measure.FluxPSF (converted to mag using the zero point)
gPSFMagErr	DVO cpm	dvo.measure.dFluxPSF (converted to mag error)
gApMag	DVO cpm	dvo.measure.FluxAp (converted to mag using the zero point)
gApMagErr	DVO cpm	dvo.measure.dFluxAp (converted to mag error)
gKronMag	DVO cpm	dvo.measure.FluxKron (converted to mag using the zero point)
gKronMagErr	DVO cpm	dvo.measure.dFluxKron (converted to mag error)
ginfoFlag	cmf file	FLAGS
ginfoFlag2	cmf file	FLAGS2
ginfoFlag3	DVO cpt	measure.dbFlags
gnFrames	cmf file, header	N_FRAMES
rippDetectID	⋯	
...	⋯	same entries repeated for *r*, *i*, *z*, and *y* filters
ynFrames	⋯	

Note. For this table, DVO cps NAME shows that this comes from the cps files in the DVO database and has a column of NAME. The sources for this table include the DVO cps files and IPPTOPSPS.

ORCID iDs

H. A. Flewelling https://orcid.org/0000-0002-1050-4056
E. A. Magnier https://orcid.org/0000-0002-7965-2815
K. C. Chambers https://orcid.org/0000-0001-6965-7789
M. E. Huber https://orcid.org/0000-0003-1059-9603
C. Z. Waters https://orcid.org/0000-0003-1989-4879
A. Calamida https://orcid.org/0000-0002-0882-7702
G. Hasinger https://orcid.org/0000-0002-0797-0646
K. S. Long https://orcid.org/0000-0002-4134-864X
N. Metcalfe https://orcid.org/0000-0001-9034-4402
G. Narayan https://orcid.org/0000-0001-6022-0484
P. Norberg https://orcid.org/0000-0002-5875-0440
R. P. Saglia https://orcid.org/0000-0003-0378-7032
J. L. Tonry https://orcid.org/0000-0003-2858-9657
R. White https://orcid.org/0000-0002-9194-2807
P. W. Draper https://orcid.org/0000-0002-7204-9802
K. W. Hodapp https://orcid.org/0000-0003-0786-2140
R. Jedicke https://orcid.org/0000-0001-7830-028X
N. Kaiser https://orcid.org/0000-0001-6511-4306
R. J. Wainscoat https://orcid.org/0000-0002-1341-0952
M. Postman https://orcid.org/0000-0002-9365-7989

References

Chambers, K. C., Magnier, E. A., Metcalfe, N., et al. 2016, arXiv:1612.05560
de Vaucouleurs, G. 1948, AnAp, 11, 247
Denneau, L., Jedicke, R., Grav, T., et al. 2013, PASP, 125, 357
Gaia Collaboration, Brown, A. G. A., Vallenari, A., et al. 2016, A&A, 595, A2
Gray, J., Szalay, A. S., Thakar, A. R., et al. 2002, arXiv:cs/0202014
Heasley, J., Smith, W., Eek, R., & Rosen, J. 2006, in The Advanced Maui Optical and Space Surveillance Technologies Conf. (Kihei, HI: Maui Economic Development Board), E51
Heasley, J. N. 2008, in AIP Conf. Ser. 1082, Classification and Discovery in Large Astronomical Surveys, ed. C. A. L. Bailer-Jones (Melville, NY: AIP), 352
Hernitschek, N., Schlafly, E. F., Sesar, B., et al. 2016, ApJ, 817, 73
Hodapp, K. W., Kaiser, N., Aussel, H., et al. 2004, AN, 325, 636
Kaiser, N., Squires, G., & Broadhurst, T. 1995, ApJ, 449, 460
Kron, R. G. 1980, ApJS, 43, 305
Magnier, E. A., Chambers, K. C., Flewelling, H. A., et al. 2020a, ApJS, 251, 3
Magnier, E. A., & Cuillandre, J.-C. 2004, PASP, 116, 449
Magnier, E. A., Schlafly, E., Finkbeiner, D., et al. 2013, ApJS, 205, 20
Magnier, E. A., Schlafly, E. F., Finkbeiner, D. P., et al. 2020c, ApJS, 251, 6
Magnier, E. A., Sweeney, W. E., Chambers, K. C., et al. 2020b, ApJS, 251, 5
Petrosian, V. 1976, ApJL, 209, L1
Sérsic, J. L. 1963, BAAA, 6, 41
Skrutskie, M. F., Cutri, R. M., Stiening, R., et al. 2006, AJ, 131, 1163
Stoughton, C., Lupton, R. H., Bernardi, M., et al. 2002, AJ, 123, 485
Szalay, A. S., Gray, J., Fekete, G., et al. 2007, arXiv:cs/0701164
Szalay, A. S., Gray, J., Thakar, A. R., et al. 2002, arXiv:cs/0202013
Taylor, M. B. 2006, in ASP Conf. Ser. 351, Astronomical Data Analysis Software and Systems XV, ed. C. Gabriel et al. (San Francisco, CA: ASP), 666
Thakar, A. R., Szalay, A. S., Vandenberg, J. V., Gray, J., & Stoughton, A. S. 2003, in ASP Conf. Ser. 295, Astronomical Data Analysis Software and Systems XII, ed. H. E. Payne, R. I. Jedrzejewski, & R. N. Hook (San Francisco, CA: ASP), 217
Tonry, J. L., Stubbs, C. W., Lykke, K. R., et al. 2012, ApJ, 750, 99
Waters, C. Z., Magnier, E. A., Price, P. A., et al. 2020, ApJS, 251, 4